

CHARLES UNIVERSITY IN PRAGUE
FACULTY OF SCIENCE
DEPARTMENT OF PLANT EXPERIMENTAL BIOLOGY



**Revealing phosphoproteins playing role in
tobacco pollen activated *in vitro***

Master thesis

Jan Fíla

Supervisor: RNDr. David Honys, Ph.D.

Consultant: RNDr. Věra Čapková, CSc.

Prague, 2012

The presented work was carried out at the Laboratory of Pollen Biology, Institute of Experimental Botany ASCR, v.v.i., Prague 6, Czech Republic, and at the Applied Biochemistry Group, Leibniz Institute of Plant Genetics and Crop Plant Research, Gatersleben, Germany.

I hereby declare that I completed this master thesis independently under the guidance of RNDr. David Honys, Ph.D., and RNDr. Věra Čapková, CSc. It documents my own work if not explicitly otherwise mentioned. I have properly acknowledged and cited all sources used. The thesis is not subject of any other defending procedure.

Prague, July 25th 2012

.....

Acknowledgements

I would like to acknowledge my supervisor RNDr. David Honys, Ph.D., for his valuable comments and meaningful discussions, and appreciate his giving me the chance to visit the Applied Biochemistry (ABC) Group at the IPK in Gatersleben. My thanks belong also to RNDr. Věra Čápková, CSc., for her guidance, patience and fruitful discussions as well as support during not only the good but also worse times. I acknowledge RNDr. Nikoleta Dupl'áková, Ph.D., for her teaching me basic laboratory skills during my beginnings of experimental work in the lab. I also thank my colleagues for creating a friendly atmosphere in the Laboratory of Pollen Biology.

Many thanks belong to Dr. Hans-Peter Mock (the head of the ABC Group, IPK Gatersleben, Germany) for starting collaboration with our laboratory, and for giving me the chance to visit his lab and learn there the phosphoproteomic techniques. The MS analyses of the MOAC-enriched phosphoproteins were performed by Dr. Andrea Matros (from the same lab), to whom belong also my thanks for a number of fruitful discussions and for introducing me to the world of mass spectrometry. I also acknowledge Annegret Wolf (from the same lab) for her excellent technical assistance during my stay in Germany. My gratefulness belongs also to other people from the ABC Group for a pleasant atmosphere and preparedness to help me in times of need.

I would also like to thank Dr. René Peiman Zahedi and Dr. Sonja Radau (Leibniz-Institut für Analytische Wissenschaften – ISAS – e.V., Dortmund, Germany) for performing titanium dioxide enrichment and subsequent MS analyses leading to the identification of particular phosphorylation sites.

I would like to acknowledge Mgr. Alena A. Fidlerová, Ph.D. for language corrections. Last but not least, I thank to my family for their support not only during my whole studies.

The project was financially supported by Czech Science Foundation (P501/11/1462, P305/12/2611), Ministry of Education, Youth and Sports of the Czech Republic (OC08011), European Science Foundation (COST Action 0603; COST-STSM-FA0603-04559 and COST-STSM-FA0603-05564), DAAD/ASCR bilateral project (D8-CZ19/2011–2012), German Academic Exchange Service (ID 50755371), and the European Fund for Regional Development, the Operational Program Prague – Competitiveness (project CZ.2.16/3.1.00/21159).

Abstract

Tobacco mature pollen rehydrates *in vivo* on a stigma tissue, and develops into the rapidly-growing pollen tube. This rehydration process is accompanied by the de-repression of stored mRNA transcripts, resulting in the synthesis of novel proteins. Furthermore, such metabolic switch is also likely to be regulated on the level of post-translational modifications of the already-present proteins, namely via phosphorylation, since it was shown to play a significant regulatory role in numerous cellular processes.

Since only a minor part of proteins is phosphorylated in a cell at a time, the employment of various enrichment techniques is usually of key importance. In this diploma project, metal oxide/hydroxide affinity chromatography (MOAC) with aluminium hydroxide matrix was applied in order to enrich phosphoproteins from the mature pollen and the 30-minute *in vitro* activated pollen crude protein extracts. The enriched fraction was separated by both 2D-GE and gel-free liquid chromatography (LC) approaches with subsequent mass spectrometric analyses. Collectively, 139 phosphoprotein candidates were identified. Additionally, to broaden the number of phosphorylation sites identified, titanium dioxide phosphopeptide enrichment of trypsin-digested mature pollen crude extract was performed. Thanks to the titanium dioxide enrichment, the position of 51 phosphorylation sites was identified giving a total of 52 phosphorylation sites present in the above phosphoprotein candidates.

Key words: male gametophyte, mature pollen, tobacco, *Nicotiana tabacum*, phosphoproteomics, phosphoprotein enrichment, MOAC, metal oxide/hydroxide affinity chromatography, titanium dioxide, TiO₂, aluminium hydroxide, Al(OH)₃

Abstract in Czech

Po dopadu na bliznu se zralý pyl tabáku rehydratuje, aktivuje a klíčí z něj pylová láčka. Rehydratace je doprovázena de-represí skladovaných mRNA, z nichž se syntetizují nové proteiny. Při vývoji zralého pylu v rychle rostoucí pylovou láčku se velmi pravděpodobně uplatňují také posttranslační modifikace proteinů, konkrétně fosforylace, jež se podílí na regulaci celé řady buněčných procesů.

Vzhledem k tomu, že pouze malý podíl proteinů je v daném okamžiku v buňce fosforylován, bývá nevyhnutelné využít nejrůznější obohacovací techniky. Pro obohacení fosfoproteinů z celkového proteinového extraktu zralého pylu a pylu aktivovaného *in vitro* 30 minut byla v této diplomové práci aplikována afinitní chromatografie s využitím kovového oxidu/hydroxidu (MOAC), kde byl matricí hydroxid hlinitý. Získaná obohacená frakce byla rozdělena nezávisle dvěma metodami; klasickou dvojrozměrnou elektroforézou (2D-GE) a kapalinovou chromatografií (LC). Hmotnostní spektrometrií (MS) byly analyzovány vzorky získané oběma způsoby dělení, a celkem tak bylo identifikováno 139 fosfoproteinových kandidátů. Fosfopeptidové obohacení využívající oxid titaničitý vedlo k lokalizaci 51 fosforylačních míst, a tak rozšířilo počet přesně identifikovaných fosforylačních míst na celkových 52.

Klíčová slova: samčí gametofyt, zralý pyl, tabák, *Nicotiana tabacum*, fosfoproteomika, obohacování o fosfoproteiny, MOAC, afinitní chromatografie s využitím kovového oxidu/hydroxidu, oxid titaničitý, TiO_2 , hydroxid hlinitý, Al(OH)_3

Contents

1	Introduction	11
2	Literature survey	12
2.1	<i>Angiosperm life cycle</i>	12
2.2	<i>Male gametophyte development</i>	13
2.3	<i>Gene expression in mature pollen</i>	15
2.4	<i>Protein phosphorylation</i>	16
2.5	<i>Phosphorylated amino acids</i>	17
2.6	<i>Enrichment techniques</i>	19
2.7	<i>Comparison of phosphoprotein and phosphopeptide enrichment</i>	19
2.8	<i>Principles of enriching protocols</i>	23
2.9	<i>Al(OH)₃-MOAC phosphoprotein enrichment</i>	25
2.10	<i>TiO₂ phosphopeptide enrichment</i>	26
3	Materials and methods	28
3.1	<i>Plant material and pollen tube activation</i>	28
3.2	<i>Protein extraction</i>	28
3.3	<i>MOAC phosphoprotein enrichment</i>	29
3.4	<i>1D SDS-PAGE of MOAC fractions</i>	30
3.5	<i>Phosphorylation in vitro</i>	31
3.6	<i>2D-GE and image analysis</i>	32
3.7	<i>Trypsin digest and MS/MS analysis of the spots</i>	33
3.8	<i>In solution trypsin digest and gel-free nLC-MS/MS</i>	34
3.9	<i>Titanium dioxide phosphopeptide enrichment</i>	36
4	Results	38
4.1	<i>Phosphoprotein enrichment</i>	38
4.2	<i>Phosphorylation in vitro</i>	40
4.3	<i>In-gel approach</i>	42
4.4	<i>Gel-free approach</i>	48
4.5	<i>The identification of phosphorylation sites</i>	55
5	Discussion	63
5.1	<i>MOAC and its specificity for phosphoprotein enrichment</i>	63
5.2	<i>Detected phosphorylation sites</i>	64
5.3	<i>Un-detectable phosphorylation sites</i>	64

5.4	<i>Biological role of the phosphorylated candidates</i>	65
5.5	<i>On-going experiments</i>	69
6	Conclusion	70
7	Publications and conferences.....	71
8	References	72
9	Supplementary tables (on a CD).....	85

Abbreviations

%C	– bisacrylamide concentration
%T	– total concentration of acrylamide and bisacrylamide monomer
1D	– one-dimensional
2D	– two-dimensional
2D-GE	– two-dimensional gel electrophoresis
ABC	– ammonium bicarbonate
ACN	– acetonitrile
Al(OH) ₃	– aluminium hydroxide
ANOVA	– analysis of variance
ATP	– adenosine triphosphate
BSA	– bovine serum albumine
CBB G250	– Coomassie Brilliant Blue G250
CHAPS	– 3-[(3-Cholamidopropyl)dimethylammonio]-1-propanesulphonate
CID	– collision-induced dissociation
Cys	– cystein
DHB	– dihydroxybenzoic acid
DTT	– dithiothreitol
EDTA	– 2,2',2'',2'''-(ethane-1,2-diyldinitrilo)tetraacetic acid
EPP	– EDTA/puromycin-resistant particle
ESI	– electrospray ionization
EST	– expressed sequence tag
HILIC	– hydrophilic interaction liquid chromatography
ICP-MS	– inductively coupled plasma mass spectrometry
IEF	– isoelectric focusing
IMAC	– immobilised metal ion affinity chromatography
LC	– liquid chromatography
ME	– 2-mercaptoethanol
MES	– 2-(<i>N</i> -morpholino)ethanesulphonic acid
Met	– methionine
MOAC	– metal oxide/hydroxide affinity chromatography
mRNA	– messenger ribonucleic acid
MS	– mass spectrometry

MS/MS	– tandem mass spectrometry
m/z	– mass-to-charge ratio
μLC	– micro liquid chromatography
nLC	– nano liquid chromatography
Phos-Tag	– 1,3-bis[bis(pyridin-2-ylmethyl)amino]propan-2-olato dizinc(II) complex
pI	– isoelectric point
pK _a	– acid dissociation constant
PLGS	– ProteinLynx GlobalSERVER
PolyMAC	– polymer-based metal ion affinity capture
ppm	– parts per million
pS	– phosphorylated serine
pT	– phosphorylated threonine
pY	– phosphorylated tyrosine
Q/TOF	– quadrupole coupled to time-of-flight MS analyzer
rRNA	– ribosomal ribonucleic acid
RuBP	– ruthenium II tris (bathophenanthroline disulphonate)
SAX	– strong anionic ion-exchange chromatography
SCX	– strong cationic ion-exchange chromatography
SDS	– sodium dodecyl sulphate
SDS-PAGE	– sodium dodecyl sulphate polyacrylamide gel electrophoresis
Ser	– serine
SMM-MES	– sucrose-mineral medium buffered with MES
TCA	– trichloroacetic acid
TFA	– trifluoroacetic acid
Thr	– threonine
TiO ₂	– titanium dioxide
Tris	– 2-amino-2-hydroxymethyl-propane-1,3-diol
Tyr	– tyrosine
v/v %	– volume percentage concentration
w/v %	– weight/volume percentage concentration

1 Introduction

Angiosperm male gametophyte represents a unique model for studies of plant polarity, tip growth, and translation regulation (Honys et al., 2000; Hepler et al., 2001). The desiccated mature pollen grain is rehydrated after reaching the stigma tissue, and subsequently, the pollen tube growth starts rapidly.

The rapid pollen tube growth is to a great extent realised due to stored mRNAs that have been repressed during the mature pollen development, and are de-repressed upon pollen activation. Such de-repression as well as functional regulation of the already-present proteins is very likely to be accompanied by protein phosphorylation.

Many phosphoproteomic techniques have newly evolved or have been notably improved in the past decade (see Dunn et al., 2010; Eyrich et al., 2011). Such development of phosphoproteomics was enabled (among others) by improvements in mass spectrometry (Boersema et al., 2009; Yates et al., 2009). Because of these newly designed or improved protocols, these techniques became more efficient and available also for less explored models such as tobacco male gametophyte.

The first aim of this diploma thesis was to apply the phosphoprotein-enriching aluminium hydroxide metal oxide/hydroxide affinity chromatography (MOAC) in order to enrich phosphoproteins both of tobacco mature pollen and of pollen activated *in vitro* for 30 min. The enriched fraction was separated by both 2D-GE, and gel-free approach applying nLC-ESI-Q/TOF resulting in a list of identified phosphoprotein candidates. The enrichment specificity was validated by phosphorylation *in vitro* and one-dimensional SDS-PAGE gel of MOAC fractions stained with ProQ Diamond Phosphoprotein Gel Stain.

The second aim of this diploma thesis was to identify exact phosphorylation site(s) in at least several phosphorylation candidates identified by the above phosphoprotein-enriching approach. To achieve this, the mature pollen crude extract was trypsin-digested and phosphopeptide-enriched by titanium dioxide.

The acquired list of phosphoprotein candidates together with several phosphorylation sites will be used in the future as a starting point for subsequent functional analyses of the selected proteins.

2 Literature survey

2.1 Angiosperm life cycle

Tobacco (*Nicotiana tabacum*) ranks among angiosperm plants (Angiospermae, Magnoliophyta). Angiosperms like other plant taxa are typical for metagenesis – the alternation of two generations differing in ploidy during the life cycle (Fig. 2.1). The adult plant represents the diploid sporophyte, and produces in its

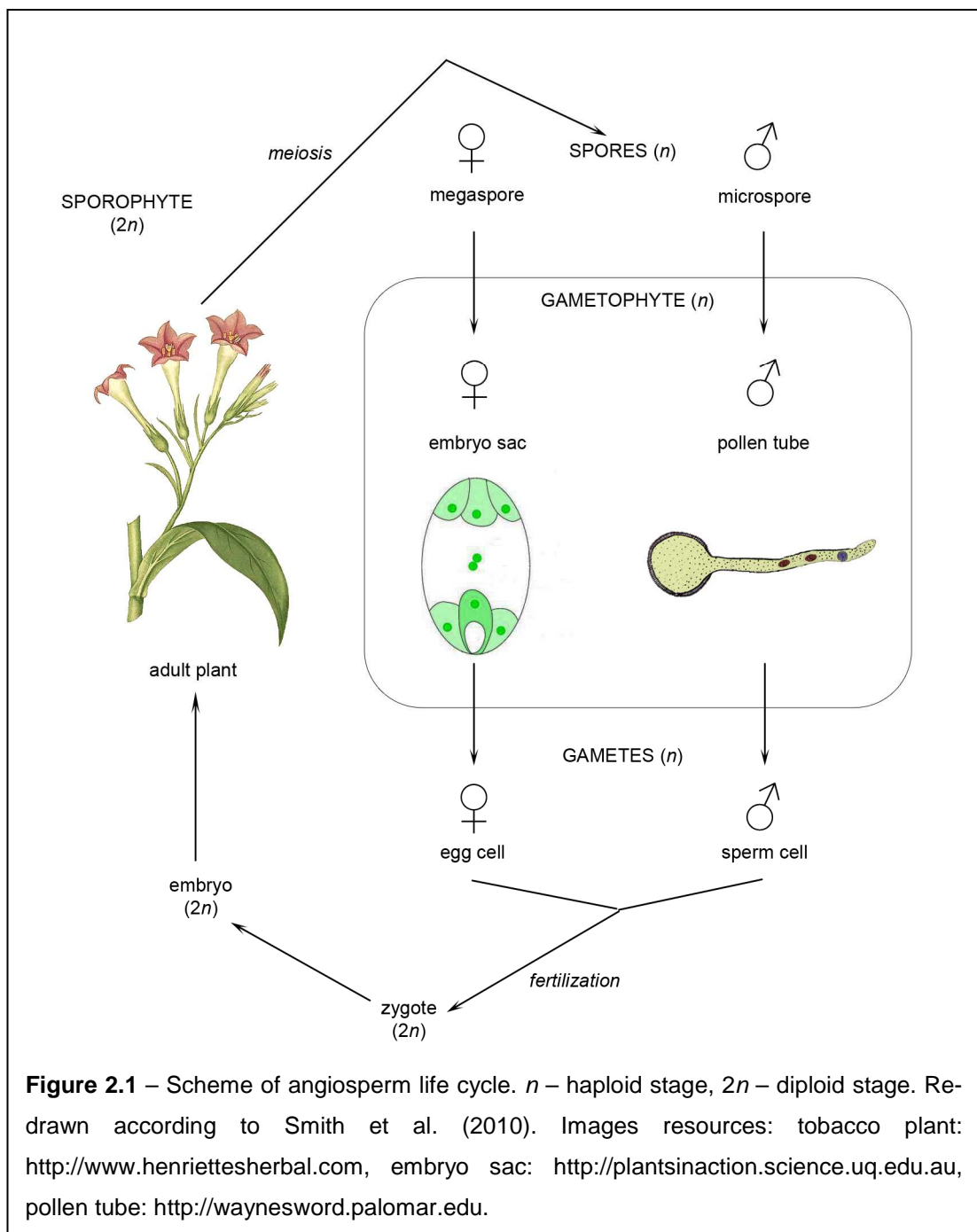


Figure 2.1 – Scheme of angiosperm life cycle. n – haploid stage, $2n$ – diploid stage. Re-drawn according to Smith et al. (2010). Images resources: tobacco plant: <http://www.henriettesherbal.com>, embryo sac: <http://plantsinaction.science.uq.edu.au>, pollen tube: <http://waynesword.palomar.edu>.

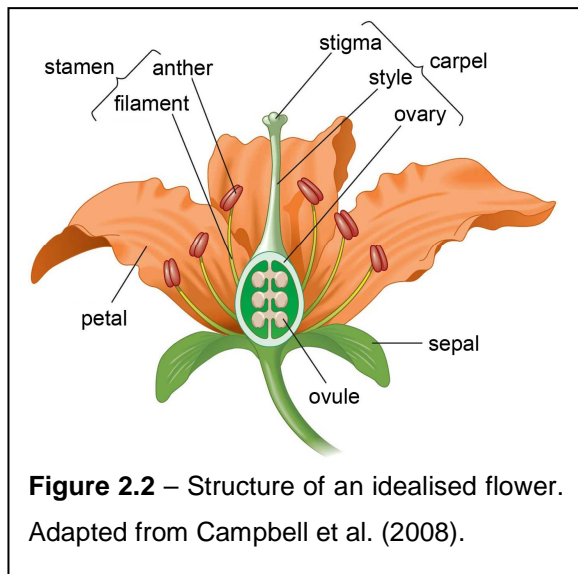
flowers haploid spores by meiosis.

The spores (being of two distinct sexes; female megaspores and male microspores) stand at the beginning of haploid gametophytic generation. Unlike the gametophyte in lower plant taxa, which is represented by a virtually independent multicellular organism, the angiosperm gametophytes are strongly reduced. Mature male gametophyte contains only three cells whereas mature female gametophyte is mostly composed of eight cells.

Inside both the male and female gametophyte, gametes are formed by mitosis. These male and female gametes fuse together giving rise to a diploid zygote, from which an embryo and subsequently adult plant emerge. The stages starting with zygote belong to the diploid sporophyte generation (Smith et al., 2010).

2.2 Male gametophyte development

Male gametophyte develops inside an anther which is a part of a flower (Fig. 2.2). The development starts with a diploid (sporophytic) archesporial cell that undergoes mitosis giving rise to pollen mother cell, and tapetal initial (McCormick, 1993; Borg et al., 2009). The pollen mother cell (called also the microsporocyte)



undergoes meiosis forming a tetrad of microspores (Fig. 2.3). These four microspores are haploid, and become separated by a mixture of enzymes containing callase that digests callose surrounding the cells.

After the microspores have been freed from the surrounding callose wall, they enlarge, and a big vacuole is formed inside each of them. Subsequently, the cells are

divided by asymmetric mitosis (called pollen mitosis I) giving rise to bi-cellular pollen. Pollen mitosis I represents a key regulatory point of male gametophyte development (Borg et al., 2009). Then, the bigger vegetative cell engulfs the smaller generative cell. After the completion of maturation processes (including cytoplasm desiccation), mature pollen grains are released into the environment. Mature pollen is in most (~70 %) plant families bicellular (including tobacco *Nicotiana tabacum* and

Solanaceae family; Brewbaker, 1967). After the pollination, the vegetative cell turns into a growing pollen tube, whereas the generative cell undergoes pollen mitosis II giving rise to two sperm cells (McCormick, 1993; Borg et al., 2009). Pollen mitosis II is thus performed only upon the start of pollen tube growth, in case of tobacco after 8–12 hours after the pollination (Tian et al., 2005; Hafidh et al., 2012b).

The remaining 30 % plant families have tricellular mature pollen (e.g. *Brassicaceae* including *Arabidopsis thaliana*). In that case, pollen mitosis II is

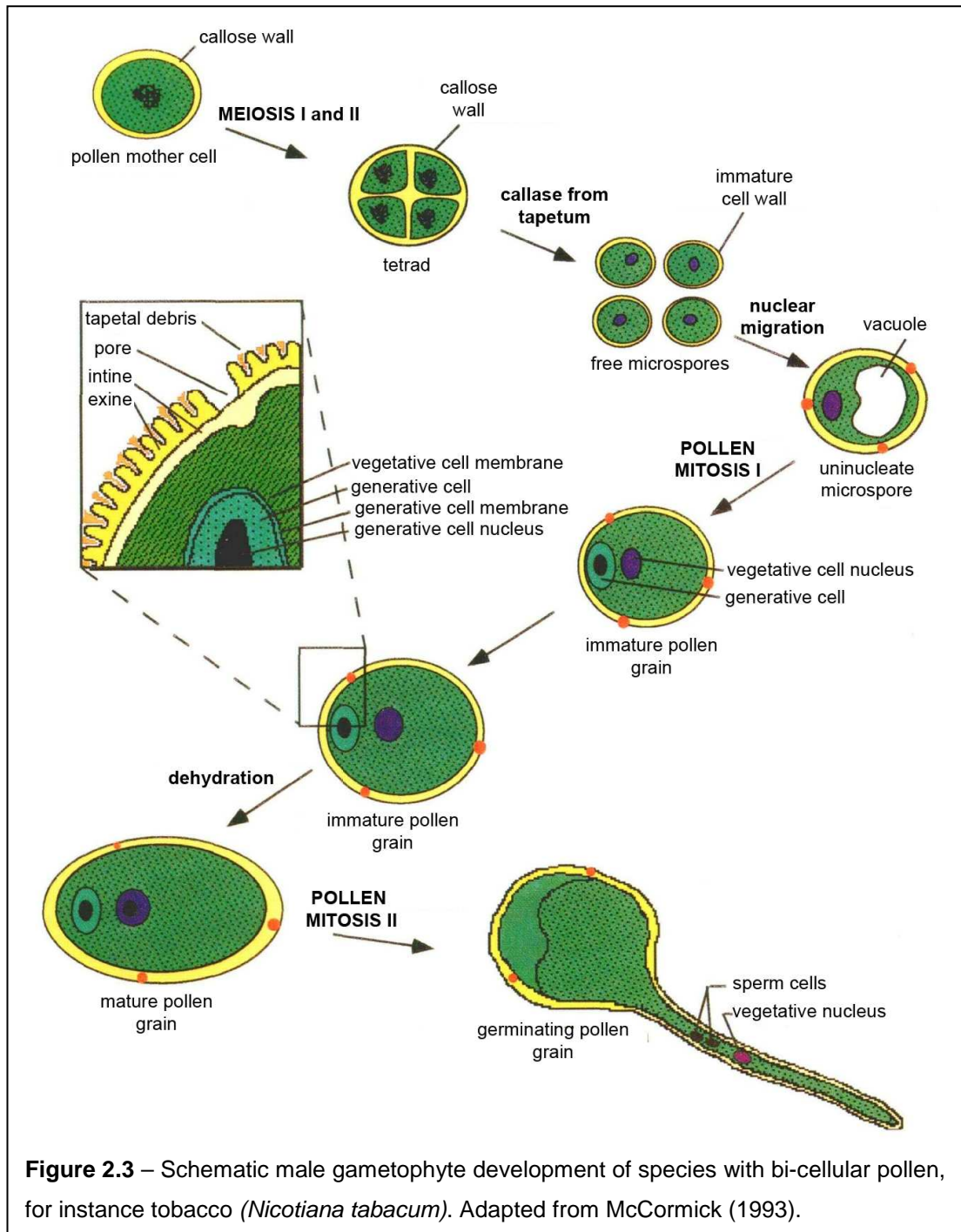


Figure 2.3 – Schematic male gametophyte development of species with bi-cellular pollen, for instance tobacco (*Nicotiana tabacum*). Adapted from McCormick (1993).

finished before the pollen grains are released. The bicellular pollen was considered as a plesiomorphic trait by Brewbaker (1967). Furthermore, it was proposed that the tricellular pollen evolved more times independently.

Both sperm cells carried to the embryo sac by a pollen tube are subsequently involved in double fertilization – the first sperm cell fuses with the egg cell giving rise to the diploid embryo, whilst the second sperm cell fuses with the central nucleus of embryo sac giving rise to the triploid endosperm.

2.3 Gene expression in mature pollen

Angiosperm mature pollen represents an extremely desiccated structure with a tough cell wall. It is metabolically quiescent since it has to be transferred in a viable state onto the stigma tissue. After pollination, it rehydrates, and subsequently the pollen tube growth starts rapidly. Desiccated mature pollen of many angiosperm species can be also rehydrated and activated *in vitro* (Mascarenhas, 1993). Even before the pollen tube emerges, the pollen vegetative cell undergoes both morphological and biochemical changes (Cresti et al., 1985; Heslop-Harrison, 1987). These biochemical changes include gradient formation essential during the pollen tube elongation (Iwano et al., 2009).

The rapid tobacco pollen tube growth was demonstrated to be largely dependent on translation but vitally independent of transcription (Čapková et al., 1988). Based on these findings, it was assumed that transcription does not occur during the pollen tube formation at all. However, the recent microarray analysis revealed that many transcripts were newly synthesised even in the growing tobacco pollen tube as long as 24 hours after germination (Hafidh et al., 2012a; 2012b).

A significant number of transcripts present in the mature pollen is stored in translationally-silent EDTA/puromycin-resistant particles (EPPs; Honys et al., 2000). These particles contain ribosomal subunits, rRNAs, mRNAs and proteins that very likely repress the transcription of present mRNAs (Honys et al., 2000; 2009). Upon pollen activation and during the pollen tube growth, the transcripts present in EPPs are being de-repressed, and translated (Honys et al., 2009). Furthermore, the EPPs are transported towards the tip of the growing pollen tube and very likely represent a transport form of the transcripts originating from mature pollen.

Such a switch between a quiescent mature pollen grain and a dynamically-growing pollen tube is very likely to be accompanied by differences in protein

phosphorylation. A similar study on *Craterostigma plantagineum*, an African xerophyte, led to the investigation of many re-hydration-related phosphoproteins (Röhrig et al., 2008). Furthermore, during preparation of this diploma thesis, the phosphoproteome of *Arabidopsis thaliana* mature pollen was published where 962 phosphopeptides present in 598 phosphoproteins were identified (Mayank et al., 2012). However, no data pertaining to activated pollen were presented in that study.

2.4 Protein phosphorylation

Phosphorylation is one of the most dynamic protein post-translational modifications. The level of protein phosphorylation is established by a huge orchestra of kinases and phosphatases (Sopory and Munshi, 1998).

Phosphorylation changes the properties of a given protein. The attached phosphate group shifts the isoelectric point (pI) of the protein to more acidic range compared to its native form. Thus, the 2D gel spot of a protein after dephosphorylation by alkaline phosphatase appeared in more basic region as documented for bovine casein (Darewicz et al., 2005).

The negative charge of the phosphate group can influence protein conformation. For instance, glycogen phosphorylase switches to the active form only upon phosphorylation (Fletterick and Sprang, 1982). Such interaction changes after the protein phosphorylation do occur not only between amino acid chains of the same polypeptide but also between more distinct polypeptide chains, thus changing the interactions between two or more proteins, as was shown for example in case of phytochrome and its partners (Kim et al., 2004), and glutamine synthetase in *Medicago truncatula* that showed an increased affinity to a 14-3-3 protein upon phosphorylation (Lima et al., 2006).

The phosphate group attached to an enzyme can influence its active site and consequently regulate its enzymatic activity. For instance, isocitrate dehydrogenase, the second enzyme of citrate cycle that converts isocitrate to α -ketoglutarate, is inhibited by phosphorylation taking place in its active site (Garnak and Reeves, 1979).

Phosphorylation plays a pivotal role in numerous cellular processes, examples of which are given below. Surely, in most of these processes also other regulatory mechanisms are known to be of key importance.

Signal transduction is mediated by cascades of kinases. One example of these signalling pathways is MAP kinase cascade (Mishra et al., 2006). Also the metabolism regulation is mediated by protein phosphorylation, for example glycolysis regulation (Plaxton, 1996). Cytoskeleton dynamics is regulated by a number of associated proteins, but protein phosphorylation is also important as shown for instance in ticklish plant (*Mimosa pudica*) where actin phosphorylation causes leaf bending (Kameyama et al., 2000). Cell cycle regulation is very important through the whole development of an organism and phosphorylation is a well established regulatory mechanism during the cell cycle (Francis and Halford, 1995). Some proteins are targeted to the cellular nucleus only after phosphorylation, for example maize Rab17 (Jensen et al., 1998), whereas others have to undergo dephosphorylation prior to their transport to the nucleus, e.g. yeast transcription factor SWI15 (Moll et al., 1991). The phosphorylation of C-terminal domain of RNA polymerase II is required for efficient transcription elongation (Baskaran et al., 1997), whereas the phosphorylation of various translation factors is essential for translation regulation (van der Kelen et al., 2009). The last but not least example of phosphorylation is its role as a marker targeting the modified species for ubiquitination and subsequent proteasome degradation (Wang et al., 2009).

2.5 Phosphorylated amino acids

Protein phosphorylation occurs mostly on serin (pS), threonine (pT), or tyrosine (pY). These amino acids bind the phosphate group by an ester bond via an oxygen atom (Fig. 2.4). The pS:pT:pY ratio in various human cell cultures was established as 78:18:3.8 (Beausoleil et al., 2004), 86.4:11.8:1.8 (Olsen et al., 2006) or 84:14:2.3 (Molina et al., 2007), depending on the cell type and protocol used.

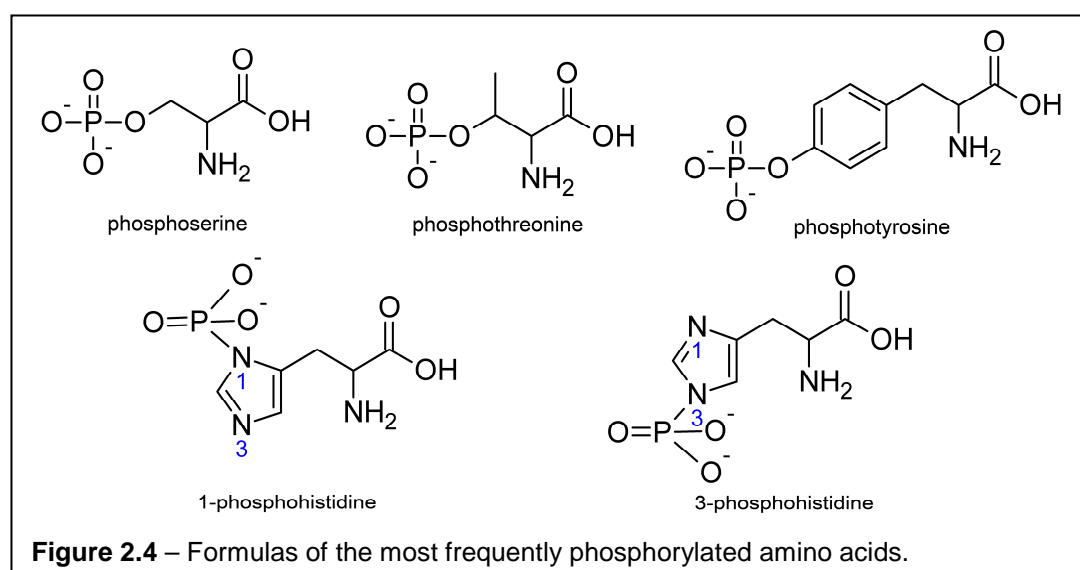
It was estimated, and afterwards experimentally shown that phosphotyrosine is less abundant in plants than in animals giving the pS:pT:pY ratio of 91.8:7.5:0.7 (van Bentem et al., 2008) and 83.81:16.18:0.01 (Benschop et al., 2007). The lower percentage of phosphotyrosine was estimated due to the lack of specific tyrosine kinases in plants. Here, tyrosine phosphorylation is thought to be carried out by dual-specificity kinases instead (Rudrabhatla et al., 2006). On the contrary, in a recent study, the proportion of the phosphoamino acids was similar to the ratio investigated in human cells, i.e. 85:10.7:4.3 (Sugiyama et al., 2008). Up to now, it remains unclear whether tyrosine phosphorylation in plants occurs really more often than

originally expected or not (reviewed in van Bentem and Hirt, 2009). In spite of the doubts about its abundance, tyrosine phosphorylation was demonstrated to play an important role in brassinosteroid signalling (Kim et al., 2009; Jaillais et al., 2011).

The conventional phosphoproteomic techniques are able to detect the *O*-phosphorylated amino acids since they are relatively stable under acidic pH which is usually applied during protein extraction and/or phosphoprotein/phosphopeptide enrichment. It was determined that the half-lives of both phosphoserine and phosphothreonine in 1 M hydrochloric acid at 100 °C were about 18 h whilst phosphotyrosine showed a half-life of about 5 h under the same conditions (Plimmer, 1941). Moreover, incubation in 1 M hydrochloric acid at 37 °C for 48 h did not result in any detectable hydrolysis of phosphoserine and phosphotyrosine and in a very subtle hydrolysis of phosphotyrosine (3.2 %; Plimmer, 1941).

The other phosphoamino acid to be found especially in bacterial and plant cells is phosphorylated histidine, to which the phosphate group is attached via a nitrogen atom (Fig. 2.4). There are two isoforms of phosphohistidine differing in the nitrogen atom in the imidazole ring to which the phosphate group is attached. These two isoforms are 1-phosphohistidine and 3-phosphohistidine, respectively, and both of them have been identified in several proteins (e.g. Wålinder, 1969a; 1969b; Spronk et al., 1976). Rarely, phosphoarginine and phospholysine can be also detected (Besant et al., 2009).

Unlike *O*-phosphorylated amino acids, both isoforms of phosphorylated histidine were unstable under the acidic pH – their half-lives in 1 M hydrochloric acid at 49 °C were 18 s for 1-phosphohistidine and 24.5 s for 3-phosphohistidine,



respectively (Hultquist, 1968). Due to the instability of both isoforms of phosphorylated histidine under the acidic pH, it was necessary to apply some of the specialised protocols in order to enable their detection (reviewed in Besant and Attwood, 2009).

Since the conventional phosphoproteomic protocols were applied in this diploma thesis, the subsequent parts of literature survey will focus exclusively on these techniques, and on the *O*-phosphorylated amino acids.

2.6 Enrichment techniques

The importance of phosphoproteins is often not reflected in their abundance since only a few per cent of cellular proteins are phosphorylated at a time in a cell. Moreover, a protein could be phosphorylated on more than one amino acid. The isoforms differing in the degree of phosphorylation could co-exist in a cell, sometimes even with the native form, which makes the identification of the phosphorylation site(s) more difficult. Some of the phosphorylation events are only temporary, which makes the detection of phosphorylated form even more complicated. Furthermore, phosphorylation is challenging also from the technical point of view since ion suppression during MS measurements could result in less efficient phosphopeptide ionization compared to their non-phosphorylated counterparts. As a result, the phosphorylated species are scarcely to be detected in a complex mixture of peptides (Marcantonio et al., 2008).

Because of these reasons, it is mostly inevitable to employ various enrichment techniques enabling the disposal of non-phosphorylated species prior to MS. In general, the enrichment can be carried out on native proteins, or on peptides arisen from the fragmentation by a specifically-cleaving agent (mostly a specific protease). Both these approaches have their advantages as well as disadvantages (reviewed in Fíla and Honys, 2011).

2.7 Comparison of phosphoprotein and phosphopeptide enrichment

Both phosphoprotein and phosphopeptide enrichment approaches start with protein extraction (Fig. 2.5). It is essential to remove nucleic acids, since their presence after the extraction would interfere with isoelectric focusing, and would decrease the enrichment specificity (Li et al., 2009). However, there are more interfering compounds that have to be removed prior to the enrichment, especially in

case of plant samples. Plant cells are surrounded by a cell wall (fragments of which would interfere with proteomic techniques), and can be filled with various secondary metabolites.

During protein extraction, it is important to keep the proteins intact and preserve their native phosphorylation pattern. Application of protease and phosphatase inhibitors is required especially when the extraction is performed in the buffers free of detergents (e.g. SDS, CHAPS), chaotropic agents (e.g. urea, guanidium chloride), and organic solvents. Furthermore, kinase activity has to be blocked in order to prevent non-biological phosphorylation. Such inhibition is important since the kinases present in the sample could overwhelm the phosphatases, resulting in an artificial phosphorylation pattern.

Phosphoprotein enrichment is usually performed on the crude protein extract immediately after the extraction. The enriched fraction of phosphoproteins is separated by either 2D-GE (Röhrig et al., 2008; Ito et al., 2009), or SDS-PAGE (Wolschin and Weckwerth, 2005; Wolschin et al., 2005). The 2D electrophoretogram usually contains a number of spots that are separated in two dimensions according to protein net charge, and molecular weight. The spots pinpointed for subsequent analysis are excised from the gel. The protein(s) inside the gel piece is/are mostly

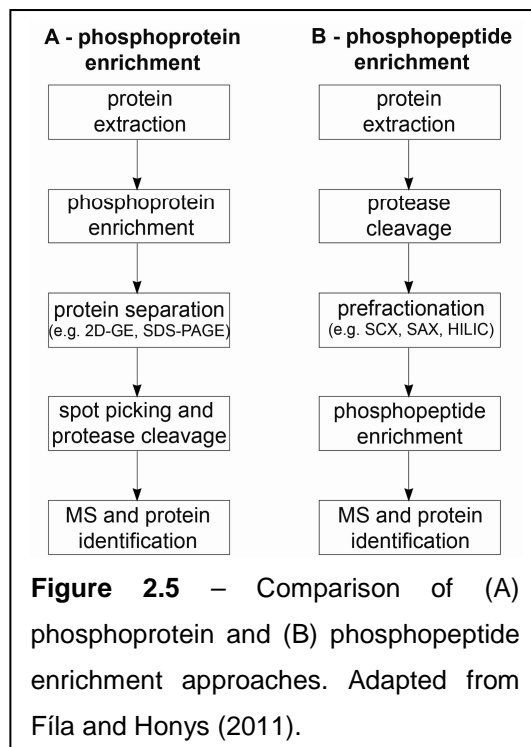


Figure 2.5 – Comparison of (A) phosphoprotein and (B) phosphopeptide enrichment approaches. Adapted from Fila and Honys (2011).

digested by a specific protease (commonly trypsin), and the obtained peptides are analysed by MS. Since this approach can show some level of non-specificity, the enriched fraction can contain some false positives. These spots would be undistinguishable from the specific ones (especially the low abundant ones). This problem can be circumvented by a parallel direct trypsinization of the enriched fraction. The acquired peptides can be separated by chromatography techniques and a second round of enrichment on the level of peptides can be performed.

The advantage of phosphoprotein enrichment is that it usually reveals molecular weight and isoelectric point of a protein. Accordingly, more isoforms of the same protein with a different molecular weight and/or isoelectric point (including the differently phosphorylated forms of the same protein) are separated as distinct spots. Furthermore, molecular weight and pI can be helpful during phosphoprotein identification – they can assist during either confirmation of the proper identification or during the rejection of less favourable identifications with a very different pI. These above advantages are related to another one – since the intact proteins are separated, the peptide spectrum for each protein(s) coming from a single excised spot is isolated from peptides that originated from other spots. The protein identification is mostly achieved according to more peptides (and not according to just one peptide as is often the case of phosphopeptide enrichment), with the assistance of native peptides (which does not occur in phosphopeptide enrichment where native species were lost during the enrichment procedure).

On the other hand, several disadvantages of phosphoprotein enrichment have to be taken into account. Firstly, some proteins are harder to resuspend (e.g. the hydrophobic ones) or impossible to separate by 2D-GE (extremely acidic or alkaline ones). Therefore, their identification is practically impossible. Furthermore, the protein losses during the procedure have to be taken into account (especially tiny and hydrophobic species). It was shown that 80 % proteins were lost during 2D-GE (Zhou et al., 2005); therefore the less abundant species are also less likely to be identified by this approach. Another disadvantage is the fact that the enrichment of intact phosphoproteins is less specific than the phosphopeptide enrichment. This is likely to be caused by the fact that protein structure is of higher complexity compared to peptide structure, and by the intactness of protein domains formed by properly folded distal chains in three-dimensional space. These structures are absent after protein cleavage into short peptides. It remains a possibility that some domain(s) could bind non-specifically even under denaturing conditions, e.g. calcium-binding domains. Finally, the phosphoprotein enrichment leads to the identification of a limited number of phosphorylation sites (Röhrig et al., 2008; Ito et al., 2009).

Phosphoprotein enrichment is beneficial especially when the most abundant proteins are studied since the low abundant species are mostly lost during the procedure. The process is also advantageous for non-sequenced organisms since the

isoelectric point and molecular weight provide valuable information for the identification. Moreover, the presence of non-phosphorylated peptides could increase sequence coverage and so increase the probability of finding a homological sequence in the database. Last but not least, it can be used as a first round of enrichment (as a pre-fractionation technique) followed by a phosphopeptide enrichment of the digested phosphoprotein-enriched sample.

As stated above, also the **phosphopeptide enrichment** starts with protein extraction. The total extract from a given tissue is usually highly complex, so multistep protein extraction resulting in more proteome fractions is advantageous, for instance three-fraction protein extraction that was successfully applied for *Arabidopsis thaliana* pollen (Holmes-Davis et al., 2005). The first extraction applied a Tris buffer in order to acquire the soluble proteins whereas the insoluble pellet was re-extracted with denaturing buffer containing urea and CHAPS. The parallel extraction (by which the third fraction composed of wall proteins was acquired) relied on a denaturing buffer with SDS. The extracted proteins are immediately fragmented by a specific protease (commonly trypsin). Since the total protein sample is usually very complex, the pre-fractionation techniques are usually required. The most common ones are SAX (strong anionic ion-exchange chromatography; Nühse et al., 2004), SCX (strong cationic ion-exchange chromatography; Beausoleil et al., 2004) and HILIC (hydrophilic interaction liquid chromatography; McNulty and Annan, 2008). An alternative approach relies on gel separation of intact proteins and subsequent work with excised bands or larger gel areas (Carrascal et al., 2008). The peptide mixture is then enriched for phosphopeptides and the enriched fraction is finally MS-analysed.

The most obvious advantage is that peptides represent less complex three-dimensional structures compared to intact proteins, and in general, are more easily to be fractionated by various chromatography techniques. These techniques are usually more sensitive than 2D-GE, making the identification of less abundant peptides feasible. Another advantage is that tiny, hydrophobic and extremely alkaline or acidic proteins are not handicapped by this approach as is the case of 2D-GE. Up to date, more experiments were performed by these techniques; this is another advantage since it is likely that the protocols applied were optimised to a higher extent. Finally, it is considered advantageous that the exact phosphorylation sites are usually identified.

The enriched fraction contains a mixture of phosphopeptides originating from a number of phosphoproteins, thus it is hard to distinguish the protein(s) from which the peptides originated. This fact can be considered disadvantageous since it represents a limitation during protein identification. Furthermore, the non-phosphorylated peptides cannot contribute to the phosphoprotein identification since they were excluded during the enrichment step. Consequently, protein identification often relies on a single phosphopeptide. Proteins containing a conserved wide-spread domain(s) could be confused with each other making the correct identification almost impossible. Another disadvantage is represented by the fact that the molecular weight and pI of a protein are not detected during this approach. In spite of the various improvements increasing selectivity of the enrichment protocols, the non-specificity issue represents still a limitation of several of these enriching strategies.

Phosphopeptide enrichment is useful when a less complex sample is analysed, e.g. mitochondrial phosphoproteome (Ito et al., 2009). Phosphopeptide enrichment is also more easily to be automated so it is very useful for high-throughput experiments (Bodenmiller et al., 2007; Han et al., 2008; Reiland et al., 2009). Last but not least, phosphopeptide enrichment is ideal for the identification of particular phosphorylation site(s).

It is impossible to consider one single enrichment method as optimal, and the others as suboptimal. Each enrichment method has its advantages and disadvantages, and its usefulness and optimality could vary according to the experimental material used. Furthermore, the enrichment methods have a complementary rather than an overlapping nature, so a reasonable coverage of phosphoproteome could be achieved only by a combination of enrichment techniques (Bodenmiller et al., 2007; Ito et al., 2009).

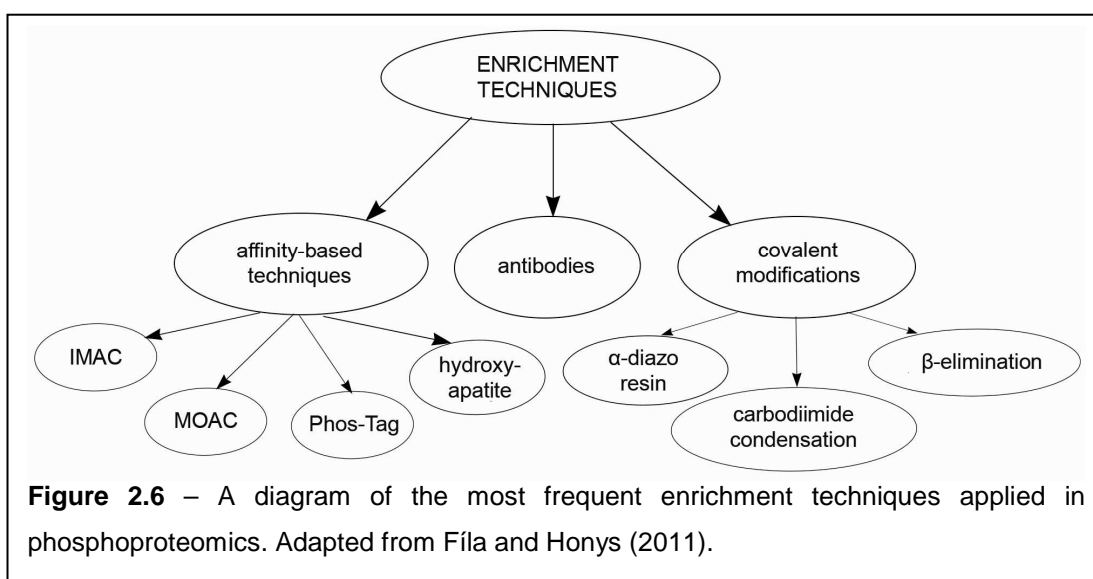
2.8 Principles of enriching protocols

The enrichment strategies rely on three basic principles (Fig. 2.6). The first one applies antibodies targeted against a given phosphorylated amino acid. This is mostly applicable for phosphotyrosine enrichment on both phosphoprotein and phosphopeptide level (Imam-Sghiouar et al., 2002; Rush et al., 2005) since anti-pY antibodies show a reasonable specificity towards their epitope. On the other hand, many antibodies raised against phosphoserine and phosphothreonine were not working properly during immunoprecipitation and/or showed specificity to the

surrounding amino acids and not exclusively to the given phosphoamino acid (Grønberg et al., 2002).

The second principle of phospho-enrichment relies on the fact that the phosphate group has a negative charge under acidic pH. Various methods apply positively-charged matrices in order to catch the phosphopeptides/proteins. IMAC (immobilised metal ion affinity chromatography) applies resin-bound metal ions (Andersson and Porath, 1986), whereas MOAC (metal oxide/hydroxide affinity chromatography) relies on a matrix composed of metal oxides themselves so metal anchoring is not needed. The MOAC matrices used were mostly aluminium hydroxide in case of phosphoprotein enrichment (Wolschin et al., 2005), and titanium dioxide (Sano and Nakamura, 2004) or zirconium dioxide (Kweon and Håkansson, 2006) in case of phosphopeptide enrichment. Rather less frequently applied affinity techniques are represented by Phos-Tag affinity chromatography (Kinoshita et al., 2005), affinity chromatography with hydroxyapatite matrix (Addeo et al., 1977; Mamone et al., 2010), and polymer-based metal ion affinity capture (PolyMAC; Iliuk et al., 2010).

The third set of phosphoprotein/phosphopeptide enrichment strategies relies on chemical modification of the phosphate group and its subsequent affinity capture via the modified residue. The techniques used were for instance β -elimination coupled with Michael addition (Oda et al., 2001), carbodiimide condensation (Zhou et al., 2001), α -diazo resin enrichment (Lansdell and Tepe, 2004), and oxidation–reduction condensation (Warthaka et al., 2006).



2.9 $Al(OH)_3$ -MOAC phosphoprotein enrichment

One of the best established phosphoprotein-enriching techniques is MOAC with aluminium hydroxide matrix (Wolschin et al., 2005). The general positives and limitations of phosphoprotein enrichment were discussed above. MOAC protocol was shown to be either of a better efficiency than any of the tested commercial kits for phosphoprotein enrichment (Wolschin et al., 2005) or at least of a comparable efficiency (Ito et al., 2009). It is noteworthy that in case of tobacco, it was advantageous to acquire the pI and molecular weight of a protein since the tobacco genome is not wholly available in the public databases and therefore these values represent valuable information about the detected proteins. Another advantage of the method is that it was successfully applied for plant samples – *Arabidopsis thaliana* leaves (Wolschin et al., 2005), *Arabidopsis thaliana* seeds, *Chlamydomonas reinhardtii* cells (Wolschin and Weckwerth, 2005), and *Craterostigma plantagineum* leaves (Röhrig et al., 2008).

The main doubts aroused about the method's specificity. The buffer composition should reduce non-specific binding since urea together with CHAPS denatures proteins. This should improve method specificity since the possibly non-specifically binding domains should be denatured and their non-specific binding reduced (Wolschin et al., 2005). However, the native conditions might be also worth applying since TiO_2 phosphoprotein enrichment under native and denaturing conditions resulted in different spectra of enriched phosphoproteins (Lenman et al., 2008). Imidazole in the incubation buffer mimicked histidine and thus competed with non-specifically binding histidine-rich proteins. The salts of acidic amino acids (glutamic and aspartic acid) competed with non-specific proteins binding via acidic amino acids, and thus the enrichment specificity was increased.

The specificity of MOAC with aluminium hydroxide matrix was tested several times. In the original study, a mixture of eight standard proteins, some of which were phosphorylated whilst others were un-phosphorylated, was enriched. The phosphorylated proteins appeared exclusively in the phosphoprotein-enriched fraction whilst the non-phosphorylated ones remained un-bound to the matrix and ended up in the flow-through (Wolschin et al., 2005). However, eight selected standard proteins could not cover the whole variability and complexity of proteome. Thus, the non-specific binding of some proteins remained possible.

Another sign of MOAC specificity was obtained by μ LC–ICP-MS where a higher phosphate-to-sulphur ratio was observed in the enriched fraction compared to the original crude extract (Krüger et al., 2007). These results strengthened the grounds for believing in the method's specificity but they did not show whether any of the proteins in the enriched fraction were false positives. Another proof of MOAC specificity was shown by Röhrig et al. (2008). The MOAC-enriched fraction was dephosphorylated by alkaline phosphatase and the dephosphorylated sample showed a lower signal when stained with phosphoprotein-specific ProQ Diamond Phosphoprotein Gel stain. However, after dephosphorylation, there remained a background signal, coming either from non-specific staining since ProQ Diamond shows quite high intensity of background (Steinberg et al., 2003), or from the incompleteness of dephosphorylation reaction. Alkaline phosphatase shows substrate specificity, and consequently could dephosphorylate some of the sites slower and/or less efficiently (Morton, 1955). Collectively, all the above data show that MOAC is likely to be (at least partially) specific but it is hard to deduce how much proteins in the enriched fraction should be regarded as false positives. The other negative of the method is that (like other phosphoprotein-enriching methods) it results in the identification of only a limited number of phosphorylation sites.

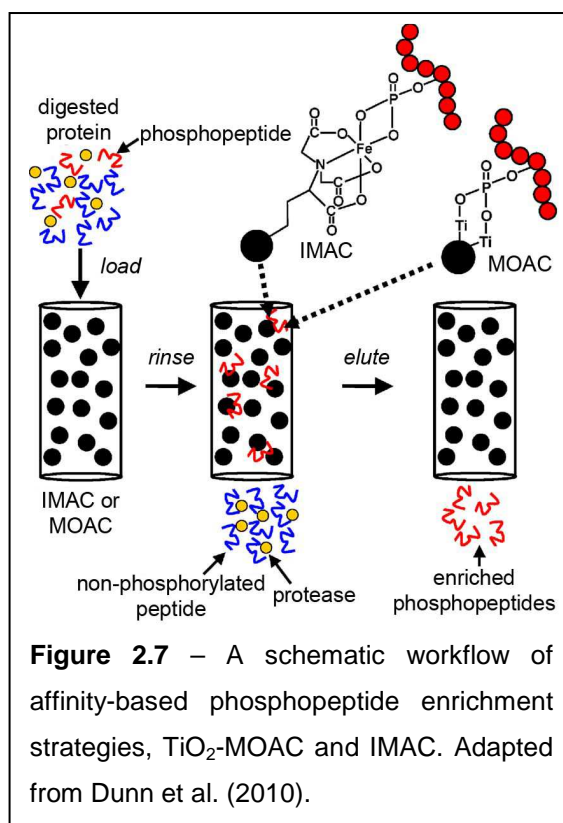
2.10 TiO₂ phosphopeptide enrichment

In order to find more phosphorylation sites, the parallel phosphopeptide enrichment is very beneficial when applying phosphoprotein-enriching protocol. One of the widely used techniques is TiO₂-MOAC (Pinkse et al., 2004). It is a widely-used technique that was mostly shown to be more specific (Larsen et al., 2005; Kweon and Håkansson, 2006; Aryal and Ross, 2010) or more sensitive (Hsieh et al., 2007) than IMAC.

The peptide mixture is usually incubated with TiO₂ beads in an acidic incubation buffer of pH round 2.5–3 (Fig. 2.7). The principle of the highest specificity under this pH is based on a different acid dissociation constant (pK_a) of acidic amino acids (glutamic and aspartic acid), and phosphate residue. The phosphate group has a pK_a of 2.1, whereas glutamic and aspartic acid 3.65 or 4.25, respectively (Kokubu et al., 2005). These specific values are valid for the free residues; if being part of a protein, the pK_a could be more or less shifted. If the pH of the loading buffer is between the pK_a values of phosphate residue and acidic amino

acids, most acidic amino acids will be protonated whereas most of the phosphate moieties will be charged. Consequently, phosphate residues exhibiting their negative charge can bind to the chromatography matrix whilst the catching of the non-specific acidic amino acids is strongly inhibited since their negative charge is masked by the bound protons. However, it is worth mentioning that a complete protonation of acidic amino acid residues could be achieved only under highly acidic pH (pH < 1–1.5). On the other hand, pH > 3 enabled a complete de-protonation of phosphate groups. It is obvious that the pH of the incubation buffer (2.5–3) is rather a compromise between the highest specificity and the highest selectivity.

Since the pH itself did not block non-specific interactions, various chemicals were added in order to reduce the method's non-specificity. The best results were obtained with dihydroxybenzoic acid (DHB), salicylic acid and phthalic acid (Larsen et al., 2005). Although DHB was in many studies applied by itself (Larsen et al., 2005; Hsieh et al., 2007) or in a combination with octanesulphonic acid (Mazanek et al., 2010), it was less efficient in others (Simon et al., 2008; Aryal and Ross, 2010). Several alternatives blocking non-specificity were successfully tested, for instance lactic acid (Sugiyama et al., 2007; Wu et al., 2007).



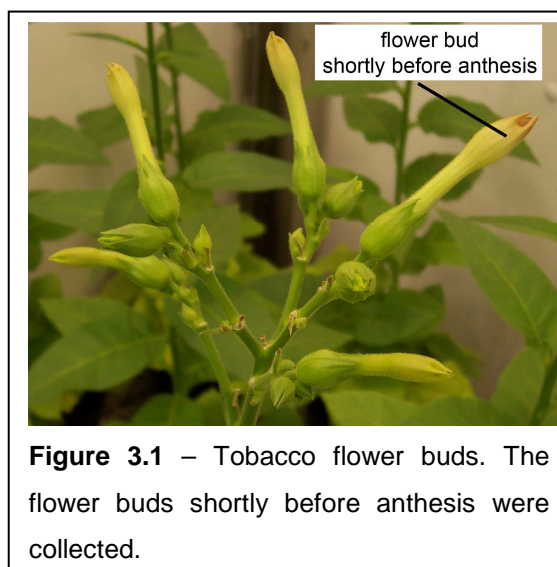
3 Materials and methods

3.1 Plant material and pollen tube activation

Tobacco plants (*Nicotiana tabacum* cv. Samsun) were grown in a growth chamber. The conditions were as follows: photoperiod 16 h/8 h (light/darkness), constant temperature 20 °C and relative humidity of 50 %.

The pollen grains were obtained according to Petru et al. (1964) with modifications. Flower buds were collected shortly before anthesis (Fig. 3.1), and the anthers were excised. They were let to dehisce overnight at room temperature. The pollen grains were sieved and stored at -20 °C. The collected pollen grains represented a bulk sample from some 30 plants.

The pollen grain activation was performed as described by Tupý and Říhová (1984). Mature pollen grains were incubated at room temperature for 10 min and then shaken as a



suspension of 10 mg pollen per 10 ml sucrose-mineral medium buffered with MES (SMM-MES; 175 mM sucrose, 1.6 mM boric acid, 3 mM $\text{Ca}(\text{NO}_3)_2 \cdot 4\text{H}_2\text{O}$, 0.8 mM $\text{MgSO}_4 \cdot \text{H}_2\text{O}$, 1 mM KNO_3 , 25 mM MES, pH 5.9). This medium is used not only for pollen activation but also for *in vitro* pollen cultivation for a longer time.

3.2 Protein extraction

Total protein was extracted from mature and activated pollen using trichloroacetic acid (TCA) / acetone (Méchin et al., 2006). The mature pollen or activated pollen, respectively, was homogenised by a pestle in a mortar and re-suspended in ten-fold volume of 10 % w/v TCA / acetone supplemented with 0.07 % v/v 2-mercaptoethanol (ME). After five-minute incubation in a ultrasonic bath, the samples were frozen in liquid nitrogen for ~20 s and kept at -20 °C for 5 min. Afterwards, the sample was mixed briefly and further incubated at -20 °C for another 5 min. The previous step was repeated twice and then the sample was

incubated for 30 min at $-20\text{ }^{\circ}\text{C}$. So in total, it was kept at $-20\text{ }^{\circ}\text{C}$ for 45 min. Subsequently, the sample was centrifuged ($23,000\times g$, 15 min, $4\text{ }^{\circ}\text{C}$).

The supernatant was discarded and the pellet containing the extracted proteins was washed with acetone supplemented with 0.07 % v/v ME, incubated for 5 min in a ultrasonic bath, cooled down in liquid nitrogen for ~ 20 s and incubated for 30 min at $-20\text{ }^{\circ}\text{C}$. After centrifugation under the above conditions, the washing step was repeated. Finally, the protein extract was dried in Concentrator Plus 5301 (Eppendorf, Hamburg, Germany) for 15 min and stored at $-20\text{ }^{\circ}\text{C}$.

3.3 MOAC phosphoprotein enrichment

TCA/acetone extract from both mature pollen and 30-minute activated pollen (1 mg per 50 μl) was resuspended in MOAC incubation buffer (30 mM MES, 20 mM imidazole, 0.2 M potassium aspartate, 0.2 M sodium glutamate, 8 M urea, 2.5 % w/v CHAPS, phosphatase inhibitors cocktail 1 – Sigma-Aldrich, cat. no. P2850, pH 6.1; Wolschin et al., 2005). The resuspended protein sample was sonicated for 5 min in a bath, and incubated at $37\text{ }^{\circ}\text{C}$ for 1 h with gentle agitation. Afterwards, the sample was centrifuged ($23,000\times g$, 15 min, $22\text{ }^{\circ}\text{C}$), and the supernatant (containing proteins) was transferred to a fresh tube. The pellet was discarded.

The protein concentration was estimated by a 2D Quant Kit (GE Healthcare, Uppsala, Sweden) according to manufacturer's instructions as follows. BSA and a blank sample were used to create a standard curve. To each standard and pollen protein sample, 500 μl Precipitant was added; the sample was vortexed and incubated for 3 min at room temperature. Then, 500 μl Co-precipitant was added; the sample was mixed and centrifuged ($23,000\times g$, 15 min, $22\text{ }^{\circ}\text{C}$). The supernatant was decanted and the pellet was resuspended in 100 μl Copper Solution and 400 μl distilled water. These re-suspended samples were mixed with 1 ml Color Reagent (spiked together 100 parts Color Reagent A together with 1 part Color Reagent B). After 20 min incubation, the samples' absorbance at 480 nm was measured by a spectrophotometer using distilled water as a reference.

A 2 mg protein sample dissolved in 3 ml MOAC incubation buffer was incubated in the presence of 160 mg aluminium hydroxide for 30 min, centrifuged ($10,400\times g$, 2 min, $4\text{ }^{\circ}\text{C}$), and the supernatant then repeatedly washed with 3.2 ml (washes 1–5) or 1.6 ml (wash 6) incubation buffer. Each washing step comprised a 1 min period of agitation, followed by centrifugation as above. Phosphoproteins were

eluted by addition of 1.6 ml elution buffer (100 mM K₂HPO₄, 8 M urea, phosphatase inhibitors cocktail 1, pH 9.0), and separated from the matrix by centrifugation under the same conditions. The MOAC enrichment was repeated at least two times for each stage from an independent TCA/acetone protein extract for both the mature and the 30-minute activated pollen.

3.4 1D SDS-PAGE of MOAC fractions

The proteins present in the MOAC fractions (namely phosphoprotein-enriched eluate, flow-through and supernatant after the first wash) together with protein crude extract were precipitated by methanol and chloroform according to Wessel and Flügge (1984). An aliquot of these samples was mixed with a 2-fold volume of methanol and thoroughly mixed. One volume of chloroform was added, and then the sample was thoroughly mixed and incubated on ice for 5 min. Afterwards, 1.5 volume distilled water was added, and the sample was centrifuged (9,000× *g*, 2 min, 4 °C). The aqueous phase was discarded and 0.75 volume methanol was added to the lower phase and this mixture was incubated on ice for 5 min. After the centrifugation (23,000× *g*, 5 min, 4 °C), the supernatant was discarded and the pellet dried in Concentrator Plus 5301 (Eppendorf, Hamburg, Germany) for 15 min.

The dried pellet was resuspended in 1D sample buffer (50 mM Tris-HCl, 10 % v/v glycerol, 2 % w/v SDS, 5 % v/v ME, 0.01 % w/v bromophenol blue). Approx. 5 µg aliquot was loaded onto an SDS-PAGE gel (stacking gel 5 %T, 2.6 %C, resolving 11.25 %T, 2.6 %C). The buffers were prepared according to Laemmli (1970) and the electrophoresis was performed on the MiniProtean system (Bio-rad, Hercules, CA, USA) at 75 V for 30 min followed by 150 V until the bromophenol blue front line reached the bottom of the gel (~45 min). SDS-PAGE standard broad range marker (Bio-rad, Hercules, CA, USA) was run in order to estimate the molecular weight of the sample proteins.

The gels were stained by phosphoprotein-specific ProQ Diamond Phosphoprotein Gel Stain (Molecular Probes, Eugene, OR, USA) according to Agrawal and Thelen (2005) with slight modifications. Briefly, the gel was incubated in fixation solution (50 % v/v methanol, 10 % v/v acetic acid) for 30 min. The buffer was exchanged for a fresh one, and the gel was incubated overnight at 4 °C. Then, it was washed six times in distilled water (resistance 18 MΩ) for 15 min. The staining

was performed in 30 ml 3× water-diluted ProQ Diamond Phosphoprotein Gel Stain. The gel was protected from light by wrapping the box in an aluminium foil. The gels were de-stained in de-staining solution (20 % v/v acetonitrile, 1 M sodium acetate pH 4.0) for 30 min. The buffer was exchanged and the de-staining step was repeated 3 times. Before scanning, the gel was submerged into distilled water for 5 min in order to become hydrated. The signal was scanned by Fuji FLA 7000 (Fujifilm, Tokyo, Japan) with 532 nm excitation laser and 580 nm emission filter.

After the ProQ signal was scanned, the gel was stained for total proteins with CBB G250 according to Kang et al. (2002). First, it was washed in distilled water for 10 min. Then, the staining was carried out for 1 hour in CBB G250 solution (0.02 % w/v CBB G250, 5 % w/v aluminium sulphate-(14-18)-hydrate, 2 % v/v ortho-phosphoric acid). The de-staining was accomplished in de-staining solution (10 % v/v ethanol, 2 % v/v ortho-phosphoric acid) within 1 hour. Subsequently, the gel was hydrated in distilled water, and scanned by G-Box CCD camera (Syngene, Frederick, MD, USA).

3.5 Phosphorylation in vitro

Both mature and 30-minute activated pollen was homogenised in extraction buffer (50 mM Tris-Cl pH 7.6, 75 mM sucrose, 5 mM ME) and centrifuged twice (500× g, 10 min, 4 °C, followed by 37,000× g; 30 min; 4 °C) to obtain the microsomal fraction, and the protein concentration was estimated by amidoblack employing BSA as a standard (Schaffner and Weissman, 1973). Aliquots of BSA and protein samples were dropped onto nitrocellulose membrane (Serva, Heidelberg, Germany). The nitrocellulose with the dried droplets was incubated in staining solution (45 % v/v methanol, 10 % v/v acetic acid, 0.1 % w/v amido black) for 5 min. After the 5-minute de-staining performed in de-staining solution (90 % v/v methanol, 2 % v/v acetic acid), the protein concentration in the sample was estimated according to signal intensity.

A phosphorylation reaction containing 50 µg proteins was performed in 50 mM Tris-Cl (pH 7.6), 10 mM potassium acetate, 1 mM magnesium acetate, 0.5 MBq γ -³²P-ATP (PerkinElmer, Waltham, MA, USA, cat. no. BLU002H500UC), 1 µM ATP at 28 °C for either 2, 5 or 15 min. The reaction was terminated by the addition of 20 % w/v TCA/acetone, and kept for 1 h at -20 °C. After centrifugation (23,000× g, 15 min, 4 °C), the pellet was washed with acetone and re-centrifuged

(23,000× g, 10 min, 4 °C). Two further washes with 80 % v/v acetone were given. The final pellet was resuspended in 30 µl 1D sample buffer (see above) and a 50 % aliquot (~25 µg proteins) was separated by SDS-PAGE (11.25 %T, 2.6 %C resolving gel) on Biometra Multigel Long apparatus (Whatman Biometra, Göttingen, Germany), as described above. The gels were stained with CBB G250 and scanned as above. After scanning, the gels were dried with gel drier D61 (Biometra, Göttingen, Germany) for 45 min and exposed overnight to a BAS-MS 2025 imaging plate (Fujifilm, Tokyo, Japan) that was scanned with a Fuji FLA 7000 (Fujifilm, Tokyo, Japan).

3.6 2D-GE and image analysis

Isoelectric focusing (IEF) was performed on 13 cm linear strips of pI 4–7 on Ettan IPGphor (GE Healthcare/Amersham Biosciences, Uppsala, Sweden). This pI range was chosen because phosphorylation is known to lower the pI of a protein (Darewicz et al., 2005). Moreover, in the preliminary experiment, the majority of spots was observed in this pI range. Fifty micrograms of both eluate and crude extract were focused under the following conditions: 14 h passive rehydration; 1 h gradient to 250 V; 1 h gradient to 500 V; 1 h gradient to 4,000 V; 5 h 35 min 4,000 V; 50 µA per strip (Witzel et al., 2007). In total, 25 kWh was reached during the IEF run.

The focused strips were equilibrated for 15 min in solution 1 (50 mM Tris-HCl pH 8.8, 6 M urea, 30 % v/v glycerol, 2 % w/v SDS, 130 mM DTT, 0.01 % w/v bromophenol blue) followed by 15 min in solution 2 (the same contents, only DTT was replaced with 135 mM iodoacetamide). The equilibrated strip was embedded onto a stacking gel by 1 % w/v agarose in SDS-PAGE electrode buffer (25 mM Tris, 192 mM glycine, 0.1 % w/v SDS, 0.005 % w/v bromophenol blue). The resolving gel was 10 %T, 2.6 %C, whilst the stacking gel was 5 %T, 2.6 %C, and the buffers were prepared according to Laemmli (1970). The run was performed on Hoefer SE600 (GE Healthcare/Amersham Biosciences, Uppsala, Sweden) at 75 V for 30 min, followed by ~4.5 h at 150 V. Molecular weights of the protein sample were estimated according to the PageRuler Prestained Protein Ladder (Fermentas, St. Leon-Rot, Germany).

The gels were stained with ruthenium II tris (bathophenanthroline disulphonate) – RuBP. The RuBP compound was synthesised according to Rabilloud

et al. (2001), and the staining procedure was performed according to Lamanda et al. (2004). First, the gel was washed for 10 min in distilled water. After overnight fixation in 200 ml fixation solution (30 % v/v ethanol, 10 % v/v acetic acid) at 4 °C, the gel was washed four times for 30 min in 20 % v/v ethanol. The staining was performed for 6 h at 4 °C by 1 µM RuBP in 20 % v/v ethanol. Upon this step until scanning, the gels were protected from light by wrapping the boxes in an aluminium foil. Two 10-minute washes in distilled water were followed by overnight de-staining in 40 % v/v ethanol / 10 % v/v acetic acid. Before scanning, the gel was swelled in distilled water. The gel was imaged by Fuji FLA 5100 (Fujifilm, Tokyo, Japan) with 473 nm excitation laser and 580 nm emission filter. To aid the precision for spot cutting, the gel was stained overnight with CBB G250 as written above; only de-staining was performed in distilled water instead of de-staining solution.

At least two independent extracts were prepared from the sample of both mature pollen, and activated pollen to generate a set of replicates. In total, there were four gels for each stage. Image analysis of the 2D gels was performed using a PDQuest Advanced 8.0.1 software (Bio-rad, Hercules, USA). The master gel was selected automatically by the software. Faint spot, small spot and largest spot cluster were chosen manually by clicking the desired spots. Normalised spot volume was expressed as a proportion to the sum of all spots present on a given gel. The spots that differed significantly 2-fold in intensity between the two stages under investigation (t-test: $p < 0.05$) were selected for subsequent analyses.

3.7 Trypsin digest and MS/MS analysis of the spots

All spots were excised from each of two selected replicate gels from the mature pollen sample, but only those which varied in intensity by at least twofold between the mature and the 30-minute activated pollen were excised from the activated pollen sample.

After the excision, the gel fragments were washed in 400 µl 10 mM ammonium bicarbonate (ABC) / 10 % v/v acetonitrile (ACN) for 30 min and dried. The proteins within the gel fragment were digested in 7.5 µl 10 ng·µl⁻¹ porcine trypsin solution (Sequencing Grade Modified Trypsin V511, Promega; Madison, WI, USA) in 5 mM ABC / 5 % v/v ACN for 5 h at 37 °C. The digest was terminated by the addition of 1 µl 1 % v/v trifluoroacetic acid (TFA).

A 5 μl aliquot of the tryptic digest was used for nLC–ESI–Q/TOF analysis and *de novo* sequencing (Witzel et al., 2007). The peptides were separated on a 180 $\mu\text{m} \times 20 \text{ mm}$ Symmetry (5 μm) C18 pre-column coupled to a 100 $\text{mm} \times 100 \mu\text{m}$ BEH (1.7 μm) C18 column (Waters Corporation, Manchester, UK) at 0.6 $\mu\text{l}\cdot\text{min}^{-1}$ under a 3–35 % v/v ACN gradient over 30 min at a column temperature of 40 °C. Mobile phase A consisted of 0.1 % v/v formic acid in water and mobile phase B of 0.1 % v/v formic acid in ACN. The mass spectrometer (Q–TOF Premier, MassLynx 4.1 software, Waters) operated in a positive ion V-mode, and the mass spectra acquired were integrated over 1 s intervals. The instrument was calibrated using Glu-Fibrinopeptide B (Sigma-Aldrich Chemie, Taufkirchen, Germany). Automatic data directed analysis was employed for MS/MS analysis on doubly- and triply-charged precursor ions. Mass spectra were collected from m/z 400–1600, and product ion MS/MS spectra were collected from m/z 50–1600. Lock mass correction of the precursor and the product ions was conducted using Glu-Fibrinopeptide B. ProteinLynx GlobalSERVER v2.3 (PLGS) software was used for data processing and database searches (Witzel et al., 2007).

The MS/MS spectra searches were conducted against the protein index of the non-redundant SwissProt database (2010/07/26), against the UniProtKB index for Viridiplantae (2010/07/26) complemented with human keratin, porcine trypsin, and yeast enolase sequences, and against the TIGR EST sequence database entries for *Solanaceae* (2010/08). The search parameters set were 10 ppm peptide, 0.1 Da fragment tolerance, one missed cleavage, and variable oxidation (Met) and carbamidomethylation (Cys). Protein identifications were accepted when at least two peptide fragments per protein were identified, and a probability score of higher than 90 % was obtained (PLGS score > 12), although in some cases a PLGS score < 12 was accepted; this occurred for proteins related to redundant entries in the database. The protein functions were assigned according to Bevan et al. (1998). Proteins falling into more than one category were assigned their prevailing activity.

3.8 In solution trypsin digest and gel-free nLC–MS/MS

A 400 μl eluate of both mature and activated pollen was precipitated by methanol/chloroform according to Wessel and Flügge (1984), and the dried pellet was re-suspended in 0.1 % w/v RapiGest (Waters, Milford, MA, USA) / 50 mM ABC. The concentration of protein present was estimated by Bradford Assay (Bio-

Rad, Hercules, CA, USA). In solution digest and MS analysis were performed as described in Kaspar et al. (2010) with minor modifications. A 30 μl sample containing 30 μg proteins was reduced by DTT and alkylated by iodoacetamide, and then incubated overnight at 37 °C with 600 ng porcine trypsin. The reaction was terminated and the detergent precipitated by lowering the pH to 2.0. After centrifugation (23,000 \times g, 30 min, 4 °C), the samples were diluted to 0.1 $\mu\text{g}\cdot\mu\text{l}^{-1}$ protein, and spiked with 100 nM pre-digested enolase (Waters, Milford, MA, USA), serving as an internal standard. A 3 μl aliquot containing an estimated 0.3 μg protein was subjected to a 90 min LC separation, with four technical replicate nLC–MS runs per sample. The same columns, solvent gradient and solvents A and B as described above were employed, as were both instrument calibration and lock mass correction. The nLC–MS data were collected in alternating high and low energy acquisition mode (multiplexed nLC–MS data processing) using MassLynx 4.1 software (Waters). The low energy mode provided accurate mass and quantitative data at the peptide level, and the high energy mode provided multiplexed MS fragmentation data from all co-eluting peptides. The spectrum acquisition time in each mode was 1 s with a 0.02 s interscan delay. In low energy mode, the constant collision energy of 4 eV was used, while in high energy mode, the collision energy was ramped from 10 to 28 eV during each 1 s data collection cycle.

For the purpose of quantification, the multiplexed nLC–MS data were processed (ion detection, accurate mass retention time pair clustering, normalization, quantification and statistical analysis) using Progenesis LC–MS v3.1 software. For sample alignment, the sensitivity was set automatically to 4. Filtering proceeded as follows: (1) at least one isotope needed to be detected, (2) both charge states 2 and 3 were included, and (3) the retention time window was set as 12–90 min. Normalization was applied automatically to all features as recommended by the Progenesis LC–MS software manual. Peptide identification was performed using the Identity Algorithm implemented in PLGS 2.3 software, by searching against the UniProt reference database (<http://www.uniprot.org/uniref>), consisting of manually assembled entries of *Arabidopsis thaliana* and *Solanaceae* with 90 % homology, complemented with sequences for human keratin and porcine trypsin to exclude background peaks, and yeast enolase. The false positive rate against a randomised database was set at 4 %. The search parameters were as follows: automatic peptide fragment tolerance, three minimum fragment ion matches per peptide,

carbamidomethylation (Cys) as fixed modification and variable oxidation (Met) and propionamide modification (Cys). Peptide results were imported into Progenesis LC-MS software for quantitative analysis and statistical evaluation. Individual peptide results were assigned to corresponding proteins. Peptides that were assigned to more than one protein were considered conflicting. Only diagnostic peptides were used for quantification at the protein level, and ANOVA values had to be $p < 0.05$. The scoring algorithm implemented in Progenesis LC-MS software was used to determine confidence values. For identification, a sample had to match at least two peptide fragments, at least one of which was diagnostic.

3.9 Titanium dioxide phosphopeptide enrichment

The TCA/acetone protein extraction from mature pollen was performed as above, and 50 mg of this extract was re-suspended in 800 μ l of 0.1 % w/v RapiGest (Waters, Eschborn, Germany) / 50 mM ABC. The tryptic peptides that were obtained as described above in the in-gel approach were desalted and concentrated using Bond Elute C18 SPE columns (200 mg, 3 ml, Varian) according to the manufacturer's instructions. The bound peptides were eluted by 200 μ l TiO₂ loading buffer (80 % v/v ACN, 6 % v/v TFA, saturated with phthalic acid). Washed titanium dioxide beads (5 μ m particles, Titansphere, GL Sciences) were mixed with tryptic peptides in a ratio of 5:1, and shaken for 30 min at laboratory temperature. Subsequent wash and elution steps were conducted as described previously (Beck et al., 2011). Briefly, two washes were performed in incubation buffer whilst for the following four washes, 80 % v/v acetonitrile acidified with 0.1 % w/v TFA was used. The elution was accomplished in three elution steps: (1) 250 mM ammonium bicarbonate (pH 9.0); (2) 125 mM ammonium bicarbonate, 50 mM phosphoric acid (pH 10.5); (3) 400 mM ammonium hydroxide (pH 11.0).

Phosphopeptide-enriched samples were analysed by nLC-MS/MS on an LTQ Orbitrap Velos (Thermo Scientific, Bremen, Germany) mass spectrometer coupled to an Ultimate 3000 nLC (Dionex, Amsterdam, the Netherlands). The peptide pre-concentration was performed on a self-packed Synergi HydroRP trapping column (100 μ m ID, 4 μ m particle size, 10 nm pore size, 2 cm length). Afterwards, the peptides were separated on a self-packed Synergi HydroRP main column (75 μ m ID, 2.5 μ m particle size, 10 nm pore size, 30 cm length) at 60 °C and a flow rate of

270 nl·min⁻¹ applying a binary gradient (A: 0.1 % formic acid, B: 0.1 % formic acid, 84 % acetonitrile) ranging from 3 % to 45 % B in 240 min.

MS survey scans were acquired from 350–2000 m/z in the Orbitrap at a resolution of 60,000 using the polysiloxane m/z 445.120030 as lock mass (Olsen et al., 2005). The ten most intense signals were subjected to collision induced decay (CID)-based MS/MS in the LTQ using normalised collision energy of 35 %, an activation time of 30 ms, and a dynamic exclusion of 12 s. AGC values were set to 10⁶ for MS and 10⁴ for MS/MS scans.

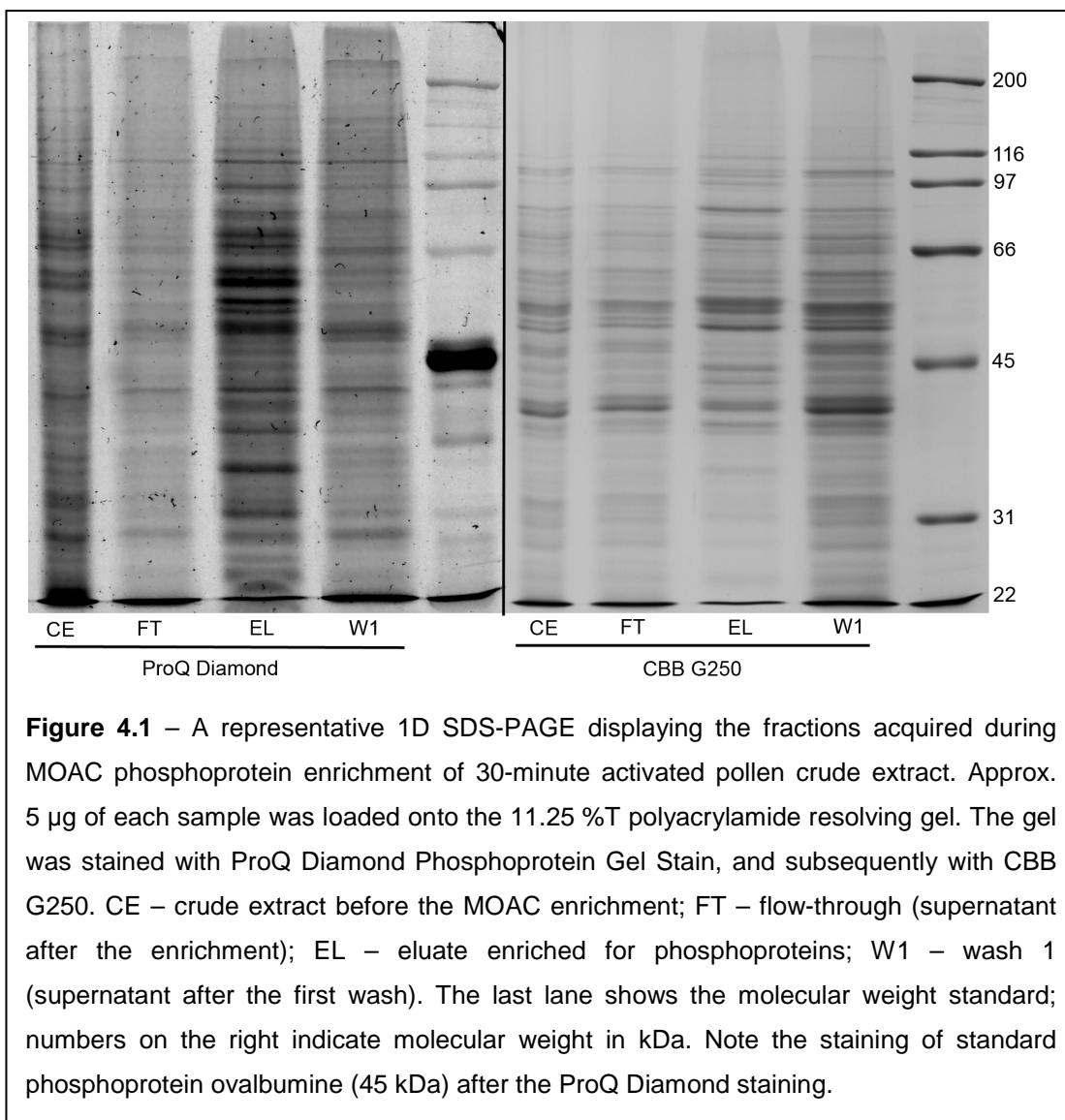
Raw data were processed by the Proteome Discoverer software V1.3 (Thermo Scientific) and searched against UniProt reference database (<http://www.uniprot.org/uniref/>), consisting of entries of *Viridiplantae* with 90 % homology (2012/02/22), complemented with sequences for human keratin and porcine trypsin to exclude background peaks, and against the TIGR EST sequence database entries for *Tobacco* (2010/08), using Mascot (version 2.3.2) and Sequest and Peptide Validator nodes with the following settings: 10 ppm MS tolerance, 0.5 Da MS/MS tolerance, trypsin as enzyme allowing a maximum of 2 missed cleavage sites, carbamidomethylation (Cys) as fixed, and oxidation (Met) as well as phosphorylation (Ser/Thr/Tyr) as variable modifications. Finally, mass deviation ≤4 ppm and high confidence (corresponding to a false discovery rate <1 %) filtering criteria were applied to the results.

4 Results

4.1 Phosphoprotein enrichment

The total proteins were extracted with TCA/acetone from mature and 30 min *in vitro* activated pollen. This extraction protocol resulted in a pellet that was easier to resuspend than the pellet originating from a phenol-based protocol (applying TRI-Reagent from Sigma) that was originally considered optimal (Fíla et al., 2011).

The protein extract was enriched for phosphoproteins by MOAC. To prove that the enrichment really had occurred, 1D SDS-PAGE of crude extract, flow-through, supernatant after the first wash, and phosphoprotein-enriched fraction was performed (Fig. 4.1).



The phosphoproteins were visualised by ProQ Diamond Phosphoprotein Gel stain. Both crude extract and phosphoprotein-enriched eluate showed a high ProQ Diamond signal revealing that the phosphorylated species were present in the originally extracted sample and in the phosphoprotein-enriched sample. On the other hand, a lower ProQ Diamond signal was observed in the flow-through and the supernatant after the first wash. These results supported the specificity of MOAC enrichment since the phosphoproteins were bound to the chromatography matrix and eluted almost exclusively during the elution step. Consequently, they were present less frequently in the flow-through and the supernatant after the first wash.

However, the origin of the lower ProQ Diamond signal in the flow-through and supernatant 1 remains unclear. The first possibility is non-specific staining resulting from a partial ProQ Diamond non-specificity (Steinberg et al., 2003) since ProQ Diamond Phosphoprotein Gel stain is a gallium resin (Agnew et al., 2006; Schilling and Knapp, 2008). A similar gallium resin showed some non-specificity also during phosphopeptide enrichment (Posewitz and Tempst, 1999; Aryal and Ross, 2010). Alternatively, the background ProQ Diamond staining can be caused by the presence of residual phosphoproteins in both fractions. It is likely that some phosphoproteins can be less tightly attached to the chromatography matrix, thus it is possible that they were not bound to the chromatography matrix at all or were freed from the matrix earlier than elution was accomplished.

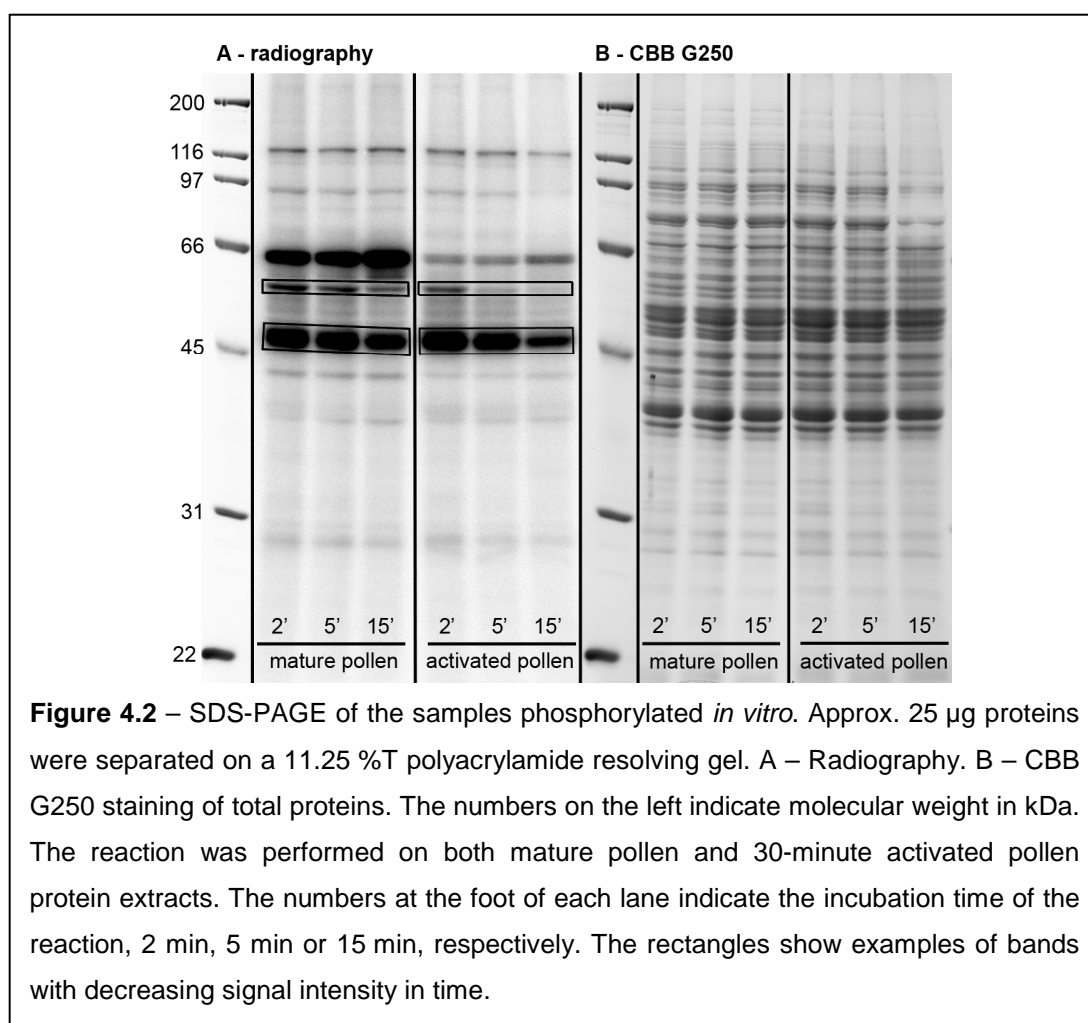
To show that the differences of ProQ Diamond staining intensity between the lanes originated from different degree of phosphorylation rather than from different amount of proteins loaded, a subsequent staining with CBB G250 was performed. The intensity of CBB G250 staining was comparable in crude extract, flow-through and phosphoprotein-enriched fraction whereas the amount of loaded proteins in supernatant 1 was somewhat higher. Such higher amount of proteins loaded was caused by too low concentration of this sample that made the accuracy of protein estimation quite limited so the loaded amount was estimated only roughly. These data supported the fact that different level of phosphorylation caused the differences in ProQ Diamond signal intensity rather than different amount of proteins loaded. The dissimilar electrophoretic spectra of the phosphoprotein-enriched eluate and the crude extract also supported the MOAC specificity since several weak bands were strengthened after phosphoprotein enrichment very likely representing the phosphorylated species. On the other hand, some bands clearly visible almost

vanished after the enrichment, possibly representing the non-phosphorylated proteins.

The mutual comparison of 1D SDS-PAGE electrophoretic patterns of several replicates (data not shown) showed high reproducibility of the applied extraction–enrichment protocol.

4.2 Phosphorylation *in vitro*

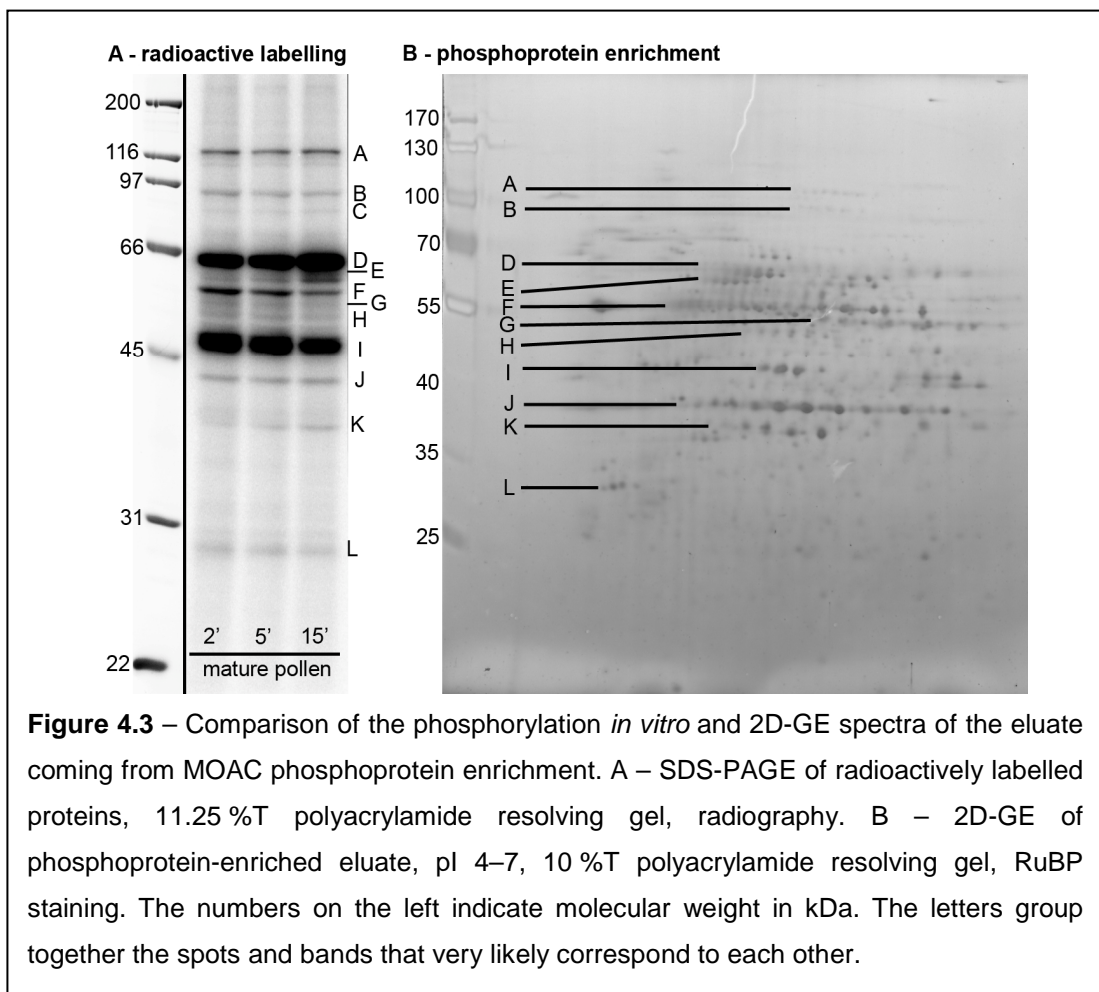
In order to further test the MOAC specificity, radioactive labelling of the newly *in vitro* phosphorylated proteins was performed. The microsomal fraction was extracted from both mature and 30 min activated pollen – this extraction relied on a “soft” extraction buffer that enabled to preserve protein conformation and function, which was essential since the kinase activity of the proteins had to be kept. TCA/acetone extract failed to be *in vitro* phosphorylated, possibly because of the fact that the proteins were denatured and subsequently incapable of proper re-folding that would lead to re-gaining of their biological function.



The microsomal fraction was incubated with γ - ^{32}P -ATP, so the newly phosphorylated proteins were radioactively labelled. These samples were separated by 1D SDS-PAGE. The electrophoretogram displayed a number of highly intensive bands (Fig. 4.2). The majority of strongly labelled proteins fell into the range of 35–70 kDa. After the various reaction times, only a little qualitative difference between the spectra was visible. Moreover, the molecular-weight range of *in vitro* phosphorylated proteins and enriched phosphoproteins was similar and many of the observed bands very likely corresponded to each other (Fig. 4.3).

Some of the strongly labelled bands were stained by CBB G250 only weakly (Fig. 4.2). These species probably represented low-abundant proteins with high incorporation of radioactive phosphorus.

It is remarkable that several proteins showed higher intensity of radioactive labelling after 2 min compared to the intensity after 5 and 15 min (see the rectangles in Fig. 4.2). This decrease in intensity can be caused by a prevailing activity of kinases during the first two minutes followed by an increased activity of



phosphatases in the subsequent incubation period thus the overall signal decreased when the reactions reached their equilibriums.

There were also notable differences between radiograms originating from mature pollen and from 30-minute activated pollen (Fig. 4.2). For instance, a 65 kDa protein was very strongly labelled in mature pollen whereas the observed signal in 30-minute activated pollen was remarkably less intense. Since the concentration of this protein was very similar in both stages, it is likely that the differences in labelling intensity did not reflect a different amount of protein but really a different level of phosphorylation in mature pollen and 30-minute activated pollen. Since the proteins after radioactive labelling were not subjected to MS, their identity and the role of their phosphorylation remained unknown.

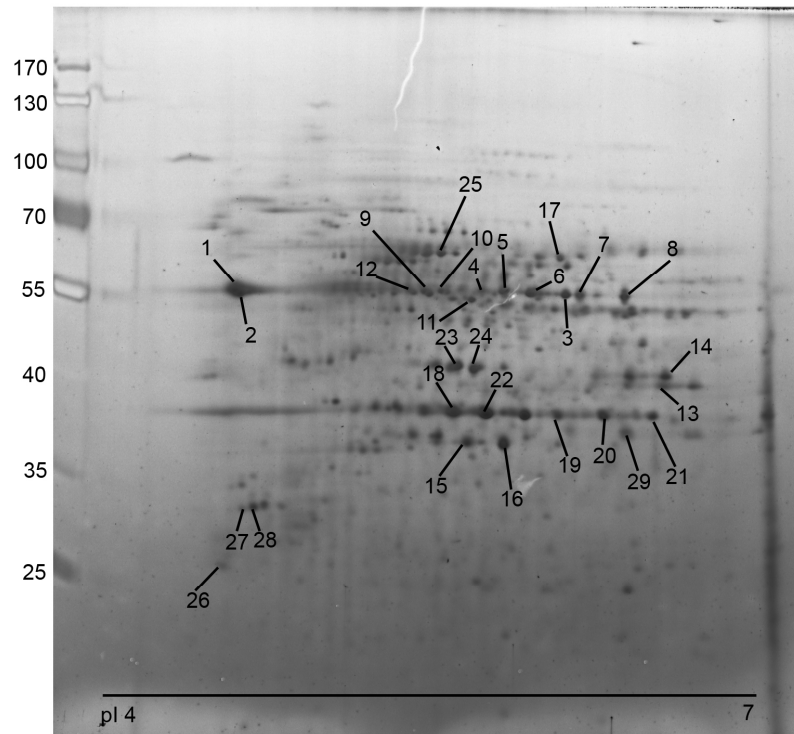
4.3 In-gel approach

Since 1D SDS-PAGE has only a limited resolution, 2D-GE separations of both phosphoprotein-enriched fractions and crude extracts were performed (Fig. 4.4 and Fig 4.5). The gels were stained with a fluorescent dye staining total proteins – RuBP. This stain represents a cheaper non-commercial alternative to the quite pricy Sypro Ruby from Invitrogen (Rabilloud et al., 2001).

The 2D spectra of the phosphoprotein-enriched fraction were different from those coming from the crude extracts (compare Fig 4.4 and Fig 4.5). Such differences represent another proof of MOAC enrichment specificity.

Mature pollen phosphoproteome was chosen as a reference, so the identification of as many proteins as possible was desired. Consequently, all visible spots from two gel replicas of mature pollen eluate were excised and analysed by nLC–ESI–Q/TOF. Afterwards, the gels of mature pollen eluate and activated pollen eluate were compared by image analysis. Fourteen spots were of a significantly two-times different abundance between the two stages ($p < 0.05$). These spots were excised also from the activated pollen gels, and analysed by MS/MS. Although each of these differentially abundant spots was picked at least from two gels, only ten of them were identified. The quantitative data of these spots are presented in Tab. 4.1 and Tab. S1, and the significantly different spots are highlighted by a superscripted “S” behind the MP/PT ratio. All presented candidates were identified according to more

A - mature pollen eluate



B - 30-minute activated pollen eluate

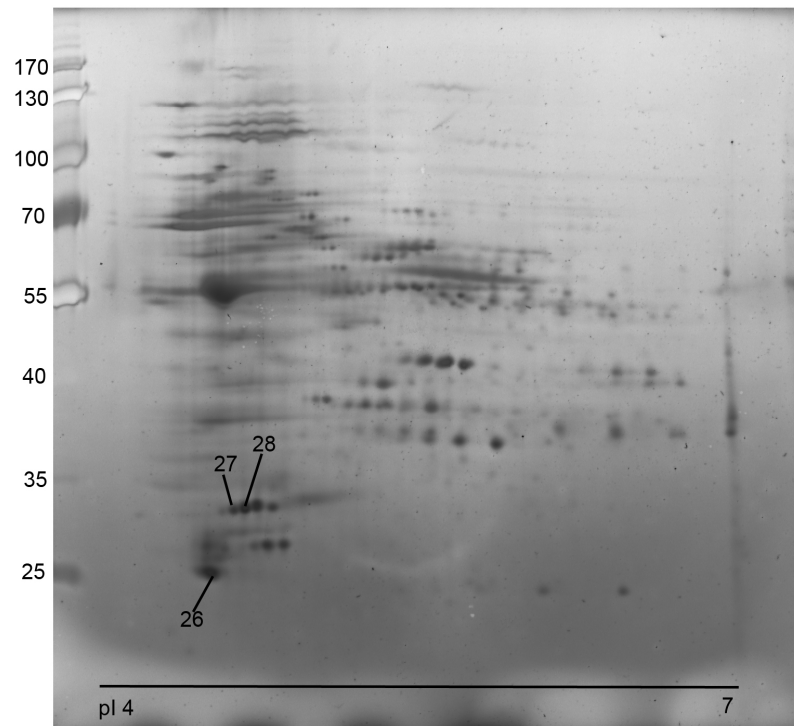


Figure 4.4 – The representative 2D-GE images of phosphoprotein-enriched eluates. A – mature pollen. B – 30-minute activated pollen. Approx. 50 µg proteins was separated in pI range 4–7, and subsequently in a 10 %T polyacrylamide resolving gel; RuBP staining. Numbered spots indicate phosphoprotein candidates that were identified by MS/MS as listed in Table 4.1. The numbers on the left indicate molecular weight in kDa.

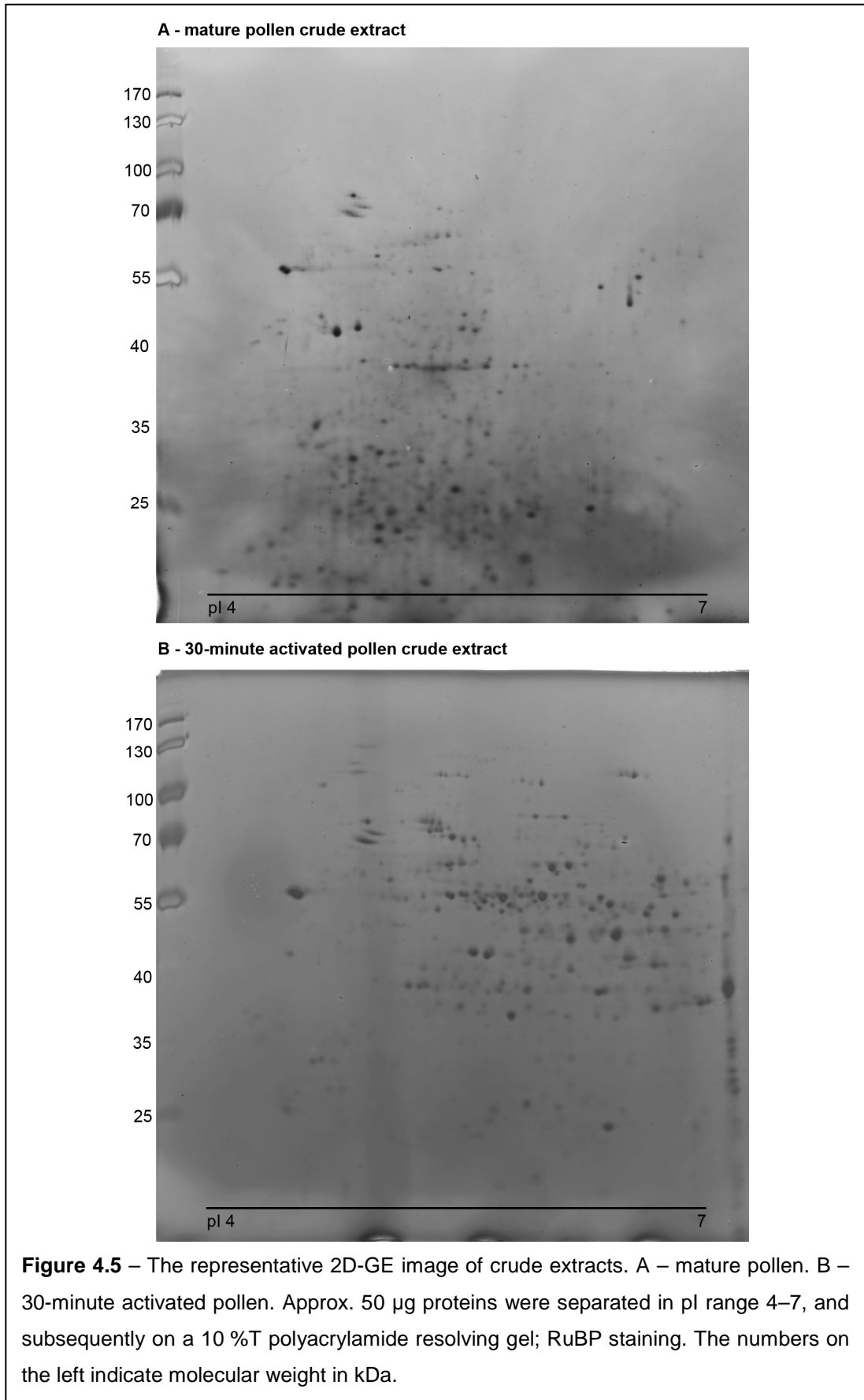


Table 4.1 – Identified phosphoprotein candidates from 2D-GE analysed as described in “Materials and methods” section. Proteins that were identified from at least two gels according to at least two peptides are pinpointed with two asterisks behind the spot number, whereas proteins that were identified only once according to at least two peptides are highlighted with one asterisk. Superscript behind accession number indicates database: a) Swissprot; b) Trembl Viridiplantae; c) TIGR EST *Solanaceae*. The superscripted S behind the MP/PT ratio means a significant change between the two stages as calculated by the PDQuest software. Note: Spot 4 was not recognised as a spot by the PDQuest software, but manually assigned. MW – molecular weight; pI – isoelectric point; Seq. coverage – sequence coverage; Num. of pept. – number of peptides; Norm. spot volume – normalised spot volume; Ver. – verified by gel-free approach; y – yes; n – no. Proteins significantly more abundant in mature pollen (MP/PT > 2.0) are highlighted in red, whilst proteins significantly more abundant in activated pollen (MP/PT < 0.5) are pinpointed in green.

Spot #	Protein name	Accession number	Functional subcategory	MW (Da)	pI	Seq. coverage	PLGS score	Num. of pept.	Mature pollen		Activated pollen (30 min)		Ratio MP/PT	Ver.
									Norm. spot volume (ppm)	Variance (ppm)	Norm. spot volume (ppm)	Variance (ppm)		
Protein destination and storage														
1**	Calreticulin (<i>Nicotiana tabacum</i>)	Q40567 ^a	folding and stability	44538	4.18	17.22	13.06	7	638.75	148.33	42153.57	35.09	0.02 ^s	y
2**	Calreticulin (<i>Nicotiana tabacum</i>)	Q40567 ^b	folding and stability	44538	4.18	21.59	13.06	9	16518.38	160.69	22452.45	118.86	0.74	n
3**	Leucine aminopeptidase 1 (<i>Arabidopsis thaliana</i>)	P30184 ^a	modification	54475	5.55	9.62	9.78	4	5476.59	20.73	141.45	44.04	38.72 ^s	n
4*	Leucine aminopeptidase 1, chloroplast precursor (<i>Solanum lycopersicum</i>)	Q10712 ^a	modification	60241	5.74	4.20	9.32	2	not identified as spot		not identified as spot		N/A	n
5**	Leucine aminopeptidase 2, chloroplast precursor (<i>Solanum lycopersicum</i>)	Q42876 ^a	modification	59511	7.94	6.85	10.01	3	5871.69	36.01	894.30	126.02	6.57	n
6**	Leucine aminopeptidase 2, chloroplast precursor (<i>Solanum lycopersicum</i>)	Q42876 ^a	modification	59511	7.94	6.85	10.01	3	5465.30	37.96	762.26	123.35	7.17	n
Energy														
7**	ATP synthase subunit alpha mitochondrial (<i>Nicotiana plumbaginifolia</i>)	P05495 ^a	respiration	55190	5.74	6.68	10.01	3	3823.90	32.68	328.49	99.49	11.64 ^s	n
8**	ATP synthase subunit alpha mitochondrial (<i>Nicotiana plumbaginifolia</i>)	P05495 ^a	respiration	55190	5.74	14.73	10.01	8	3739.60	44.41	1340.33	74.05	2.79	n
9**	ATP synthase subunit beta, mitochondrial precursor (<i>Nicotiana plumbaginifolia</i>)	P17614 ^a	respiration	59819	5.90	21.07	10.01	9	4172.27	63.63	3545.61	15.12	1.18	y
10**	ATP synthase subunit beta, mitochondrial precursor (<i>Nicotiana plumbaginifolia</i>)	P17614 ^a	respiration	59819	5.90	11.61	10.01	5	2845.01	66.17	2440.58	45.58	1.17	n
11**	ATP synthase subunit beta (<i>Nicotiana sylvatica</i>)	Q9ZR78 ^b	respiration	59475	6.12	6.51	13.06	3	3500.72	61.66	2052.00	58.46	1.71	n

12*	ATP synthase subunit beta (<i>Oryza sativa</i>)	Q5N7P8 ^b	respiration	45208	5.09	5.73	11.27	2	2373.51	86.35	1671.26	71.92	1.42	n
13**	Alcohol dehydrogenase, fragment (<i>Nicotiana tabacum</i>)	Q42953 ^b	fermentation	41296	6.63	4.75	13.06	2	4326.88	3.97	1672.66	47.47	2.59 ^s	n
14**	Alcohol dehydrogenase (<i>Nicotiana tabacum</i>)	Nt_TC4884 ^c	fermentation	41324	6.64	9.29	11.79	3	4345.27	19.43	2097.85	88.69	2.07	n
15**	Fructokinase (<i>Nicotiana tabacum</i>), fragment	Nt_EB427949 ^c	glycolysis	–	–	23.23	11.91	6	5744.92	29.43	4657.99	41.31	1.23	n
16**	Fructokinase (<i>Nicotiana tabacum</i>), fragment	Nt_EB427949 ^c	glycolysis	–	–	27.95	11.91	7	9955.21	51.15	7480.28	57.68	1.33	n
17**	Phosphoglycerate mutase (<i>Nicotiana tabacum</i>)	P35494 ^a	glycolysis	61029	5.95	5.55	10.01	3	2507.34	28.94	1246.50	90.65	2.01	n
Cell structure														
18**	Homologue to UP Q69F96 PHAVU – reversibly glycosylated protein (<i>Nicotiana tabacum</i>)	Nt_TC5256 ^c	cell wall	40193	5.82	6.27	11.91	2	12685.47	30.21	721.98	122.34	17.57 ^s	n
19**	Homologue to UP Q69F96 PHAVU – reversibly glycosylated protein (<i>Nicotiana tabacum</i>)	Nt_TC5256 ^c	cell wall	40193	5.82	12.54	11.91	4	4660.57	12.05	195.51	70.97	23.84 ^s	n
20**	Alpha 1-4 glucan protein synthase UDP forming (<i>Solanum tuberosum</i>)	Q9SC19 ^a	cell wall	41777	6.18	5.75	8.90	2	4218.53	66.70	51.62	125.44	81.73	y
21*	Alpha 1-4 glucan protein synthase UDP forming (<i>Solanum tuberosum</i>)	Q9SC19 ^a	cell wall	41777	6.18	5.75	8.90	2	3798.14	17.30	313.49	97.48	12.12 ^s	n
22*	Alpha 1-4 glucan protein synthase UDP forming (<i>Pisum sativum</i>)	O04300 ^a	cell wall	41545	5.65	4.40	9.31	2	16665.02	66.73	522.52	115.06	31.89	n
23**	Actin (<i>Nicotiana tabacum</i>)	Q05214 ^a	cytoskeleton	41711	5.34	10.08	5.75	3	9243.99	92.67	12044.63	42.78	0.77	n
24**	Actin (<i>Solanum tuberosum</i>)	P30170 ^a	cytoskeleton	21681	5.87	19.49	9.69	3	7507.36	51.89	6803.83	28.20	1.10	n
25*	Actin (<i>Chlamydomonas reinhardtii</i>)	A8JAV1 ^b	cytoskeleton	41836	5.30	19.71	13.05	6	4395.38	42.64	1173.76	38.31	3.74	n
Protein synthesis														
26**	Alpha chain of nascent polypeptide associated complex (<i>Nicotiana benthamiana</i>)	A2PYH3 ^b	translation control	21910	4.12	13.43	13.06	2	1479.72	124.27	10014.09	13.46	0.15 ^s	y
27**	Ripening regulated protein (<i>Solanum tuberosum</i>)	Nt_TC4064 ^c	translation factors	25318	4.47	10.64	11.53	3	721.43	64.81	4596.24	37.79	0.16 ^s	n
28*	Elongation factor 1 delta 2 (<i>Oryza sativa</i>)	Q40682 ^a	translation factors	24639	4.20	7.52	9.34	2	2044.42	79.44	13668.64	10.38	0.15 ^s	n
Unclassified														
29*	Similar to UniRef100_Q8LA49 globulin like protein (<i>Arabidopsis thaliana</i>)	Lg_TC190764 ^c	–	38311	5.83	8.24	11.66	2	2097.53	99.61	5390.07	21.11	0.39	n

than two peptides, several of them only in one replica, whilst others were identified twice, independently from both gel replicas.

Tab. 4.1 and Tab. S1 list differentially abundant spots between the two stages together with further 19 spots that did not show significantly different abundance between the two stages. Collectively, the gel approach led to the identification of 29 spots. The identification of many proteins relied on the similarity to the homologues from different species. This is not uncommon since tobacco genomic sequences available in the public databases do not cover the whole genome. Consequently, it remains unclear whether several isoforms identified from other species represent true isoforms in tobacco – two identifiers from two independent species might represent the same tobacco homologue.

In the following part, a protein is defined as a distinct identification number in a database, i.e. each protein isoform is regarded as a single protein. Seven proteins were identified in more spots: calreticulin in spots #1 and #2, leucine aminopeptidase 2 in #5 and #6, ATP synthase subunit α in #7 and #8, ATP synthase subunit β in #9 and #10, fructokinase in #15 and #16, reversibly glycosylated protein in #18 and #19, and α 1-4 glucan protein synthase UDP forming in #20 and #21. These groups of spots were usually clustered in the strings of the same molecular weight differing in the pI – they very likely represented the differently-phosphorylated forms of the very same protein. However, they might also represent products of different genes (with substitutions in their sequence).

Collectively, 29 identified spots contained 22 distinct proteins (again, different isoforms were counted as a single protein). Amongst the ten proteins present in the spots with a different abundance in mature and 30-minute activated pollen, four were over-represented in the activated pollen – calreticulin (#1), α -chain of a nascent polypeptide associated complex (#26), ripening regulated protein homologue (#27), and elongation factor 1 δ 2 (#28). Six identified spots that had lower concentration in the activated pollen eluates were leucine aminopeptidase 1 (#3), ATP synthase subunit α (#7), alcohol dehydrogenase (#13), and three spots of a reversibly glycosylated protein / α 1-4 glucan protein synthase UDP forming (#18, #19, and #21).

It should be mentioned that the up- or down-regulation of a spot did not necessarily mean total higher or lower concentration of the respective proteins. Many proteins were present in more spots, referring to more forms, which differed in their

phosphorylation level. However, several isoforms could have remained undetected since not all the spots were identified successfully. Moreover, the appearance or disappearance of a particular spot might or might not be referring to *de novo* synthesis of the respective isoform – it can be caused by its sole phosphorylation/dephosphorylation since a protein appeared in the eluate if phosphorylated but remained in the flow-through in its non-phosphorylated form.

Although the majority of the in-gel identified proteins (or their different isoforms) was also revealed by the gel-free approach (see below), leucine aminopeptidase 1 and 2, elongation factor 1 δ 2 and a globulin like protein were identified exclusively from 2D-GE separations. These results highlighted the importance of 2D-GE approach although it identified a lower number of proteins in comparison with the gel-free technique.

However, several spots remained unidentified. These spots were mostly less abundant, and resulted in poor MS/MS spectra that prevented successful protein identification. It is likely that RuBP is too sensitive and can also display proteins below the MS/MS detection limits.

4.4 Gel-free approach

Since the in-gel approach discriminates several groups of proteins (tiny, large, low-abundant and those with an extremely acidic or alkaline pI), the gel-free method was applied in parallel to broaden the list of identified proteins. The eluate was directly fragmented by trypsin so the peptides represented a mixture coming from all present proteins. The peptides that could have belonged to more than one protein (because of sequence homology) were called conflicting peptides. Since their origin remained unclear, only diagnostic peptides could be taken into consideration when calculating the abundance of a protein. The quantitative data for each single peptide in both mature and 30-minute activated pollen were calculated as an average from three replicates. The data regarding diagnostic peptides were combined and statistically evaluated by ANOVA in order to obtain the abundance of a protein.

The gel-free approach discovered 121 proteins if different isoforms were calculated as different proteins (Tab. 4.2 and Tab. S2). Four of these IDs verified the proteins identified by the in-gel approach whilst 117 of them were unique for the gel-free approach. Such difference in number of identified proteins by the respective

approaches was quite likely since during 2D-GE, as high as 80 % of the sample can be lost (Zhou et al., 2005).

Many of the proteins were present in more isoforms, for instance alcohol dehydrogenase (#43 and #44), fructokinase (#50–53), fructose-bisphosphate aldolase (#54–56), glyceraldehyde 3-phosphate dehydrogenase (#57–65), adenosyl homocysteinase (#85–88), calreticulin (#102–105), luminal binding protein (#113–116), and 14-3-3 protein (#136–139).

The most identified proteins fell into the categories connected with energy production (39 proteins), protein destination and storage (24), and metabolism (19). Other categories were also represented, namely protein synthesis (11), cell structure (11), signal transduction (8), transport (3), and disease/defence (2). Interestingly, four proteins were listed as unclassified.

Only proteins with a two-fold difference in abundance were considered as differentially abundant, and are shown in Tab. 4.2 in red (more abundant in mature pollen) or green (more abundant in activated pollen). Proteins taking part in energy production were usually more concentrated in the activated pollen – e.g. phosphoglycerate kinase (#68), and fructose-bisphosphate aldolase (#55). Certain isoforms of glyceraldehyde 3-phosphate dehydrogenase were up-regulated (#58, #62, #63, and #65) or down-regulated (#60) in activated pollen. On the other hand, fructokinase (#50), pyruvate decarboxylase (#46) and ATP synthase subunit α (#74–76) were more abundant in mature pollen. On the contrary, a higher concentration in activated pollen was demonstrated for proteins playing role in protein destination and storage, calreticulin (#102–104), luminal binding protein 4 (#115) and a GrpE protein (#121, and #122). Heat shock protein 81-3 (#112), endoplasmic reticulum chaperone protein (#107) and luminal-binding protein 3 (#114) were more common in mature pollen. Many proteins playing role in amino acid metabolism were also less abundant in the activated pollen – homocysteine methyltransferase (#82–84), and adenosyl homocysteinase (#86–88). Other proteins less abundant in the activated pollen were the translation factors #131, #133, and #134 whereas other translation factors (#126, #127, and #132) were present in higher abundance. Differentially expressed signal transducers and proteins involved in determining cell structure, in the disease and defence response, and in transport were mostly less common in the activated pollen – 14-3-3 protein (#136–139), Rab-GDP dissociation inhibitor (#142), tubulin (#38, and #39), and V-type proton ATPase (#145).

Table 4.2 – Identified phosphoprotein candidates by the gel-free approach analysed as described in “Materials and methods” section. Number of peptides indicates the total number of peptides, according to which the protein was identified. The number in the brackets represents number of unique peptides that contribute to the calculation of protein abundance. Proteins more abundant in mature pollen (MP/PT > 2.0) are highlighted in red, whilst proteins more concentrated in activated pollen (MP/PT < 0.5) are pinpointed in green.

Protein #	Protein name	Accession number (UniRef90 -)	Functional subcategory	LC-MS score	Number of peptides (diagnostic peptides)	Normalised abundance (mature pollen)	Normalised abundance (30-minute activated pollen)	Ratio (MP/PT)	ANOVA (p)
Cell structure									
30	Alpha-1,4-glucan-protein synthase [UDP-forming] 1 (<i>Solanum tuberosum</i>)	Q9SC19	cell wall	362.75	6 (5)	1392.89	1013.50	1.37	4.85E-03
31	Reversibly glycosylated polypeptide-3 (<i>Arabidopsis thaliana</i>)	Q8LB19	cell wall	218.32	3 (2)	414.16	373.34	1.11	2.00E-02
32	Actin 2, fragment (<i>Vitis vinifera</i>)	Q94KC0	cytoskeleton	442.95	4 (1)	260.98	182.40	1.43	8.92E-04
33	Actin, fragment (<i>Solanum melongena</i>)	D5LXP0	cytoskeleton	1223.75	8 (1)	168.18	116.01	1.45	3.00E-02
34	Actin-12 (<i>Arabidopsis thaliana</i>)	P53497	cytoskeleton	2151.77	20 (4)	890.18	707.85	1.26	5.28E-03
35	Actin-46, fragment (<i>Solanum tuberosum</i>)	P93586	cytoskeleton	1427.58	12 (1)	539.81	316.07	1.71	4.66E-03
36	Actin-54, fragment (<i>Nicotiana tabacum</i>)	P93373	cytoskeleton	1826.46	12 (1)	237.95	200.64	1.19	2.00E-02
37	Actin-75 (<i>Solanum tuberosum</i>)	P30169	cytoskeleton	1708.56	19 (5)	2286.58	1793.35	1.28	1.00E-02
38	Tubulin alpha-2 chain (<i>Oryza sativa</i> var. <i>japonica</i>)	Q53M52	cytoskeleton	589.99	8 (4)	1264.59	421.10	3.00	1.63E-07
39	Tubulin alpha-2/alpha-4 chain (<i>Arabidopsis thaliana</i>)	P29510	cytoskeleton	700.15	8 (4)	1189.79	591.45	2.01	2.28E-06
40	Tubulin beta-4 chain (<i>Arabidopsis thaliana</i>)	P24636	cytoskeleton	229.96	3 (1)	539.88	310.39	1.74	9.60E-05
Disease/defence									
41	Monodehydroascorbate reductase (<i>Solanum lycopersicum</i>)	Q43497	detoxification	129.44	2	653.25	440.49	1.48	6.19E-03
42	Chilling-responsive protein (<i>Nicotiana tabacum</i>)	B6RCM0	stress responses	163.16	3	847.58	770.27	1.10	1.94E-05
Energy									
43	Alcohol dehydrogenase 1 (<i>Petunia hybrida</i>)	P25141	fermentation	1596.71	16 (10)	3104.63	4344.41	0.71	2.01E-05
44	Alcohol dehydrogenase, fragment (<i>Nicotiana acaulis</i>)	D4I613	fermentation	751.49	7 (2)	881.00	1118.26	0.79	2.86E-06
45	Aldehyde dehydrogenase, NAD ⁺ (<i>Nicotiana tabacum</i>)	P93344	fermentation	121.92	3	215.58	188.83	1.14	2.20E-04
46	Pyruvate decarboxylase isozyme 2 (<i>Nicotiana tabacum</i>)	P51846	fermentation	728.32	12	2914.82	1258.51	2.32	1.12E-05
47	2,3-bisphosphoglycerate-independent phosphoglycerate mutase (<i>Nicotiana tabacum</i>)	P35494	glycolysis	1255.20	15 (6)	1112.67	1557.40	0.71	2.53E-05

48	2,3-bisphosphoglycerate-independent phosphoglycerate mutase 1 (<i>Arabidopsis thaliana</i>)	O04499	glycolysis	445.10	6 (1)	47.81	82.05	0.58	8.77E-04
49	E1 alpha subunit of pyruvate dehydrogenase (<i>Petunia hybrida</i>)	Q5ECP6	glycolysis	409.60	4 (3)	312.29	370.58	0.84	1.10E-03
50	Fructokinase (<i>Solanum lycopersicum</i>)	O04897	glycolysis	184.01	3 (1)	180.79	79.33	2.28	7.62E-03
51	Fructokinase (<i>Solanum tuberosum</i>)	P37829	glycolysis	415.56	5 (2)	592.36	531.95	1.11	7.50E-03
52	Probable fructokinase-1 (<i>Arabidopsis thaliana</i>)	Q9SID0	glycolysis	355.26	4 (1)	77.91	76.14	1.02	1.64E-05
53	Putative fructokinase-5 (<i>Arabidopsis thaliana</i>)	O82616	glycolysis	432.03	5 (4)	1923.92	2581.26	0.75	1.61E-05
54	Fructose-bisphosphate aldolase (<i>Arabidopsis thaliana</i>)	Q9LF98	glycolysis	517.91	6 (1)	255.12	357.51	0.71	6.31E-04
55	Fructose-bisphosphate aldolase (<i>Solanum tuberosum</i>)	Q2PYX3	glycolysis	749.53	8 (2)	339.19	1192.89	0.28	3.22E-09
56	Fructose-bisphosphate aldolase, fragment (<i>Solanum lycopersicum</i>)	Q94FU4	glycolysis	437.92	5 (1)	132.69	259.80	0.51	4.75E-05
57	Glyceraldehyde 3-phosphate dehydrogenase (<i>Solanum lycopersicum</i>)	O04106	glycolysis	987.41	9 (1)	44.87	62.76	0.71	3.72E-03
58	Glyceraldehyde 3-phosphate dehydrogenase, fragment (<i>Solanum tuberosum</i>)	Q43833	glycolysis	693.80	7 (2)	538.15	2003.99	0.27	6.68E-05
59	Glyceraldehyde-3-phosphate dehydrogenase (<i>Arabidopsis thaliana</i>)	P25858	glycolysis	1130.05	11 (2)	378.14	641.63	0.59	9.96E-07
60	Glyceraldehyde-3-phosphate dehydrogenase (<i>Atriplex nummularia</i>)	P34783	glycolysis	822.00	8 (1)	9.90	1.83	5.41	1.00E-02
61	Glyceraldehyde-3-phosphate dehydrogenase (<i>Capsicum annuum</i>)	Q8VWN9	glycolysis	143.59	2 (1)	229.50	224.21	1.02	2.00E-02
62	Glyceraldehyde-3-phosphate dehydrogenase (<i>Magnolia liliiflora</i>)	P26518	glycolysis	469.57	5 (1)	9.47	124.03	0.08	4.53E-04
63	Glyceraldehyde-3-phosphate dehydrogenase, fragment (<i>Coelogyne fimbriata</i>)	C7E4Z7	glycolysis	691.06	7 (3)	693.90	1807.04	0.38	4.26E-06
64	Glyceraldehyde-3-phosphate dehydrogenase, fragment (<i>Nicotiana attenuata</i>)	A1BQW0	glycolysis	1097.34	12 (3)	575.17	1122.67	0.51	3.00E-02
65	Glyceraldehyde-3-phosphate dehydrogenase (<i>Vitis vinifera</i>)	D7TAM6	glycolysis	791.03	7 (2)	643.54	1739.31	0.37	1.09E-05
66	Phosphoglucomutase (<i>Solanum tuberosum</i>)	Q9M4G4	glycolysis	368.04	5	1121.77	643.51	1.71	5.91E-04
67	Phosphoglycerate kinase (<i>Nicotiana tabacum</i>)	Q42962	glycolysis	2113.18	18 (8)	3854.27	5512.84	0.70	4.90E-04
68	Phosphoglycerate kinase (<i>Solanum tuberosum</i>)	Q2V9C6	glycolysis	1344.20	12 (2)	322.16	702.96	0.46	3.69E-04
69	Phosphoglycerate mutase, fragment (<i>Nicotiana attenuata</i>)	A1BQW7	glycolysis	899.42	8 (2)	212.48	400.61	0.53	2.23E-06
70	Putative UDP-glucose dehydrogenase 1 (<i>Nicotiana tabacum</i>)	Q6IVK7	glycolysis	1934.62	20 (12)	4281.77	3016.86	1.42	3.33E-04
71	Triosephosphate isomerase (<i>Petunia hybrida</i>)	P48495	glycolysis	495.55	5 (4)	420.21	764.28	0.55	6.27E-07

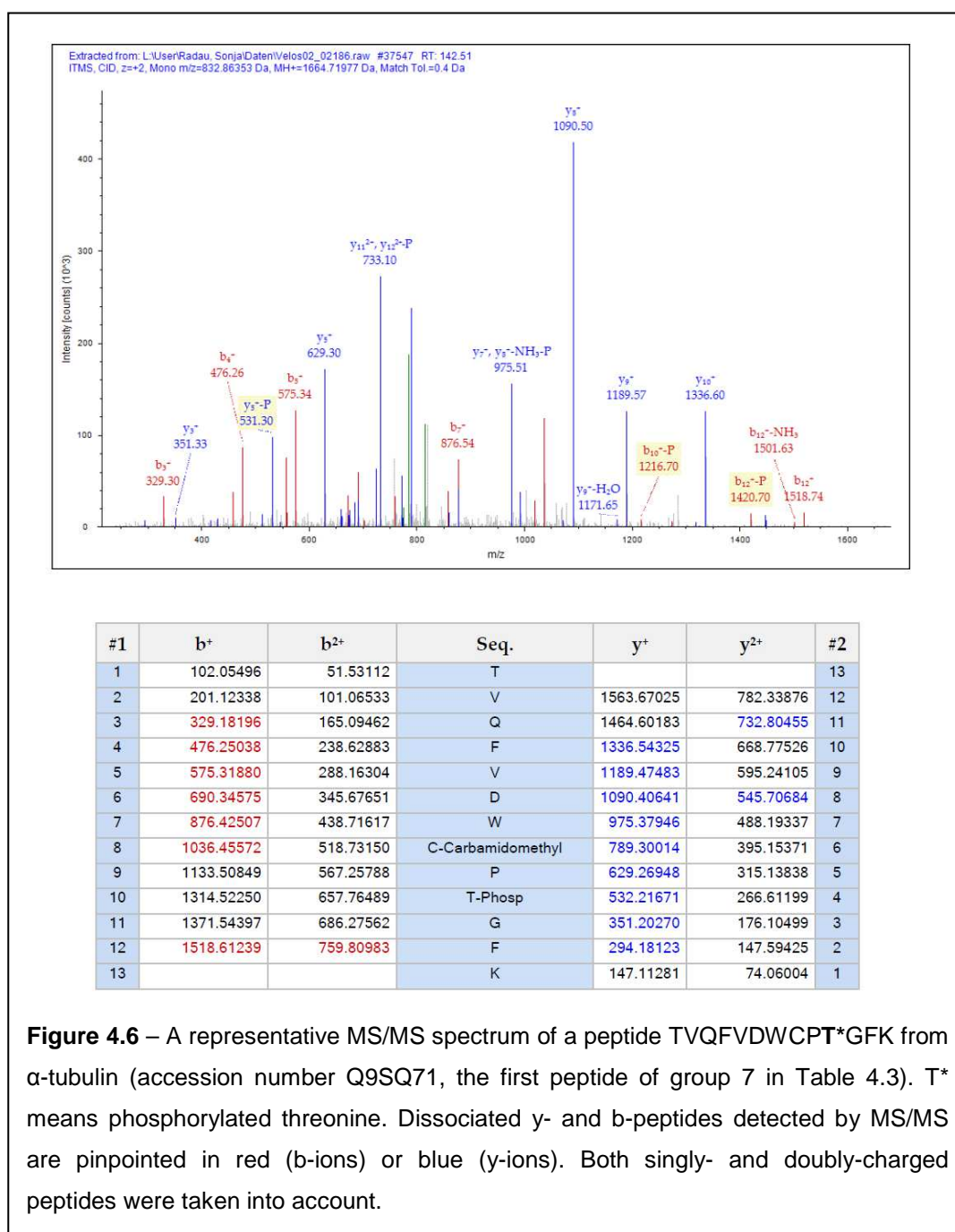
72	Triosephosphate isomerase (<i>Solanum tuberosum</i>)	Q3HRV9	glycolysis	250.61	2 (1)	823.85	1142.91	0.72	2.85E-04
73	ATP synthase subunit alpha (<i>Arabidopsis thaliana</i>)	P92549	respiration	1066.26	12 (1)	153.75	157.98	0.97	2.00E-02
74	ATP synthase subunit alpha, fragment (<i>Arabidopsis thaliana</i>)	A7KNE3	respiration	1011.16	12 (3)	422.66	124.81	3.39	7.70E-04
75	F1-ATP synthase subunit alpha, fragment (<i>Nicotiana repanda</i>)	O63701	respiration	408.71	4	3101.34	1515.44	2.05	5.48E-05
76	F1-ATPase alpha subunit (<i>Gymnosiphon divaricatus</i>)	B3FTT5	respiration	290.12	2 (1)	1223.70	593.89	2.06	2.15E-04
77	Truncated putative F1-ATP synthase subunit alpha (<i>Nicotiana tabacum</i> x <i>Nicotiana bigelovii</i>)	Q37046	respiration	442.01	7 (2)	691.83	391.37	1.77	3.81E-03
78	ATP synthase subunit beta (<i>Nicotiana plumbaginifolia</i>)	P17614	respiration	2086.19	20 (6)	2433.39	2196.57	1.11	2.53E-05
79	ATP synthase subunit beta (<i>Sorghum bicolor</i>)	C5XGT6	respiration	1487.99	14 (2)	687.51	528.96	1.30	6.80E-03
80	Aconitase, fragment (<i>Solanum pennellii</i>)	Q84NI5	TCA pathway	332.75	6	501.97	445.33	1.13	5.25E-04
81	Isocitrate dehydrogenase, NADP ⁺ (<i>Solanum tuberosum</i>)	P50217	TCA pathway	139.23	4 (2)	158.48	89.29	1.77	4.00E-02
Metabolism									
82	5-methyltetrahydropteroyltriglutamate- homocysteine methyltransferase (<i>Arabidopsis thaliana</i>)	O50008	amino acid	1499.64	11 (4)	1311.06	394.29	3.33	4.01E-05
83	5-methyltetrahydropteroyltriglutamate- homocysteine methyltransferase (<i>Catharanthus roseus</i>)	Q42699	amino acid	1574.83	15 (8)	4608.80	1801.35	2.56	1.61E-06
84	5-methyltetrahydropteroyltriglutamate- homocysteine S-methyltransferase-like protein, fragment (<i>Arabidopsis thaliana</i>)	Q0WP70	amino acid	663.45	6 (2)	397.85	121.88	3.26	8.84E-05
85	Adenosylhomocysteinase (<i>Catharanthus roseus</i>)	P35007	amino acid	1424.50	16 (1)	238.58	124.40	1.92	1.45E-04
86	Adenosylhomocysteinase 1 (<i>Arabidopsis thaliana</i>)	O23255	amino acid	1623.63	16 (1)	382.44	189.53	2.02	2.31E-05
87	Adenosylmonocysteinase (<i>Arabidopsis thaliana</i>)	A8MQP1	amino acid	1181.17	9 (1)	309.13	144.14	2.14	1.76E-04
88	Adenosylhomocysteinase (<i>Arabidopsis thaliana</i>)	C0Z3F3	amino acid	1007.21	10 (1)	272.04	133.79	2.03	3.00E-02
89	Glutamine synthetase (<i>Nicotiana plumbaginifolia</i>)	P12424	amino acid	143.00	2 (1)	227.71	120.68	1.89	4.57E-04
90	Glutamine synthetase (<i>Solanum tuberosum</i>)	Q9FPT8	amino acid	131.76	2 (1)	241.42	171.19	1.41	4.00E-02
91	S-adenosyl-L-homocysteine hydrolase, fragment (<i>Solanum chacoense</i>)	Q9SP98	amino acid	832.39	6 (1)	3183.51	2742.16	1.16	4.16E-03
92	S-adenosylmethionine synthase 3 (<i>Arabidopsis thaliana</i>)	Q9SJL8	amino acid	788.78	10 (6)	994.84	1460.75	0.68	1.79E-06
93	S-adenosylmethionine synthase 4 (<i>Arabidopsis thaliana</i>)	Q9LUT2	amino acid	734.85	8 (4)	458.52	837.72	0.55	4.10E-06
94	S-adenosylmethionine synthase, fragment (<i>Plantago major</i>)	Q2YHN7	amino acid	464.32	5 (1)	45.35	74.15	0.61	3.92E-03
95	Serine hydroxymethyltransferase (<i>Arabidopsis thaliana</i>)	O23254	amino acid	140.57	2	299.50	423.09	0.71	3.85E-05
96	Adenosine kinase isoform 1T-like protein (<i>Solanum tuberosum</i>)	Q2XPV0	nucleotides	695.87	6 (2)	944.20	948.08	1.00	2.80E-03
97	Adenosine kinase, fragment (<i>Nicotiana benthamiana</i>)	Q5XPZ0	nucleotides	670.62	7 (3)	242.97	317.51	0.77	4.00E-02

98	Nucleoside diphosphate kinase (<i>Solanum tuberosum</i>)	D3U1X1	nucleotides	281.74	4	483.27	631.99	0.76	1.41E-03
99	UDP-glucose 6-dehydrogenase (<i>Glycine max</i>)	Q96558	sugars and polysaccharides	937.90	9 (2)	222.07	127.20	1.75	3.00E-02
100	UTP-glucose-1-phosphate uridylyltransferase (<i>Solanum tuberosum</i>)	P19595	sugars and polysaccharides	464.84	5 (4)	637.04	790.52	0.81	8.20E-04
Protein destination and storage									
101	Calnexin-like protein (<i>Solanum lycopersicum</i>)	Q4W5U7	folding and stability	142.41	2	873.77	1020.11	0.86	2.57E-04
102	Calreticulin (<i>Nicotiana plumbaginifolia</i>)	Q40401	folding and stability	2605.91	20 (1)	774.09	5806.43	0.13	9.98E-05
103	Calreticulin, fragment (<i>Nicotiana tabacum</i>)	Q40567	folding and stability	3291.73	30 (9)	4798.06	36500.00	0.13	3.96E-09
104	Calreticulin-like protein, fragment (<i>Solanum melongena</i>)	Q9ST29	folding and stability	1753.30	16 (2)	383.90	1896.18	0.20	2.74E-05
105	Calreticulin (<i>Solanum tuberosum</i>)	Q38HV3	folding and stability	1391.14	13 (2)	944.32	1231.83	0.77	5.24E-04
106	Chaperonin CPN60 (<i>Arabidopsis thaliana</i>)	P29197	folding and stability	291.16	4	639.99	741.14	0.86	3.78E-06
107	Endoplasmic homolog (<i>Arabidopsis thaliana</i>)	Q9STX5	folding and stability	142.61	2	865.50	401.55	2.16	1.74E-04
108	Heat shock cognate 70 kDa (<i>Petunia hybrida</i>)	P09189	folding and stability	1548.23	16 (1)	842.91	1037.77	0.81	2.51E-04
109	Heat shock cognate 70 kDa protein 2 (<i>Solanum lycopersicum</i>)	P27322	folding and stability	2091.32	21 (3)	941.49	1039.93	0.91	5.62E-03
110	Heat shock protein 70, fragment (<i>Nicotiana benthamiana</i>)	Q6L9F6	folding and stability	904.63	7 (3)	186.10	197.91	0.94	1.79E-04
111	Heat shock protein cognate 70, fragment (<i>Sorghum bicolor</i>)	Q41291	folding and stability	608.59	6 (1)	1100.39	1608.43	0.68	3.00E-02
112	Heat shock protein 81-3 (<i>Arabidopsis lyrata</i> subsp. <i>lyrata</i>)	D7ML65	folding and stability	471.30	5 (1)	593.37	169.34	3.50	5.26E-04
113	Luminal-binding protein 1 (<i>Arabidopsis thaliana</i>)	Q9LKR3	folding and stability	1228.99	13 (1)	46.08	63.54	0.73	4.82E-04
114	Luminal-binding protein 3, fragment (<i>Nicotiana tabacum</i>)	Q03683	folding and stability	253.00	5 (1)	69.79	32.81	2.13	2.00E-02
115	Luminal-binding protein 4 (<i>Nicotiana tabacum</i>)	Q03684	folding and stability	1767.80	17 (3)	160.86	451.84	0.36	9.30E-04
116	Luminal-binding protein 8, fragment (<i>Nicotiana tabacum</i>)	Q03686	folding and stability	489.41	6 (1)	102.28	129.13	0.79	7.92E-05
117	Uncharacterised protein (<i>Arabidopsis thaliana</i>)	Q3E8J0	folding and stability	1501.56	15 (1)	1.94	60.28	0.03	9.25E-03
118	Predicted protein (<i>Populus trichocarpa</i>)	B9GIR0	folding and stability	420.97	5 (4)	844.45	492.50	1.71	4.73E-06
119	Alanine aminotransferase (<i>Capsicum annuum</i>)	Q6VEJ5	modification	594.64	8	960.27	1869.54	0.51	8.43E-05
120	Polyubiquitin 8 (<i>Arabidopsis thaliana</i>)	Q39256	modification	252.81	3	1533.59	1663.93	0.92	4.37E-03
121	GrpE protein homolog (<i>Nicotiana tabacum</i>)	Q9ZSP4	targeting	336.66	5 (4)	547.91	2171.18	0.25	3.79E-05
122	GrpE protein homolog (<i>Nicotiana tabacum</i>)	Q9ZSP3	targeting	262.70	3 (2)	106.92	308.59	0.35	2.52E-05
123	GTP-binding nuclear protein Ran-1 (<i>Arabidopsis thaliana</i>)	P41916	targeting	181.15	3 (1)	299.49	417.14	0.72	2.00E-02
124	Mitochondrial processing peptidase (<i>Solanum tuberosum</i>)	Q41440	targeting	254.20	3	165.99	179.56	0.92	2.36E-05
Protein synthesis									
125	60S acidic ribosomal protein-like protein (<i>Solanum tuberosum</i>)	Q3HVP0	ribosomal proteins	390.49	3	730.48	3621.96	0.20	1.11E-08
126	Alpha chain of nascent polypeptide associated complex (<i>Nicotiana benthamiana</i>)	A2PYH3	translation control	1442.00	9 (6)	1485.21	24000.00	0.06	2.54E-06

127	Predicted protein (<i>Arabidopsis lyrata</i> subsp. <i>lyrata</i>)	D7KZS1	translation control	734.27	5 (3)	537.74	5678.95	0.09	1.01E-06
128	Elongation factor 1 alpha, fragment (<i>Capsicum chinense</i>)	Q08IG4	translation factors	883.87	7 (1)	296.32	154.07	1.92	8.23E-05
129	Elongation factor 1-alpha (<i>Ricinus communis</i>)	B9RWF3	translation factors	803.59	7 (1)	2584.72	4239.83	0.61	4.96E-04
130	Elongation factor 1-alpha (<i>Arabidopsis thaliana</i>)	P13905	translation factors	1351.04	13 (3)	759.06	769.82	0.99	1.00E-02
131	Elongation factor 2 (<i>Beta vulgaris</i>)	O23755	translation factors	242.01	3 (2)	531.38	231.57	2.29	2.44E-03
132	Elongation factor-like protein (<i>Solanum tuberosum</i>)	Q3HVL1	translation factors	520.84	9 (7)	1380.84	3088.50	0.45	9.38E-07
133	Eukaryotic initiation factor 4A-13, fragment (<i>Nicotiana tabacum</i>)	Q40466	translation factors	262.19	2	1179.60	468.21	2.52	1.89E-06
134	Putative elongation factor, fragment (<i>Arabidopsis thaliana</i>)	Q8H145	translation factors	348.11	5 (2)	683.51	311.96	2.19	9.78E-04
135	Ripening regulated protein DDTFR10 (<i>Solanum lycopersicum</i>)	Q9FR30	translation factors	544.59	5 (3)	1506.39	2319.32	0.65	9.78E-06
Signal transduction									
136	14-3-3 protein, fragment (<i>Nicotiana tabacum</i>)	Q948K2	mediators	361.45	6 (1)	50.69	13.04	3.89	6.88E-03
137	14-3-3-like protein 16R (<i>Solanum tuberosum</i>)	P93784	mediators	784.61	8 (3)	972.82	254.28	3.83	7.06E-05
138	14-3-3-like protein B (<i>Nicotiana tabacum</i>)	O49995	mediators	674.29	8 (1)	331.01	141.93	2.33	7.01E-05
139	14-3-3-like protein GF14 iota (<i>Arabidopsis thaliana</i>)	Q9C5W6	mediators	160.34	2 (1)	170.08	17.28	9.84	5.78E-04
140	GDP dissociation inhibitor (<i>Arabidopsis thaliana</i>)	Q9LXC0	others	326.95	5 (2)	335.20	294.27	1.14	7.86E-03
141	Pollen tube RhoGDI2 (<i>Nicotiana tabacum</i>)	Q1ZZN8	others	157.87	2	582.36	1625.61	0.36	1.14E-05
142	Rab-GDP dissociation inhibitor (<i>Nicotiana benthamiana</i>)	C0LSK7	others	397.37	6 (1)	23.36	2.78	8.40	3.49E-03
143	Rab-GDP dissociation inhibitor (<i>Solanum lycopersicum</i>)	A5CKE3	others	666.88	9 (3)	1163.17	933.58	1.25	5.17E-03
Transporters									
144	ADP/ATP carrier protein 1, mitochondrial (<i>Arabidopsis thaliana</i>)	P31167	purine/pyrimidines	152.95	2	522.66	526.99	0.99	4.23E-03
145	V-type proton ATPase catalytic subunit A (<i>Arabidopsis thaliana</i>)	O23654	transport ATPases	161.04	3	689.26	236.15	2.92	5.12E-05
146	V-type proton ATPase subunit B2 (<i>Arabidopsis thaliana</i>)	Q9SZN1	transport ATPases	184.46	3	1098.07	903.28	1.22	2.00E-02
Unclassified									
147	ArcA 3 protein, fragment (<i>Nicotiana tabacum</i>)	O65851	–	160.59	2	1006.45	545.49	1.85	9.11E-04
148	AT1G07750 protein, fragment (<i>Arabidopsis thaliana</i>)	B9DHT6	–	258.93	3	1951.12	5154.57	0.91	1.92E-03
149	Putative uncharacterised protein (<i>Arabidopsis thaliana</i>)	Q56WY3	–	200.94	4 (1)	100.28	79.27	1.27	1.35E-04
150	Putative uncharacterised protein (<i>Solanum tuberosum</i>)	Q38HU5	–	549.18	6	1699.91	1026.93	1.66	1.12E-05

4.5 The identification of phosphorylation sites

Amongst the 139 proteins identified by both in-gel and gel-free approaches performed on the phosphoprotein-enriched sample, only one exact phosphorylation site was unambiguously identified, particularly phosphorylated threonine in the KYT*EVKPALK peptide from 5-methyltetrahydropteroyltriglutamate–homocysteine methyltransferase (#82). Thus it was of a key importance to identify the phosphorylation sites in more of the phosphoprotein candidates since the MS-



identification of a phosphorylation site is a definite proof that a protein was really phosphorylated, and was not a false positive.

To enable the unambiguous identification of a higher number of phosphorylation sites, parallel phosphopeptide enrichment using titanium dioxide (a technique known also as TiO₂-MOAC) was performed (Pinkse et al., 2004; Beck et al., 2011). The total proteins extracted by TCA/acetone from mature pollen were trypsin-digested and the peptide mixture was enriched. The phosphopeptide-enriched fraction was analysed by nLC-MS/MS (for a representative MS/MS spectrum, see Fig. 4.6).

Since it was difficult (if not impossible) to assign a given phosphopeptide to a particular homologue, and many of the proteins were identified by homologous sequences from different plant species, the identified phosphorylation sites were listed into protein groups containing more isoforms of the same protein. In total, 69 phosphopeptides catalogued into 19 protein groups were identified by titanium dioxide enrichment (Tab. 4.3 and Tab. S3).

Although all of these 69 peptides were shown to be phosphorylated, the exact position of phosphorylation site could not be assigned in case of six peptides pinpointed in Tab. 4.3 in gray. Furthermore, several of these peptides led to the identification of the same phosphorylation site (e.g. a couple of peptides where one was completely cleaved and the second contained one mis-cleavage site or a couple of peptides where one represented the native form and the other the modified form, for instance containing carbamylated cysteine), so only 51 distinct phosphorylation sites present in 50 phosphopeptides (one peptide was doubly phosphorylated) were identified after phosphopeptide enrichment. Together with the only phosphorylation site from the gel-free approach following phosphoprotein enrichment, 52 individual phosphorylation sites from 18 groups of proteins were revealed (Tab. 4.3). The phosphorylation sites were detected exclusively on serine (35 sites) and threonine (17); there was not identified any site on tyrosine.

Only one of the phosphorylated peptides was doubly phosphorylated – peptide MHLFVSRLS*HSTQRSIFGT*VK from ATPase subunit 8. The other phosphopeptides with an unambiguous phosphorylation site were singly phosphorylated.

Several phosphoprotein candidates were shown to be multiply phosphorylated, for instance vacuolar H⁺ ATPase (#1), a ripening regulated protein

homologue (#5), globulin-like protein (#6), fructose biphosphate aldolase (#9), glyceraldehyde-3-phosphate dehydrogenase (#10), 5-methyltetrahydropteroyl-triglutamate–homocysteine methyltransferase (#11), adenosyl homocysteinase (#12), 60S ribosomal protein (#15), and RhoGDI (#18). Besides, only one phosphorylation site was identified in 2,3-bisphosphoglycerate-independent phosphoglycerate mutase (#3), and heat shock protein 90 (#13), amongst others.

Table 4.3 – List of phosphorylation sites identified after the TiO₂-MOAC phosphopeptide enrichment from mature pollen. The proteins are grouped according to their names, in some cases listing together several isoforms of the same protein since they are hard to be distinguished from each other due to tobacco not being completely sequenced. The phosphorylation site is highlighted in bold and the given phosphorylated amino acid is followed by an asterisk. The oxidised methionine is pinpointed as M^{ox} whereas carbamidomethylated cystein is written as C^{cm}. The peptides with ambiguous position of phosphorylation site are shown in gray. The superscripted number behind the accession number indicates database: a) UniProt, 90 % homology clusters, *Viridiplantae*; b) TIGR EST *Nicotiana tabacum*. MH⁺ [Da] – molecular weight in daltons; pRS sc. – pRS score; Mascot ion sc. – Mascot ion score; # MC – number of mis-cleavages.

	Protein name	Sequence	Protein group accessions	pRS site probabilities	MH ⁺ [Da]	pRS sc.	Mascot ion sc.	Sequester XCorr	# MC
1	Plasma membrane ATPase 4 (<i>Nicotiana plumbaginifolia</i>)	GLDIETIQQH Y T*V	NT_TC82708_1 ^a	T(6): 0.0; Y(11): 0.0; T(12): 100.0	1596.73	201	55	2.89	0
	ATPase subunit 8 (<i>Desmarestia viridis</i>)	M ^{ox} HLFVS R LS*HSTQRSIFGT*VK	NT_TC78171_1 ^a	S(6): 13.0; S(9): 60.9; S(11): 13.1; T(12): 13.1; S(15): 5.4; T(19): 94.5	2607.24	37		3.40	2
	Vacuolar H ⁺ -ATPase A1 subunit isoform (<i>Solanum lycopersicum</i>)	P S*LFGGPM T TFEDSEK	NT_TC79070_1 ^a	S(2): 100.0; T(9): 0.0; T(10): 0.0; S(14): 0.0	1822.76	171	72		0
	Vacuolar H ⁺ -ATPase A1 subunit isoform (<i>Solanum lycopersicum</i>)	P S*LFGGPM ^{ox} T TFEDSEK	NT_TC79070_1 ^a	S(2): 100.0; T(9): 0.0; T(10): 0.0; S(14): 0.0	1838.75	117	49		0
	Vacuolar H ⁺ -ATPase A1 subunit isoform (<i>Solanum lycopersicum</i>)	G V S *VPALDK	NT_TC79070_1 ^a	S(3): 100.0	965.47	95	33		0
2	Allyl alcohol dehydrogenase (<i>Nicotiana tabacum</i>)	IEGSYVESFAP G S*PITGYGVAK	Q9SLN8 ^b	S(4): 0.0; Y(5): 0.0; S(8): 0.0; S(13): 100.0; T(16): 0.0; Y(18): 0.0	2309.07	177	60	4.14	0
	Allyl alcohol dehydrogenase (<i>Nicotiana tabacum</i>)	KIEGSYVESFAP G S*PITGYGVAK	NT_TC78085_1 ^a	S(5): 0.0; Y(6): 0.0; S(9): 0.0; S(14): 99.5; T(17): 0.2; Y(19): 0.2	2437.17	72	46		1
3	2,3-bisphosphoglycerate-independent phosphoglycerate mutase (<i>Nicotiana tabacum</i>)	AHGNAVGLPTEDDM ^{ox} G N S *EVGHN ALGAGR	NT_TC77653_1 ^a , NT_TC80529_1 ^a	T(10): 0.2; S(17): 99.8	2842.23	77	36	3.30	0

4	Actin, cytoplasmic 2 (<i>Triakis scyllium</i>)	C ^{cm} DVDIRKDLYANTVLSGGTTM ^{ox} YP GIADR	NT_TC90723_1 ^a	Y(10): 4.7; T(13): 38.2; S(16): 8.1; T(19): 16.4; T(20): 16.4; Y(22): 16.4	3197.45	9		2.93	2
5	Ripening regulated protein DDTFR10-like (<i>Solanum tuberosum</i>)	ISGVSGEGAGVTVEGSAPITEEAVAT *PPAADTK	NT_TC77461_1 ^a	S(2): 0.0; S(5): 0.0; T(12): 0.0; S(16): 0.0; T(20): 0.0; T(26): 99.9; T(32): 0.0	3148.50	129	49	3.61	0
	Ripening regulated protein DDTFR10-like (<i>Solanum lycopersicum</i>)	DSDQEDGSIAPFS*GK	NT_TC87771_1 ^a	S(2): 0.0; S(8): 0.0; S(13): 100.0	1632.64	121	34		0
6	Globulin-like protein (<i>Arabidopsis thaliana</i>)	TLVSS*QTAQGIVK	NT_TC79679_1 ^a , NT_TC84734_1 ^a NT_TC86230_1 ^a	T(1): 0.0; S(4): 1.7; S(5): 96.6; T(7): 1.7	1411.72	152	76		0
	Globulin-like protein (<i>Arabidopsis thaliana</i>)	LDS*GFQMPEPK	NT_TC79679_1 ^a , NT_TC84734_1 ^a NT_TC86230_1 ^a	S(3): 100.0	1328.56	144	51	2.94	0
7	Alpha-tubulin, Fragment (<i>Gossypium hirsutum</i>)	TVQFVDWC ^{cm} PT*GFK	Q9SQ71 ^b	T(1): 0.0; T(10): 100.0	1664.72	200	51	3.58	0
	Tubulin alpha-4 chain (<i>Gossypium hirsutum</i>)	TIQFVDWC ^{cm} PT*GFK	B9DFF8 ^b	T(1): 0.0; T(10): 100.0	1678.74	186	51	3.79	0
	Alpha-tubulin (<i>Nicotiana tabacum</i>)	RTIQFVDWC ^{cm} PT*GFK	NT_TC77583_1 ^a , NT_TC77710_1 ^a NT_TC78231_1 ^a , NT_TC80038_1 ^a	T(2): 0.0; T(11): 100.0	1834.84	193	51	3.18	1
	Alpha-tubulin (<i>Nicotiana tabacum</i>)	TIQFVDWC ^{cm} PT*GFK ^{cm} GINYQPPT VVPGGDLAK	NT_TC77583_1 ^a , NT_TC77710_1 ^a NT_TC78231_1 ^a , NT_TC80038_1 ^a	T(1): 1.4; T(10): 96.8; Y(18): 1.4; T(22): 0.4	3545.68	40		3.67	1
8	Pyruvate decarboxylase isozyme (<i>Nicotiana tabacum</i>)	IFVPEGT*PLK	NT_TC80900_1 ^a	T(7): 100.0	1180.60	115	38		0
	Pyruvate decarboxylase isozyme (<i>Nicotiana tabacum</i>)	IFVPEGT*PLKSEPNEPLR	NT_TC80900_1 ^a	T(7): 100.0; S(11): 0.0	2103.06	138	37	3.46	1
	Pyruvate decarboxylase isozyme (<i>Nicotiana tabacum</i>)	RIFVPEGT*PLK	NT_TC80900_1 ^a	T(8): 100.0	1336.70	125	36		1
9	Fructose-bisphosphate aldolase (<i>Ricinus communis</i>)	GILAADES*GTIGKR	B9SRH4 ^b ; Q2PYX3 ^b	S(8): 97.0; T(9): 2.9; T(11): 0.1	1568.77	151	61	4.57	1
	Fructose-bisphosphate aldolase (<i>Ricinus communis</i>)	GILAADES*GTIGK	B9SRH4 ^b ; Q2PYX3 ^b	S(8): 96.3; T(9): 3.5; T(11): 0.2	1412.67	150	53		0
	Fructose-bisphosphate aldolase (<i>Ricinus communis</i>)	YADELIANAAYIGT*PGK	B9SRH4 ^b	Y(1): 0.0; Y(11): 0.0; T(14): 100.0	1846.86	276	92	4.02	0
	Fructose-bisphosphate aldolase (<i>Solanum lycopersicum</i>)	YAGSSNLSEGA*S*ESLHVK	NT_FG156892_1 ^a	Y(1): 0.0; S(4): 0.0; S(5): 0.0; S(8): 0.0; S(12): 0.0; S(14): 100.0	1915.84	164	67	4.43	0
	Fructose-bisphosphate aldolase (<i>Solanum lycopersicum</i>)	TMPAAVPAVVFLS*GGQSEEEATR	NT_FG156892_1 ^a	T(1): 0.0; S(13): 100.0; S(17): 0.0; T(22): 0.0	2427.14	185	66	4.19	0

	Fructose-bisphosphate aldolase (<i>Solanum lycopersicum</i>)	TM ^{ox} PAAVPAVVFLS*GGQSEEEATR	NT_FG156892_1 ^a	T(1): 0.0; S(13): 100.0; S(17): 0.0; T(22): 0.0	2443.12	167	44	4.42	0
	Fructose-bisphosphate aldolase (<i>Solanum tuberosum</i>)	YAGATNLSEGASES*LHVK	NT_TC78239_1 ^a	Y(1): 0.0; T(5): 0.0; S(8): 0.0; S(12): 0.0; S(14): 100.0	1913.87	191	73	3.95	0
	Fructose-bisphosphate aldolase (<i>Solanum tuberosum</i>)	TMPAAVPAVVFLS*GGQSEEEATVNLNAMNK	NT_TC78239_1 ^a	T(1): 0.0; S(13): 97.8; S(17): 2.2; T(22): 0.0	3155.48	93	46	4.02	0
	Fructose-bisphosphate aldolase (<i>Solanum tuberosum</i>)	TM ^{ox} PAAVPAVVFLSGGQSEEEAT*VNLNAMNK	NT_TC78239_1 ^a	T(1): 0.0; S(13): 0.4; S(17): 0.4; T(22): 99.3	3171.47	87	35		0
	Fructose-bisphosphate aldolase (<i>Solanum tuberosum</i>)	RFS*SINVENVESNR	NT_TC78239_1 ^a NT_TC118911_1 ^a	S(3): 99.9; S(4): 0.1; S(12): 0.0	1730.78	194	64	3.59	1
	Fructose-bisphosphate aldolase (<i>Solanum tuberosum</i>)	YAII ^{cm} QQNGLVPIVEPEILVDGS*HDINK	NT_TC78239_1 ^a NT_TC118911_1 ^a	Y(1): 0.0; S(23): 100.0	3214.59	124	49	3.18	0
10	Glyceraldehyde-3-phosphate dehydrogenase (<i>Dimocarpus longan</i>)	FGIVEGLM ^{ox} TTVHSITAT*QK	C0LDX1 ^b , D7UBG8 ^b , D0EF74 ^b , C0SQK4 ^b	T(9): 0.0; T(10): 0.0; S(13): 0.0; T(15): 0.0; T(17): 100.0	2129.03	163	54	3.98	0
	Glyceraldehyde-3-phosphate dehydrogenase (<i>Tamarix hispida</i>)	FGIVEGLMTTVHSLTAT*QK	D0EF74 ^b , C0LDX1 ^b , D7UBG8 ^b , C0SQK4 ^b	T(9): 0.0; T(10): 0.0; S(13): 0.0; T(15): 0.0; T(17): 100.0	2113.04	217	59	4.91	0
	Glyceraldehyde-3-phosphate dehydrogenase, Fragment (<i>Antirrhinum majus</i>)	FGIVEGLMATVHS*ITATQK	B9V155 ^b	T(10): 0.8; S(13): 98.4; T(15): 0.8; T(17): 0.0	2083.04	107		3.38	0
	Glyceraldehyde-3-phosphate dehydrogenase, cytosolic (<i>Petroselinum crispum</i>)	LTGMSFRVPTVDVSVDLTAR	NT_TC82500_1 ^a	T(2): 49.3; S(5): 49.3; T(10): 1.4; S(14): 0.0; T(19): 0.0	2343.19	105	50	4.06	1
11	5-methyltetrahydropteroyltriglutamate-homocysteine methyltransferase (<i>Arabidopsis thaliana</i>)	YGAGIGPGVYDIHS*PR	O50008 ^b , Q42699 ^b , Q2QLY5 ^b	Y(1): 0.0; Y(10): 0.0; S(14): 100.0	1738.80	198	58	3.74	0
	5-methyltetrahydropteroyltriglutamate-homocysteine methyltransferase (<i>Quercus mongolica</i> subsp. <i>Crispula</i>)	M ^{ox} ARGNASVPAM ^{ox} EMT*K	B0M0H3 ^b	S(7): 7.8; T(14): 92.2	1705.71	20		3.55	1
12	Adenosylhomocysteinase (<i>Zea mays</i>)	LVGSEET*TTGVKR	Q8W530 ^b ; Q9SP98 ^b	S(5): 0.0; T(8): 95.2; T(9): 4.5; T(10): 0.2	1555.77	121	56		1
	Adenosylhomocysteinase (<i>Nicotiana glauca</i>)	VKDMS*QADFGR	NT_TC120215_1 ^a NT_TC79998_1 ^a	S(5): 100.0	1333.56	161	47		1
	Adenosylhomocysteinase (<i>Nicotiana glauca</i>)	VKDM ^{ox} S*QADFGR	NT_TC120215_1 ^a NT_TC79998_1 ^a	S(5): 100.0	1349.56	227	45	2.92	1
13	Heat shock protein 90 (<i>Nicotiana tabacum</i>)	EGLKLEDES*EDEK	NT_TC98434_1 ^a NT_TC93842_1 ^a	S(8): 100.0	1471.62	125	31	2.83	1
14	Luminal-binding protein 5 precursor (<i>Nicotiana tabacum</i>)	NQIDEIVLVGGSTRIPK	NT_TC77897_1 ^a	S(12): 50.0; T(13): 50.0	1918.98	0		2.85	1

15	60S ribosomal protein L12-2 (<i>Physcomitrella patens</i> subsp. <i>Patens</i>)	IGPLGLS*PK	A9RZZ0 ^b , B6T1W9 ^b , Q9ZSL1 ^b	S(7): 100.0	961.51	158	57		0
	60S ribosomal protein L24-1 (<i>Populus balsamifera</i> subsp. <i>Trichocarpa</i>)	S*IVGATLEVIQK	B9NJD1 ^b	S(1): 100.0; T(6): 0.0	1337.71	200	71		0
	60S ribosomal protein L24-1 (<i>Populus balsamifera</i> subsp. <i>Trichocarpa</i>)	S*IVGATLEVIQKK	B9NJD1 ^b	S(1): 100.0; T(6): 0.0	1465.80	124	50		1
	60S ribosomal protein L8 (<i>Solanum lycopersicum</i>)	FRS*LDFGER	NT_TC101390_1 ^a	S(3): 100.0	1206.53	171	54		1
	60S ribosomal protein L19 (<i>Capsicum annuum</i>)	LAQGPGERPVQPAAPAAAAPQAQPAQGS*K	NT_TC78366_1 ^a	S(27): 100.0	2716.36	78	37	4.58	0
	60S ribosomal protein L19 (<i>Capsicum annuum</i>)	EKTLS*DQFEAR	NT_TC78366_1 ^a NT_TC78371_1 ^a NT_TC78814_1 ^a NT_TC80876_1 ^a	T(3): 0.0; S(5): 100.0	1403.62	167	54		1
	60S ribosomal protein L19 (<i>Capsicum annuum</i>)	TLS*DQFEAR	NT_TC78366_1 ^a NT_TC78371_1 ^a NT_TC78814_1 ^a NT_TC80876_1 ^a	T(1): 0.1; S(3): 99.9	1146.48	118	34		0
	60S ribosomal protein L19 (<i>Capsicum annuum</i>)	LAQGPGERPAQPAAPAASAQTAQGG*KK	NT_TC80876_1 ^a	S(18): 1.4; T(21): 10.5; S(26): 88.1	2725.34	82	34	4.01	1
	60s acidic ribosomal protein-like protein (<i>Solanum tuberosum</i>)	LASVPC ^{cm} GGGGGGVAVAAPAGGAA AAAS*AAEEKK	NT_TC91479_1 ^a	S(3): 0.0; S(27): 100.0	2860.37	77		3.18	1
16	Nascent polypeptide-associated complex subunit alpha-like protein 2 (<i>Arabidopsis thaliana</i>)	SDVSPSTAAAEEDEEEVEDETGVEPR	NT_TC77572_1 ^a	S(1): 25.0; S(4): 25.0; S(6): 25.0; T(7): 25.0; T(21): 0.0	2799.14	82	39	3.44	0
	Nascent polypeptide-associated complex subunit alpha-like protein 2 (<i>Arabidopsis thaliana</i>)	SDVSPSTAAAEEDEEEVEDETGVEPR	NT_TC79086_1 ^a	S(1): 25.0; S(4): 25.0; S(6): 25.0; T(7): 25.0; T(22): 0.0	2928.18	94		3.38	0
	Alpha chain of nascent polypeptide associated complex (<i>Nicotiana tabacum</i>)	APNLS*NVISKPEPSTVAQDDEDVDETGVEPK	NT_TC80057_1 ^a NT_TC92601_1 ^a	S(5): 90.3; S(9): 8.1; S(14): 0.8; T(15): 0.8; T(26): 0.0	3360.54	105	50	4.33	0
17	Eukaryotic translation initiation factor 2 beta subunit-like (<i>Solanum tuberosum</i>)	VVIQDPADDS*VDSLAEK	Q2V9B2 ^b	S(10): 100.0; S(13): 0.0	1880.86	220	67	3.59	0
	Eukaryotic translation initiation factor 2 beta subunit-like (<i>Solanum tuberosum</i>)	TENLS*VSEGLEATFSGK	Q2V9B2 ^b	T(1): 0.0; S(5): 100.0; S(7): 0.0; T(13): 0.0; S(15): 0.0	1848.83	200	85	4.16	0
	Eukaryotic translation initiation factor 2 family protein (<i>Arabidopsis thaliana</i>)	IGDNSFSSALLDEEEADTSVSK	NT_DV158562_1 ^a	S(5): 0.0; S(7): 0.0; S(8): 0.0; T(19): 2.1; S(20): 48.9; S(22): 48.9	2523.07	72	39	4.08	0
	Eukaryotic translation initiation factor 2 family protein (<i>Arabidopsis thaliana</i>)	ETVEEGAVES*AAAK	NT_TC85822_1 ^a	T(2): 0.0; S(10): 100.0	1470.64	182	63	3.48	0
	Eukaryotic translation initiation factor 3 subunit B (<i>Nicotiana tabacum</i>)	LRDGEAS*DEEEYEAK	P56821 ^b	S(7): 100.0; Y(13): 0.0	1949.77	206	62	3.84	1
	Eukaryotic translation initiation factor 4g, putative (<i>Vitis vinifera</i>)	AEPDDWEDAADIST*PK	F6GVD5 ^b	S(13): 0.0; T(14): 100.0	1839.73	274	103		0

	Translation initiation factor eIF4E (<i>Nicotiana tabacum</i>)	VDEVEKPAS*LEESK	D3UW24 ^b	S(9): 100.0; S(13): 0.0	1639.75	126	50		0
	Translation initiation factor eIF4E (<i>Nicotiana tabacum</i>)	VDEVEKPVSLLEESKNT*R	NT_DV158475_1 ^a	S(9): 0.0; S(13): 4.4; T(16): 91.2; T(17): 4.4	2140.02	51	34		1
	Eukaryotic initiation factor 4B (<i>Arabidopsis thaliana</i>)	S*EGPAALQGGVM ^{ox} EVKPKPK	NT_FG166442_1 ^a	S(1): 100.0	2019.00	87		2.83	0
	Eukaryotic translation initiation factor 3 subunit 8 (<i>Nicotina tabacum</i>)	LAELT*EGEGEAESIEENK	NT_TC79735_1 ^a	T(5): 100.0; S(13): 0.0	2027.87	206	77		0
	Eukaryotic initiation factor 4B (<i>Arabidopsis thaliana</i>)	S*PWGNIGAWAAEAER	NT_TC95936_1 ^a	S(1): 100.0	1694.73	189	79	4.50	0
18	Pollen tube RhoGDI2 (<i>Nicotiana tabacum</i>)	T*PIADSDSEIEHEPVGEK	Q1ZZN8 ^b	T(1): 100.0; S(6): 0.0; S(8): 0.0	2032.88	165	70		0
	Pollen tube RhoGDI2 (<i>Nicotiana tabacum</i>)	GGTKT*PIADSDSEIEHEPVGEK	NT_TC77816_1 ^a	T(3): 5.0; T(5): 94.7; S(10): 0.3; S(12): 0.0	2376.06	112	35	3.54	1
	Pollen tube RhoGDI2 (<i>Nicotiana tabacum</i>)	GIIVGSDSDPEIENENVGNNNDNRV*S* R	NT_TC93883_1 ^a	S(7): 0.0; S(25): 100.0	2906.29	84	35		1
19	RabGAP/TBC domain-containing protein-like (<i>Solanum tuberosum</i>)	SLGS*ASGGFPPVER	NT_TC84637_1 ^a	S(1): 0.2; S(4): 99.5; S(6): 0.2	1472.64	99	39		0

5 Discussion

5.1 MOAC and its specificity for phosphoprotein enrichment

This diploma thesis presents a list of phosphoprotein candidates that likely play a role in the switch from quiescent mature pollen to the 30-minute activated pollen. To acquire these data, a combination of phosphoprotein enrichment using MOAC with aluminium hydroxide matrix, and phosphopeptide enrichment applying TiO₂-MOAC was performed.

The specificity of MOAC phosphoprotein enrichment applying aluminium hydroxide matrix was demonstrated by six indirect evidences.

(1) The SDS-PAGE of the MOAC fractions stained with ProQ Diamond Phosphoprotein Gel Stain showed a remarkably higher signal in the phosphoprotein-enriched eluate compared to the flow-through and supernatant after the first wash. This shows that the majority of phosphoproteins was captured by the aluminium hydroxide particles, and subsequently appeared in the eluate.

(2) CBB G250 staining of the same gel revealed a different protein pattern of the enriched eluate compared to the original crude extract. Again, this indicates the enrichment to be at least partly specific.

(3) When looking on 2D-GE protein spectra of the phosphoprotein-enriched eluates, it was obvious that some of the identified proteins were detected in two or multiple spots of the same molecular weight but of different pI. Such two neighbouring spots represented very likely the same isoform of a protein, differing in the degree of phosphorylation. Protein phosphorylation causes a shift to more acidic pI whereas molecular weight remains virtually unchanged.

(4) The newly-phosphorylated proteins during *in vitro* phosphorylation had mostly the molecular weight of 35–70 kDa. This range practically overlapped with the proteins identified after phosphoprotein enrichment.

(5) The functional categories, which were over-represented in the presented data set, were very likely involved in the pollen re-hydration and activation processes. Furthermore, their regulation via phosphorylation is very suggestive.

(6) Fifty-two particular phosphorylation sites in several of the identified phosphoprotein candidates were experimentally assigned by MS.

However, it remained a speculation how many false positives could have appeared on the list of phosphoprotein candidates. It is possible that metal-binding proteins were caught via their domain(s) with a high metal-affinity. Amongst the presented candidates, calreticulin could be bound by the calcium-binding site (Hrubá et al., 2005), actin by its magnesium/calcium-binding site (Selden et al., 1987), and alcohol dehydrogenase by its zinc-binding site (Thompson et al., 2007).

5.2 Detected phosphorylation sites

Collectively, the unambiguous position of 52 phosphorylation sites was experimentally assigned by MS following phosphopeptide (51 sites), and phosphoprotein (1 site) enrichment. The most frequently phosphorylated amino acid was serine (35 sites), followed by threonine (17). No site was identified on tyrosine. Such ratio is in accordance with the published data from *Arabidopsis thaliana* (Benschop et al., 2007; Sugiyama et al., 2008; van Bentem et al., 2008; Mayank et al., 2012). However, the data presented in this diploma thesis represent only a limited set of 52 phosphorylation sites so they could be more or less biased.

Although additional phosphopeptides were identified after TiO₂ phosphopeptide enrichment, only the peptides that confirmed the position of a phosphorylation site in any of the phosphoprotein candidates identified after phosphoprotein enrichment were presented in this diploma thesis.

5.3 Un-detectable phosphorylation sites

Although 52 phosphorylation sites present in 18 groups of proteins were unambiguously assigned, the position of the phosphorylation site(s) was not successfully determined in all phosphoprotein candidates identified after the phosphoprotein enrichment. This could be caused by three reasons.

(1) Only peptides that are ionisable and thus detectable during MS contribute to protein identification. If the peptides produced by the enzymatic digest are too short or too long, they are not accessible by MS. If the phosphorylation site occurred on such undetectable peptide, it could not be identified. Trypsin is a specific protease that cleaves the polypeptide chain behind lysine or arginine (if either is not followed by proline) but there are also alternative specific proteases with different specificities so the peptides inaccessible by trypsin can be detectable if an alternative specific protease was applied instead (Gauci et al., 2009). Furthermore, the digestion by a

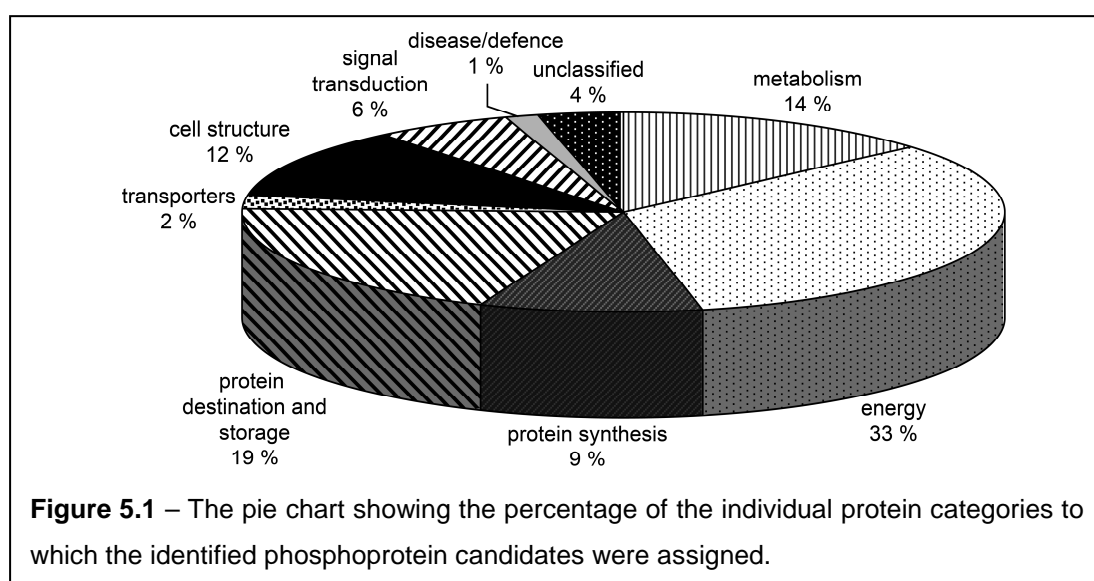
pair of alternative specific proteases can be performed sequentially (Gilmore et al., 2012). If a single protein was to be mapped, even the low-specificity proteases can be applied (Schlosser et al., 2005).

(2) A single peptide could carry one or more phosphorylation sites. The multiply-phosphorylated peptides are harder to be ionised and/or fragmented by MS/MS, and consequently their identification is more challenging. Moreover, TiO₂ phosphopeptide enrichment was repeatedly shown to be less efficient in catching the multiply-phosphorylated peptides compared to IMAC (Bodenmiller et al., 2007; Aryal and Ross, 2010). If a particular protein contained two proximal phosphorylation sites, it could result in a phosphopeptide with multiple phosphorylation sites, identification of which would be more challenging.

(3) The last reason is that every phosphoproteomic method biases towards a different group of phosphopeptides (Bodenmiller et al., 2007). Therefore, even the rarely-used phosphoproteomic methods can show their importance although they could be considered less selective and/or sensitive than the more efficient and/or more frequently-used ones. They are worth applying since they will very likely reveal a different subset of phosphopeptides. Furthermore, it is usually worth employing both phosphoprotein- and phosphopeptide-enriching methods since their advantages and disadvantages are practically complementary.

5.4 *Biological role of the phosphorylated candidates*

As mentioned above, a majority of the identified phosphoprotein candidates is likely to play an important role during pollen activation. Their possible function will



now be discussed in more detail. However, this section should not comprehensively discuss the role of all identified phosphoprotein candidates but rather should highlight the function of several of the most interesting ones.

The 139 identified phosphoprotein candidates fell into categories that show a broad range of biological functions (Fig. 5.1). Nine per cent of the candidates are involved in protein synthesis, comprising for instance 60S acidic ribosomal protein-like protein, a variety of translation initiation and elongation factors, a ripening-regulated protein homologue and α -subunit of a nascent polypeptide-associated complex. Eukaryotic initiation factor 4A isoform 13 (eIF4A-13) was of a higher abundance in mature pollen compared to the activated pollen. We can only hypothesise that its inhibitory phosphorylation was important in mature pollen, and was reduced in the activated pollen where active translation is of vital importance. In tobacco, there are more than ten isoforms of initiation factor 4A (Owtrim et al., 1994) with the eIF4A-8 specifically expressed in male gametophyte (Brander and Kuhlemeier, 1995). This pollen-specific isoform was phosphorylated upon pollen rehydration (op den Camp and Kuhlemeier, 1998). The antagonistic level of phosphorylation between more protein isoforms documents the need for acquiring the experimental data for each isoform separately since the data extrapolation from a distinct isoform is not sufficient.

Protein destination and storage represented a process where 19 % phosphoprotein candidates were involved. Chaperones play an important role during protein folding – i.e. acquiring the proper tertiary structure, which is very important for protein function. The importance of chaperones is mostly obvious under stress conditions and/or during intense translation, as is the case of activated pollen grain. Since mature pollen is a quiescent structure, it is likely that the chaperones are ready but inactive, and that their activity after the switch to the rapidly-growing pollen tube is regulated via phosphorylation or dephosphorylation as was demonstrated in rat liver (Cvoro et al., 1999). The proper protein folding in the endoplasmic reticulum is checked by luminal-binding protein, endoplasmin and calreticulin. The last one also sequestered calcium ions in endoplasmic reticulum during pollen tube growth (Hrubá et al., 2005), and was shown to be phosphorylated by CK2 kinase (Baldan et al., 1996). Leucine aminopeptidases cleave the terminal amino acids (mostly but not exclusively leucine) from their target protein (Matsui et al., 2006). In plants, they play an important role during wound responses and other various stresses, beside

other functions (Waditee-Sirisattha et al., 2011). The pollen maturation resembling drought stress quite likely requires the activity of leucine aminopeptidases as well as their phosphorylation regulation.

About one third of the identified phosphoprotein candidates was related to energy production. The phosphorylation regulation of the energy-related proteins upon pollen rehydration is very probable since the activated pollen has very different energetic demands compared to the quiescent mature pollen. It is a well established fact that metabolic processes are controlled, amongst other mechanisms, via protein phosphorylation. Several glycolytic enzymes, pyruvate dehydrogenase, and citric acid cycle enzymes are few examples of the proteins regulated by phosphorylation (Garnak and Reeves, 1979; Plaxton, 1996; Kolobova et al., 2001). The antagonistic energy demands of mature pollen and 30-minute activated pollen will probably be also reflected in the ATP requirements of the respective stages. It is likely that F_0F_1 ATPase will be regulated via phosphorylation. The last example of energy-related protein to be mentioned is alcohol dehydrogenase. Together with pyruvate decarboxylase it is responsible for pyruvate fermentation. The presence of these enzymes during tobacco pollen development was reported by Tadege and Kuhlemeier (1997), and their regulatory phosphorylation was strongly suggestive.

The non-energy metabolic processes were represented by 14 % phosphoprotein candidates. The phosphorylation sites were identified in several of them, for instance 5-methyltetrahydropteroyltriglutamate–homocysteine *S*-methyltransferase, adenosylhomocysteinase, and nucleoside diphosphate kinase. Inorganic nitrogen is incorporated into organic molecules by glutamine synthetase, phosphorylation of which was reported in *Medicago truncatula*, where it increased affinity to the 14-3-3 protein (Lima et al., 2006). Glutamine synthetase in complex with the 14-3-3 protein is directed to proteolytic cleavage. The higher concentration of 14-3-3 protein was detected in mature pollen that leads to speculation that a higher activity of glutamine synthetase will be expected in the activated pollen whereas its majority should be degraded in mature pollen. However, such conclusion cannot be solid since 14-3-3 proteins were reported to interact with several of the identified phosphoprotein candidates, for instance V-type of H^+ -ATPase (Svennelid et al., 1999), and glyceraldehyde-3-phosphate dehydrogenase (Bustos and Iglesias, 2003).

Regulatory proteins are highly important for switching between the quiescent mature pollen and the rapidly-growing pollen tube. Moreover, regulatory

mechanisms are necessary for pollen tube guidance *in vivo*. The signalling role was assigned to 6 % phosphoprotein candidates. It is likely that many of the signalling-related proteins remained unidentified possibly because they tend to be of lower abundance (e.g. Eidelman et al., 2010). The dimerisation of the above-mentioned regulatory 14-3-3 proteins is regulated via phosphorylation (Shen et al., 2003). The Rab GTPases play a crucial role during endocytosis, vesicular trafficking, and exocytosis – all these processes are of a vital importance during pollen tube elongation (Cheung et al., 2002; de Graaf et al., 2005). Rab GTPases bind GTP in the active membrane whilst Rab associated with a GDP remains in its inactive form in cytosol. Rab and other groups of small GTPases dimerise with guanine-nucleotide dissociation inhibitors (GDI). These proteins hold the GTPases in cytoplasm and prevent the GTP/GDP exchange. RhoGDI, phosphorylation site of which was presented in this diploma thesis, was previously reported to play an important role in pollen tube growth (Klahre et al., 2006).

Cell structure category contains proteins that are parts of cytoskeleton and that take part in cell wall formation. These processes vital for pollen tube growth are connected with 12 % phosphoprotein candidates. Cytoskeleton is composed of microtubules and microfilaments, and its dynamics is regulated by a variety of microtubule-associated and actin-binding proteins (Raudaskoski et al., 2001). However, phosphorylation of actin monomers themselves was also demonstrated – it caused bending of leaves in ticklish plant (*Mimosa pudica*; Kameyama et al., 2000). A similar regulatory role of tubulin phosphorylation is suggestive. A rapid cell wall formation starts after the pollen activation, thus the enzymes catalysing this process are very likely inhibited inside mature pollen. Cell wall synthesis is connected with carbohydrate metabolism, so many phosphoprotein candidates of this nature are listed to the metabolic category. A reversibly glycosylated protein (alternatively named also α -1,4-glucan-protein synthase) is required for polysaccharide anabolism, and its important role during male gametophyte development was documented in *Arabidopsis thaliana* (Drakakaki et al., 2006).

Amongst 2 % transport proteins were listed for instance V-H⁺-ATPase and ADP/ATP mitochondrial carrier. Mitochondrial ATP synthase could have been also included in this category but because of its prevailing function, it was placed among proteins playing role during energy metabolism. Only one percent of the identified phosphoprotein candidates was listed into disease/defence category, for example

monodehydroascorbate reductase. The last 4 % proteins belonged to the unclassified category, which was not surprising due to the fact that a majority of male gametophyte-specific proteins are not known and tobacco genome is not fully available in the public sequence databases.

5.5 On-going experiments

The list of the presented phosphoprotein candidates did not reveal the exact function of the proteins. It is rather a starting point for choosing the most interesting proteins for further analyses.

Most likely, the functional analysis of several phosphoprotein candidates will be the aim of my doctoral thesis. The localization of the selected candidates will be determined by a GFP-fused protein expressed in transiently transformed pollen. Subsequently, the protein will be over-expressed and a knock-down using small RNAs will be created.

In parallel, antibodies raised against the selected candidates will be produced. Firstly, they will be used for revealing a different set of isoforms, which will be displayed on a 2D IEF-PAGE during distinct stages of male gametophyte. Secondly, the immuno-purified proteins will be MS-analysed and possibly further phosphorylation sites will be identified. Thirdly, the protein partners of the selected candidates will be co-immunoprecipitated with the selected proteins. The pulled-down partners will be verified by a yeast two-hybrid system.

6 Conclusion

The first objective of this diploma thesis was the identification of phosphoprotein candidates present in mature pollen and 30-minute activated pollen. The applied phosphoprotein-enriching $\text{Al}(\text{OH})_3$ -MOAC led to the identification of a set of 139 phosphoprotein candidates present in the above stages of male gametophyte development. The MOAC feasibility together with its specificity was proven by a series of our results – a strong ProQ signal of phosphoprotein-enriched fraction on 1D SDS-PAGE, a different CBB G250 pattern of the enriched fraction compared to the crude extract prior to any enrichment, the string of spots of the same molecular weight but a different pI expressed on 2D-GE, and a similar molecular weight of the enriched and *in vitro* labelled proteins.

The second objective of this diploma thesis was to show exact phosphorylation site(s) of at least some phosphoprotein candidates. TiO_2 enrichment resulted in the unambiguous identification of 51 phosphorylation sites in 17 protein groups, so 52 phosphorylation sites in 18 protein groups were identified together with the only phosphorylation site identified after phosphoprotein enrichment. However, the phosphorylation site(s) of the remaining candidates were not shown. This does not necessarily mean that they were not phosphorylated – their phosphorylation site(s) may not have been achievable by the techniques used, and a set of alternative phosphoproteomic techniques would have been necessary to apply.

Collectively, the majority of candidates (even the ones without phosphorylation site presented) are likely to be connected with the metabolic switch from quiescent mature pollen to the rapidly-growing pollen tube. There is a number of interesting phosphoprotein candidates connected with translation regulation (a ripening regulated protein homologue, α -subunit of nascent-polypeptide-associated complex, and various translation initiation and translation elongation factors), function of which is likely to be characterised by the on-going experiments.

7 Publications and conferences

Impacted publications

- Fíla J, Matros A, Radau S, Zahedi RP, Čapková V, Mock HP, Honys D (2012):
Revealing phosphoproteins playing role in tobacco pollen activated *in vitro*.
Proteomics, *in revision*.
- Fíla J, Honys D (2011): Enrichment techniques employed in phosphoproteomics.
Amino Acids, *on-line first*, doi: 10.1007/s00726-011-1111-z.
- Fíla J, Čapková V, Feciková J, Honys D (2011): Impact of homogenization and
protein extraction conditions on the obtained tobacco pollen proteomic patterns.
Biologia Plantarum 55: 499–506.

Unimpacted publications

- Baláž V, Balážová A, Fíla J, Kolář F, Mikát M (2012): Láska, sex a něžnosti. *in
press*
- Fíla J, Pánek T, Sekereš J (2011): Tvary v živé přírodě. 153 pp. [ISBN 978-80-213-
2191-5]

Conferences

The results were presented at 8 international (4 oral presentations and 4 posters) and
2 Czech conferences (2 oral presentations).

8 References

- Addeo F, Chobert JM, Ribadeaudumas B** (1977) Fractionation of whole casein on hydroxyapatite – application to a study of buffalo kappa-casein. *J Dairy Res* **44**: 63–68
- Agnew B, Beechem J, Gee K, Haugland R, Liu J, Martin V, Patton W, Steinberg T** (2006) Compositions and methods for detection and isolation of phosphorylated molecules. U.S. Patent 7102005
- Agrawal GK, Thelen JJ** (2005) Development of a simplified, economical polyacrylamide gel staining protocol for phosphoproteins. *Proteomics* **5**: 4684–4688
- Andersson L, Porath J** (1986) Isolation of phosphoproteins by immobilized metal (Fe^{3+}) affinity chromatography. *Anal Biochem* **154**: 250–254
- Aryal UK, Ross ARS** (2010) Enrichment and analysis of phosphopeptides under different experimental conditions using titanium dioxide affinity chromatography and mass spectrometry. *Rapid Commun Mass Spectrometry* **24**: 219–231
- Baldan B, Navazio L, Friso A, Mariani P, Meggio F** (1996) Plant calreticulin is specifically and efficiently phosphorylated by protein kinase CK2. *Biochem Biophys Res Commun* **221**: 498–502
- Baskaran R, Chiang GG, Mysliwiec T, Kruh GD, Wang JYJ** (1997) Tyrosine phosphorylation of RNA polymerase II carboxyl-terminal domain by the Abl-related gene product. *J Biol Chem* **272**: 18905–18909
- Beausoleil SA, Jedrychowski M, Schwartz D, Elias JE, Villen J, Li JX, Cohn MA, Cantley LC, Gygi SP** (2004) Large-scale characterization of HeLa cell nuclear phosphoproteins. *Proc Natl Acad Sci USA* **101**: 12130–12135
- Beck F, Lewandrowski U, Wiltfang M, Feldmann I, Geiger J, Sickmann A, Zahedi RP** (2011) The good, the bad, the ugly: Validating the mass spectrometric analysis of modified peptides. *Proteomics* **11**: 1099–1109
- Benschop JJ, Mohammed S, O’Flaherty M, Heck AJR, Slijper M, Menke FLH** (2007) Quantitative phosphoproteomics of early elicitor signaling in Arabidopsis. *Mol Cell Proteomics* **6**: 1198–1214
- Besant PG, Attwood PV** (2009) Detection and analysis of protein histidine phosphorylation. *Mol Cell Biochem* **329**: 93–106

- Besant PG, Attwood PV, Piggott MJ** (2009) Focus on phosphoarginine and phospholysine. *Curr Protein Peptide Sci* **10**: 536–550
- Bevan M, Bancroft I, Bent E, Love K, Goodman H, Dean C, Bergkamp R, Dirkse W, van Staveren M, Stiekema W, et al.** (1998) Analysis of 1.9 Mb of contiguous sequence from chromosome 4 of *Arabidopsis thaliana*. *Nature* **391**: 485–488
- Bodenmiller B, Mueller LN, Mueller M, Domon B, Aebersold R** (2007) Reproducible isolation of distinct, overlapping segments of the phosphoproteome. *Nature Methods* **4**: 231–237
- Boersema PJ, Mohammed S, Heck AJR** (2009) Phosphopeptide fragmentation and analysis by mass spectrometry. *J Mass Spectrometry* **44**: 861–878
- Borg M, Brownfield L, Twell D** (2009) Male gametophyte development: a molecular perspective. *J Exp Botany* **60**: 1465–1478
- Brander KA, Kuhlemeier C** (1995) A pollen-specific DEAD-box protein related to translation initiation factor eIF-4A from tobacco. *Plant Mol Biol* **27**: 637–649
- Brewbaker JL** (1967) Distribution and phylogenetic significance of binucleate and trinucleate pollen grains in angiosperms. *Am J Botany* **54**: 1069–1083
- Bustos DM, Iglesias AA** (2003) Phosphorylated non-phosphorylating glyceraldehyde-3-phosphate dehydrogenase from heterotrophic cells of wheat interacts with 14-3-3 proteins. *Plant Physiol* **133**: 2081–2088
- Campbell NA, Reece JB, Urry LA, Cain ML, Wasserman SA, Minorsky PV, Jackson RB** (2008) *Biology*, 8th edition. Pearson Education, San Francisco
- Carrascal M, Ovefletro D, Casas V, Gay M, Ablan J** (2008) Phosphorylation analysis of primary human T lymphocytes using sequential IMAC and titanium oxide enrichment. *J Proteome Res* **7**: 5167–5176
- Cheung AY, Chen CYH, Glaven RH, de Graaf BHJ, Vidali L, Hepler PK, Wu HM** (2002) Rab2 GTPase regulates vesicle trafficking between the endoplasmic reticulum and the Golgi bodies and is important to pollen tube growth. *Plant Cell* **14**: 945–962
- Cresti M, Ciampolini F, Mulcahy DLM, Mulcahy G** (1985) Ultrastructure of *Nicotiana glauca* pollen, its germination and early tube formation. *Am J Botany* **72**: 719–727

- Cvoro A, Dundjerski J, Trajkovic D, Matic G** (1999) The level and phosphorylation of Hsp70 in the rat liver cytosol after adrenalectomy and hyperthermia. *Cell Biol Internatl* **23**: 313–320
- Čapková V, Hrabětová E, Tupý J** (1988) Protein synthesis in pollen tubes: preferential formation of new species independent of transcription. *Sex Plant Reprod* **1**: 150–155
- Darewicz M, Dziuba J, Minkiewicz P** (2005) Some properties of beta-casein modified via phosphatase. *Acta Alimentaria* **34**: 403–415
- de Graaf BHJ, Cheung AY, Andreyeva T, Levasseur K, Kieliszewski M, Wu HM** (2005) Rab11 GTPase-regulated membrane trafficking is crucial for tip-focused pollen tube growth in tobacco. *Plant Cell* **17**: 2564–2579
- Drakakaki G, Zobotina O, Delgado I, Robert S, Keegstra K, Raikhel N** (2006) Arabidopsis reversibly glycosylated polypeptides 1 and 2 are essential for pollen development. *Plant Physiol* **142**: 1480–1492
- Dunn JD, Reid GE, Bruening ML** (2010) Techniques for phosphopeptide enrichment prior to analysis by mass spectrometry. *Mass Spectrometry Rev* **29**: 29–54
- Eidelman O, Jozwik C, Huang W, Srivastava M, Rothwell SW, Jacobowitz DM, Ji X, Zhang X, Guggino W, Wright J, Kiefer J, Olsen C, Adimi N, Mueller GP, Pollard HB** (2010) Gender dependence for a subset of the low-abundance signaling proteome in human platelets. *Hum Genomics Proteomics* **2010**: 164906
- Eyrich B, Sickmann A, Zahedi RP** (2011) Catch me if you can: Mass spectrometry-based phosphoproteomics and quantification strategies. *Proteomics* **11**: 554–570
- Fíla J, Čapková V, Feciková J, Honys D** (2011) Impact of homogenization and protein extraction conditions on the obtained tobacco pollen proteomic patterns. *Biol Plant* **55**: 499–506
- Fíla J, Honys D** (2011) Enrichment techniques employed in phosphoproteomics. *Amino Acids*, **on-line first**: doi: 10.1007/s00726-011-1111-z
- Fletterick RJ, Sprang SR** (1982) Glycogen-phosphorylase structures and function. *Acc Chem Res* **15**: 361–369
- Francis D, Halford NG** (1995) The plant cell cycle. *Physiol Plant* **93**: 365–374

- Garnak M, Reeves HC** (1979) Phosphorylation of isocitrate dehydrogenase of *Escherichia coli*. *Science* **203**: 1111–1112
- Gauci S, Helbig AO, Slijper M, Krijgsveld J, Heck AJR, Mohammed S** (2009) Lys-N and trypsin cover complementary parts of the phosphoproteome in a refined SCX-based approach. *Anal Chem* **81**: 4493–4501
- Gilmore JM, Kettenbach AN, Gerber SA** (2012) Increasing phosphoproteomic coverage through sequential digestion by complementary proteases. *Anal Bioanal Chem* **402**: 711–720
- Grønborg M, Kristiansen TZ, Stensballe A, Andersen JS, Ohara O, Mann M, Jensen ON, Pandey A** (2002) A mass spectrometry-based proteomic approach for identification of serine/threonine-phosphorylated proteins by enrichment with phospho-specific antibodies – Identification of a novel protein, Frigg, as a protein kinase A substrate. *Mol Cell Proteomics* **1**: 517–527
- Hafidh S, Breznenová K, Honys D** (2012a) *De novo* post-pollen mitosis II tobacco pollen tube transcriptome. *Plant Signal Behav* **7**: in press
- Hafidh S, Breznenová K, Růžička P, Feciková J, Čapková V, Honys D** (2012b) Comprehensive analysis of tobacco pollen transcriptome unveils common pathways in polar cell expansion and underlying heterochronic shift during spermatogenesis. *BMC Plant Biol* **12**: 24
- Han GH, Ye ML, Zhou HJ, Jiang XN, Feng S, Jiang XG, Tian RJ, Wan DF, Zou HF, Gu JR** (2008) Large-scale phosphoproteome analysis of human liver tissue by enrichment and fractionation of phosphopeptides with strong anion exchange chromatography. *Proteomics* **8**: 1346–1361
- Hepler PK, Vidali L, Cheung AY** (2001) Polarized cell growth in higher plants. *Annu Rev Cell Dev Biol* **17**: 159–187
- Heslop-Harrison J** (1987) Pollen germination and pollen tube growth. In Giles KL, Prakash J (eds), *Pollen: Cytology and Development*, Vol 107. Academic Press, London, pp. 1–78
- Holmes-Davis R, Tanaka CK, Vensel WH, Hurkman WJ, McCormick S** (2005) Proteome mapping of mature pollen of *Arabidopsis thaliana*. *Proteomics* **5**: 4864–4884

- Honys D, Combe JP, Twell D, Čapková V** (2000) The translationally repressed pollen-specific ntp303 mRNA is stored in non-polysomal mRNPs during pollen maturation. *Sex Plant Reprod* **13**: 135–144
- Honys D, Reňák D, Feciková J, Jedelský PL, Nebesářová J, Dobrev P, Čapková V** (2009) Cytoskeleton-associated large RNP complexes in tobacco male gametophyte (EPPs) are associated with ribosomes and are involved in protein synthesis, processing, and localization. *J Proteome Res* **8**: 2015–2031
- Hrubá P, Honys D, Tupý J** (2005) Expression and thermotolerance of calreticulin during pollen development in tobacco. *Sex Plant Reprod* **18**: 143–148
- Hsieh HC, Sheu C, Shi FK, Li DT** (2007) Development of a titanium dioxide nanoparticle pipette-tip for the selective enrichment of phosphorylated peptides. *J Chromatogr A* **1165**: 128–135
- Hultquist DE** (1968) The preparation and characterization of phosphorylated derivatives of histidine. *Biochim Biophys Acta* **153**: 329–340
- Iliuk AB, Martin VA, Alicie BM, Geahlen RL, Tao WA** (2010) In-depth analyses of kinase-dependent tyrosine phosphoproteomes based on metal ion-functionalized soluble nanopolymers. *Mol Cell Proteomics* **9**: 2162–2172
- Imam-Sghiouar N, Laude-Lemaire I, Labas V, Pflieger D, Le Caer JP, Caron M, Nabias DK, Joubert-Caron R** (2002) Subproteomics analysis of phosphorylated proteins: Application to the study of B-lymphoblasts from a patient with Scott syndrome. *Proteomics* **2**: 828–838
- Ito J, Taylor NL, Castleden I, Weckwerth W, Millar AH, Heazlewood JL** (2009) A survey of the *Arabidopsis thaliana* mitochondrial phosphoproteome. *Proteomics* **9**: 4229–4240
- Iwano M, Entani T, Shiba H, Kakita M, Nagai T, Mizuno H, Miyawaki A, Shoji T, Kubo K, Isogai A, Takayama S** (2009) Fine-tuning of the cytoplasmic Ca²⁺ concentration is essential for pollen tube growth. *Plant Physiol* **150**: 1322–1334
- Jaillais Y, Hothorn M, Belkhadir Y, Dabi T, Nimchuk ZL, Meyerowitz EM, Chory J** (2011) Tyrosine phosphorylation controls brassinosteroid receptor activation by triggering membrane release of its kinase inhibitor. *Genes Dev* **25**: 232–237

- Jensen AB, Goday A, Figueras M, Jessop AC, Pagès M** (1998) Phosphorylation mediates the nuclear targeting of the maize Rab17 protein. *Plant J* **13**: 691–697
- Kameyama K, Kishi Y, Yoshimura M, Kanzawa N, Sameshima M, Tsuchiya T** (2000) Tyrosine phosphorylation in plant bending – Puckering in a ticklish plant is controlled by dephosphorylation of its actin. *Nature* **407**: 37–37
- Kang DH, Gho YS, Suh MK, Kang CH** (2002) Highly sensitive and fast protein detection with coomassie brilliant blue in sodium dodecyl sulfate–polyacrylamide gel electrophoresis. *Bull Korean Chem Soc* **23**: 1511–1512
- Kaspar S, Weier D, Weschke W, Mock HP, Matros A** (2010) Protein analysis of laser capture micro-dissected tissues revealed cell-type specific biological functions in developing barley grains. *Anal Bioanal Chem* **398**: 2883–2893
- Kim J, Shen Y, Han YJ, Park JE, Kirchenbauer D, Soh MS, Nagy F, Schafer E, Song PS** (2004) Phytochrome phosphorylation modulates light signaling by influencing the protein–protein interaction. *Plant Cell* **16**: 2629–2640
- Kim TW, Guan SH, Sun Y, Deng ZP, Tang WQ, Shang JX, Burlingame AL, Wang ZY** (2009) Brassinosteroid signal transduction from cell-surface receptor kinases to nuclear transcription factors. *Nature Cell Biol* **11**: 1254–U1233
- Kinoshita E, Yamada A, Takeda H, Kinoshita-Kikuta E, Koike T** (2005) Novel immobilized zinc(II) affinity chromatography for phosphopeptides and phosphorylated proteins. *J Sep Sci* **28**: 155–162
- Klahre U, Becker C, Schmitt AC, Kost B** (2006) Nt-RhoGDI2 regulates Rac/Rop signaling and polar cell growth in tobacco pollen tubes. *Plant J* **46**: 1018–1031
- Kokubu M, Ishihama Y, Sato T, Nagasu T, Oda Y** (2005) Specificity of immobilized metal affinity-based IMAC/C18 tip enrichment of phosphopeptides for protein phosphorylation analysis. *Anal Chem* **77**: 5144–5154
- Kolobova E, Tuganova A, Boulatnikov I, Popov KM** (2001) Regulation of pyruvate dehydrogenase activity through phosphorylation at multiple sites. *Biochem J* **358**: 69–77

- Krüger R, Wolschin F, Weckwerth W, Bettmer J, Lehmann WD** (2007) Plant protein phosphorylation monitored by capillary liquid chromatography-element mass spectrometry. *Biochem Biophys Res Commun* **355**: 89–96
- Kweon HK, Håkansson K** (2006) Selective zirconium dioxide-based enrichment of phosphorylated peptides for mass spectrometric analysis. *Anal Chem* **78**: 1743–1749
- Laemmli UK** (1970) Cleavage of structural proteins during assembly of head of bacteriophage T4. *Nature* **227**: 680–685
- Lamanda A, Zahn A, Roder D, Langen H** (2004) Improved ruthenium II tris (bathophenanthroline disulfonate) staining and destaining protocol for a better signal-to-background ratio and improved baseline resolution. *Proteomics* **4**: 599–608
- Lansdell TA, Tepe JJ** (2004) Isolation of phosphopeptides using solid phase enrichment. *Tetrahedron Lett* **45**: 91–93
- Larsen MR, Thingholm TE, Jensen ON, Roepstorff P, Jorgensen TJD** (2005) Highly selective enrichment of phosphorylated peptides from peptide mixtures using titanium dioxide microcolumns. *Mol Cell Proteomics* **4**: 873–886
- Lenman M, Sorensson C, Andreasson E** (2008) Enrichment of phosphoproteins and phosphopeptide derivatization identify universal stress proteins in elicitor-treated Arabidopsis. *Mol Plant–Microbe Interact* **21**: 1275–1284
- Li YJ, Luo YM, Wu SZ, Gao YH, Liu YX, Zheng DX** (2009) Nucleic acids in protein samples interfere with phosphopeptide identification by immobilized-metal-ion affinity chromatography and mass spectrometry. *Mol Biotechnol* **43**: 59–66
- Lima L, Seabra A, Melo P, Cullimore J, Carvalho H** (2006) Phosphorylation and subsequent interaction with 14-3-3 proteins regulate plastid glutamine synthetase in *Medicago truncatula*. *Planta* **223**: 558–567
- Mamone G, Picariello G, Ferranti P, Addeo F** (2010) Hydroxyapatite affinity chromatography for the highly selective enrichment of mono- and multi-phosphorylated peptides in phosphoproteome analysis. *Proteomics* **10**: 380–393

- Marcantonio M, Trost M, Courcelles M, Desjardins M, Thibault P** (2008) Combined enzymatic and data mining approaches for comprehensive phosphoproteome analyses. *Mol Cell Proteomics* **7**: 645–660
- Mascarenhas JP** (1993) Molecular mechanisms of pollen tube growth and differentiation. *Plant Cell* **5**: 1303–1314
- Matsui M, Fowler JH, Walling LL** (2006) Leucine aminopeptidases: diversity in structure and function. *Biol Chem* **387**: 1535–1544
- Mayank P, Grossman J, Wuest S, Boisson-Dernier A, Roschitzki B, Nanni P, Nühse T, Grossniklaus U** (2012) Characterization of the phosphoproteome of mature *Arabidopsis* pollen. *Plant J*, **on-line first**: doi: 10.1111/j.1365-313X.2012.05061.x
- Mazanek M, Roitinger E, Hudecz O, Hutchins JRA, Hegemann B, Mitulovic G, Taus T, Stingl C, Peters JM, Mechtler K** (2010) A new acid mix enhances phosphopeptide enrichment on titanium- and zirconium dioxide for mapping of phosphorylation sites on protein complexes. *J Chromatogr B – Anal Technol Biomed Life Sci* **878**: 515–524
- McCormick S** (1993) Male gametophyte development. *Plant Cell* **5**: 1265–1275
- McNulty DE, Annan RS** (2008) Hydrophilic interaction chromatography reduces the complexity of the phosphoproteome and improves global phosphopeptide isolation and detection. *Mol Cell Proteomics* **7**: 971–980
- Méchin V, Damerval C, Zivy M** (2006) Total protein extraction with TCA-acetone. *In* Thiellement H, Zivy M, Damerval C, Méchin V (eds) *Methods in Molecular Biology*. Springer, pp. 1–8
- Mishra NS, Tuteja R, Tuteja N** (2006) Signaling through MAP kinase networks in plants. *Archives Biochem Biophys* **452**: 55–68
- Molina H, Horn DM, Tang N, Mathivanan S, Pandey A** (2007) Global proteomic profiling of phosphopeptides using electron transfer dissociation tandem mass spectrometry. *Proc Natl Acad Sci USA* **104**: 2199–2204
- Moll T, Tebb G, Surana U, Robitsch H, Nasmyth K** (1991) The role of phosphorylation and the CDC28 protein kinase in cell-cycle regulated nuclear import of the *Saccharomyces cerevisiae* transcription factor SWI15. *Cell* **66**: 743–758
- Morton RK** (1955) Substrate specificity and inhibition of alkaline phosphatases of cows milk and calf intestinal mucosa. *Biochem J* **61**: 232–240

- Nühse TS, Stensballe A, Jensen ON, Peck SC** (2004) Phosphoproteomics of the Arabidopsis plasma membrane and a new phosphorylation site database. *Plant Cell* **16**: 2394–2405
- Oda Y, Nagasu T, Chait BT** (2001) Enrichment analysis of phosphorylated proteins as a tool for probing the phosphoproteome. *Nature Biotechnol* **19**: 379–382
- Olsen JV, Blagoev B, Gnäd F, Macek B, Kumar C, Mortensen P, Mann M** (2006) Global, *in vivo*, and site-specific phosphorylation dynamics in signaling networks. *Cell* **127**: 635–648
- Olsen JV, de Godoy LMF, Li GQ, Macek B, Mortensen P, Pesch R, Makarov A, Lange O, Horning S, Mann M** (2005) Parts per million mass accuracy on an orbitrap mass spectrometer via lock mass injection into a C-trap. *Mol Cell Proteomics* **4**: 2010–2021
- op den Camp RGL, Kuhlemeier C** (1998) Phosphorylation of tobacco eukaryotic translation initiation factor 4A upon pollen tube germination. *Nucleic Acids Res* **26**: 2058–2062
- Owtrim GW, Mandel T, Trachsel H, Thomas AAM, Kuhlemeier C** (1994) Characterization of the tobacco eIF-4A gene family. *Plant Mol Biol* **26**: 1747–1757
- Petrů E, Hrabětová E, Tupý J** (1964) The technique of obtaining germinating pollen without microbial contamination. *Biol Plant* **6**: 68–69
- Pinkse MWH, Uitto PM, Hilhorst MJ, Ooms B, Heck AJR** (2004) Selective isolation at the femtomole level of phosphopeptides from proteolytic digests using 2D–nanoLC–ESI–MS/MS and titanium oxide precolumns. *Anal Chem* **76**: 3935–3943
- Plaxton WC** (1996) The organization and regulation of plant glycolysis. *Annu Rev Plant Physiol Plant Mol Biol* **47**: 185–214
- Plimmer RHA** (1941) Esters of phosphoric acid: Phosphoryl hydroxyamino-acids. *Biochem J* **35**: 461–469
- Posewitz MC, Tempst P** (1999) Immobilized gallium(III) affinity chromatography of phosphopeptides. *Anal Chem* **71**: 2883–2892
- Rabilloud T, Strub JM, Luche S, van Dorsselaer A, Lunardi J** (2001) Comparison between Sypro Ruby and ruthenium II tris (bathophenanthroline disulfonate) as fluorescent stains for protein detection in gels. *Proteomics* **1**: 699–704

- Raudaskoski M, Åström H, Laitinen E** (2001) Pollen tube cytoskeleton: Structure and function. *J Plant Growth Regul* **20**: 113–130
- Reiland S, Messerli G, Baerenfaller K, Gerrits B, Endler A, Grossmann J, Gruissem W, Baginsky S** (2009) Large-scale Arabidopsis phosphoproteome profiling reveals novel chloroplast kinase substrates and phosphorylation networks. *Plant Physiol* **150**: 889–903
- Röhrig H, Colby T, Schmidt J, Harzen A, Facchinelli F, Bartels D** (2008) Analysis of desiccation-induced candidate phosphoproteins from *Craterostigma plantagineum* isolated with a modified metal oxide affinity chromatography procedure. *Proteomics* **8**: 3548–3560
- Rudrabhatla P, Reddy MM, Rajasekharan R** (2006) Genome-wide analysis and experimentation of plant serine/threonine/tyrosine-specific protein kinases. *Plant Mol Biol* **60**: 293–319
- Rush J, Moritz A, Lee KA, Guo A, Goss VL, Spek EJ, Zhang H, Zha XM, Polakiewicz RD, Comb MJ** (2005) Immunoaffinity profiling of tyrosine phosphorylation in cancer cells. *Nature Biotechnol* **23**: 94–101
- Sano A, Nakamura H** (2004) Titanias as a chemo-affinity support for the column-switching HPLC analysis of phosphopeptides: Application to the characterization of phosphorylation sites in proteins by combination with protease digestion and electrospray ionization mass spectrometry. *Anal Sci* **20**: 861–864
- Schaffner W, Weissman C** (1973) Rapid, sensitive, and specific method for determination of protein in dilute solution. *Anal Biochem* **56**: 502–514
- Schilling M, Knapp DR** (2008) Enrichment of phosphopeptides using biphasic immobilized metal affinity-reversed phase microcolumns. *J Proteome Res* **7**: 4164–4172
- Schlosser A, Vanselow JT, Kramer A** (2005) Mapping of phosphorylation sites by a multi-protease approach with specific phosphopeptide enrichment and nanoLC–MS/MS analysis. *Anal Chem* **77**: 5243–5250
- Selden LA, Gershman LC, Kinoshita H, Estes JE** (1987) Conversion of ATP-actin to ADP-actin reverses the affinity of monomeric actin for Ca^{2+} vs. Mg^{2+} . *FEBS Lett* **217**: 89–93

- Shen YH, Godlewski J, Bronisz A, Zhu J, Comb MJ, Avruch J, Tzivion G** (2003) Significance of 14-3-3 self-dimerization for phosphorylation-dependent target binding. *Mol Biol Cell* **14**: 4721–4733
- Simon ES, Young M, Chan A, Bao ZQ, Andrews PC** (2008) Improved enrichment strategies for phosphorylated peptides on titanium dioxide using methyl esterification and pH gradient elution. *Anal Biochem* **377**: 234–242
- Smith AM, Coupland G, Dolan L, Harberd N, Jones J, Martin C, Sablowski R, Amey A** (2010) *Plant biology*. Garland Science, New York and Abingdon
- Sopory SK, Munshi M** (1998) Protein kinases and phosphatases and their role in cellular signaling in plants. *Crit Rev Plant Sci* **17**: 245–318
- Spronk AM, Yoshida H, Wood HG** (1976) Isolation of 3-phosphohistidine from phosphorylated pyruvate-phosphate dikinase. *Proc Natl Acad Sci USA* **73**: 4415–4419
- Steinberg TH, Agnew BJ, Gee KR, Leung WY, Goodman T, Schulenberg B, Hendrickson J, Beechem JM, Haugland RP, Patton WF** (2003) Global quantitative phosphoprotein analysis using multiplexed proteomics technology. *Proteomics* **3**: 1128–1144
- Sugiyama N, Masuda T, Shinoda K, Nakamura A, Tomita M, Ishihama Y** (2007) Phosphopeptide enrichment by aliphatic hydroxy acid-modified metal oxide chromatography for nano-LC–MS/MS in proteomics applications. *Mol Cell Proteomics* **6**: 1103–1109
- Sugiyama N, Nakagami H, Mochida K, Daudi A, Tomita M, Shirasu K, Ishihama Y** (2008) Large-scale phosphorylation mapping reveals the extent of tyrosine phosphorylation in Arabidopsis. *Mol Syst Biol* **4**: 7
- Svennelid F, Olsson A, Piotrowski M, Rosenquist M, Ottman C, Larsson C, Oecking C, Sommarin M** (1999) Phosphorylation of Thr-948 at the C terminus of the plasma membrane H⁺-ATPase creates a binding site for the regulatory 14-3-3 protein. *Plant Cell* **11**: 2379–2391
- Tadege M, Kuhlemeier C** (1997) Aerobic fermentation during tobacco pollen development. *Plant Mol Biol* **35**: 343–354
- Thompson CE, Salzano FM, de Souza ON, Freitas LB** (2007) Sequence and structural aspects of the functional diversification of plant alcohol dehydrogenases. *Gene* **396**: 108–115

- Tian HQ, Yuan T, Russell SD** (2005) Relationship between double fertilization and the cell cycle in male and female gametes of tobacco. *Sex Plant Reprod* **17**: 243–252
- Tupý J, Říhová L** (1984) Changes and growth effect of pH in pollen tube culture. *J Plant Physiol* **115**: 1–10
- van Bentem SD, Anrather D, Dohnal I, Roitinger E, Csaszar E, Joore J, Buijnink J, Carreri A, Forzani C, Lorkovic ZJ, Barta A, Lecourieux D, Verhounig A, Jonak C, Hirt H** (2008) Site-specific phosphorylation profiling of Arabidopsis proteins by mass spectrometry and peptide chip analysis. *J Proteome Res* **7**: 2458–2470
- van Bentem SD, Hirt H** (2009) Protein tyrosine phosphorylation in plants: more abundant than expected? *Trends Plant Sci* **14**: 71–76
- van der Kelen K, Beyaert R, Inze D, de Veylder L** (2009) Translational control of eukaryotic gene expression. *Crit Rev Biochem Mol Biol* **44**: 143–168
- Waditee-Sirisattha R, Shibato J, Rakwal R, Sirisattha S, Hattori A, Nakano T, Takabe T, Tsujimoto M** (2011) The Arabidopsis aminopeptidase LAP2 regulates plant growth, leaf longevity and stress response. *New Phytologist* **191**: 958–969
- Wålinder O** (1969a) Evidence of presence of 1-phosphohistidine as main phosphorylated component at active site of bovine liver nucleoside diphosphate kinase. *Acta Chem Scand* **23**: 339–341
- Wålinder O** (1969b) Protein-bound acid-labile phosphate – Isolation of 1-³²P-phosphohistidine and 3-³²P-phosphohistidine from some mammalian and microbial cell extracts incubated with adenosine triphosphate-³²P. *J Biol Chem* **244**: 1065–1069
- Wang YQ, Liao MX, Hoe N, Acharya P, Deng CH, Krutchinsky AN, Correia MA** (2009) A role for protein phosphorylation in cytochrome P450 3A4 ubiquitin-dependent proteasomal degradation. *J Biol Chem* **284**: 5671–5684
- Warthaka M, Karwowska-Desaulniers P, Pflum MKH** (2006) Phosphopeptide modification and enrichment by oxidation–reduction condensation. *ACS Chem Biol* **1**: 697–701
- Wessel D, Flügge UI** (1984) A method for the quantitative recovery of protein in dilute solution in the presence of detergents and lipids. *Anal Biochem* **138**: 141–143

- Witzel K, Surabhi GK, Jyothsnakumari G, Sudhakar C, Matros A, Mock HP** (2007) Quantitative proteome analysis of barley seeds using ruthenium(II)-tris-(bathophenanthroline-disulphonate) staining. *J Proteome Res* **6**: 1325–1333
- Wolschin F, Weckwerth W** (2005) Combining metal oxide affinity chromatography (MOAC) and selective mass spectrometry for robust identification of *in vivo* protein phosphorylation sites. *Plant Methods* **1**: 9
- Wolschin F, Wienkoop S, Weckwerth W** (2005) Enrichment of phosphorylated proteins and peptides from complex mixtures using metal oxide/hydroxide affinity chromatography (MOAC). *Proteomics* **5**: 4389–4397
- Wu J, Shakey Q, Liu W, Schuller A, Follettie MT** (2007) Global profiling of phosphopeptides by titania affinity enrichment. *J Proteome Res* **6**: 4684–4689
- Yates JR, Ruse CI, Nakorchevsky A** (2009) Proteomics by mass spectrometry: Approaches, advances, and applications. *Ann Rev Biomed Eng* **11**: 49–79
- Zhou HL, Watts JD, Aebersold R** (2001) A systematic approach to the analysis of protein phosphorylation. *Nature Biotechnol* **19**: 375–378
- Zhou SB, Bailey MJ, Dunn MJ, Preedy VR, Emery PW** (2005) A quantitative investigation into the losses of proteins at different stages of a two-dimensional gel electrophoresis procedure. *Proteomics* **5**: 2739–2747

9 Supplementary tables (on a CD)

Table S1 – Identified phosphoprotein candidates from the excised 2D-GE spots analysed as described in “Materials and methods” with additional data (identified peptides, their m/z and ladder scores). Proteins that were identified from at least two gels according to at least two peptides are marked with two asterisks behind the spot number, whereas proteins that were identified only once according to at least two peptides are marked with one asterisk. Superscript behind accession number indicates database: a) Swissprot; b) Trembl *Viridiplantae*; c) TIGR EST *Solanaceae*. The superscripted S behind the MP/PT ratio means a significant change between the two stages as calculated by the PDQuest software. Note: Spot 4 was not recognised as a spot by the PDQuest software, but manually assigned. Norm. spot volume – normalised spot volume.

Table S2 – Complete set of identified phosphoprotein candidates by the non-gel approach analysed as described in “Materials and methods” section with additional data (identified peptides, their mass, charge, scores and individual quantity data). Number of peptides indicates the total number of peptides, according to which the protein was identified. The number in the brackets represents number of unique peptides that contribute to protein identification (the peptides common for more proteins were excluded). The data regarding diagnostic peptides are shown in black whereas the conflicting ones are displayed in gray.

Table S3 – List of phosphorylation sites identified after the TiO₂-MOAC phosphopeptide enrichment from mature pollen with additional information. The proteins are grouped according to their names, in some cases listing together several isoforms of the same protein since they are hard to be distinguished between each other due to tobacco being not completely sequenced. The phosphorylation site is pinpointed in bold and the given phosphorylated amino acid is followed by an asterisk. The peptides with ambiguous position of phosphorylation site are shown in gray. The superscripted number behind the accession number indicates database: a) UniProt, 90% homology clusters, *Viridiplantae*, b) TIGR EST *Nicotiana tabacum*.